Technische Universität München
Fakultät für Medizin

# The role of p22phox in the cardiovascular response to obesity

Mathieu Edouard Klop

Vollständiger Abdruck der von der Fakultät für Medizin der Technischen Universität München zur Erlangung eines

Doktors der Medizinischen Wissenschaft (Dr. med. sci.)

genehmigten Dissertation.

Vorsitz: Prof. Dr. Michael Joner

Prüfer*innen der Dissertation:

1. Prof. Dr. Agnes Görlach
2. Priv.- Doz. Dr. Thorsten Keßler

Die Dissertation wurde am 17.02.2023 bei der Technischen Universität München eingereicht und durch die Fakultät für Medizin am 14.06.2023 angenommen.

# Table of contents

# 1 Summary

Obesity is a major burden worldwide which has increased substantially in the last 20 years. It is strongly associated with metabolic and cardiovascular disorders and has been recognized as an independent risk factor for heart failure (Poirier et al., 2006). Obesity has been reported to elevate the levels of reactive oxygen species (ROS) not only in adipocytes but also in cardiovascular tissues (Fernández-Sánchez et al., 2011; Furukawa et al., 2017).

NADPH oxidases are important sources of ROS in the cardiovascular system and have been discussed to contribute to the pathogenesis of many cardiovascular diseases (Brown & Griendling, 2009; Petry et al., 2010). However, their contribution to cardiovascular complications in obesity including obesity cardiomyopathy is not well understood.

The aim of this study was to better understand the role of NADPH oxidases in the obese heart. To this end, mice lacking functional NADPH oxidases due to a point mutation in the Cyba gene coding for the essential NADPH oxidase subunit p22phox (nmf333) and wildtype mice were exposed to a high fat diet for 20 weeks.

This regimen resulted in the development of obesity induced cardiomyopathy in wildtype mice characterized by increased left ventricular pressure, cardiac hypertrophy and dysfunction with reduced ejection fraction as well as left and right ventricular remodeling and pulmonary vascular remodelling. However, NADPH oxidase-deficient nmf333 mice were protected against the development of obesity induced cardiomyopathy. In fact, lack of p22phox reduced ROS generation not only in the obese heart, but also in isolated cardiomyocytes exposed to treatment with the unsaturated fatty acid palmitate.

To better understand the pathways dysregulated in obesity induced cardiomyopathy we performed microRNA sequencing (miRNAseq) analysis in lean and obese hearts derived from wildtype and NADPH oxidase deficient mice. We identified miRNA-1a (miR1a) as specifically downregulated in obese hearts from wildtype mice while this response was not observed in hearts from nmf333 mice after high fat diet treatment. In line, the expression of miR-1a target genes was increased in the heart from wildtype mice but not from nmf333 mice following high fat diet. Pathway analyses performed on the data sets derived from miRNA-seq pointed towards several stress pathways, emphasizing oxidative stress, the unfolded protein response (UPR) as well as programmed cell death dysregulated by obesity and p22phox.

In fact, p22phox as well as the NADPH oxidase subunits NOX2 and NOX4 were not only increased in hearts, but also in lungs from high fat diet treated wildtype mice but not from nmf333 mice. In line, oxidative DNA damage and lipid peroxidation were elevated in hearts and lungs from high fat diet treated wildtype mice but not from nmf333 mice, confirming that nmf333 mice were protected against oxidative stress pathways in heart and lungs induced by high fat diet.

Subsequently, markers for endoplasmic reticulum (ER) stress and the UPR as well as for programmed cell death were elevated in hearts from wildtype mice, but not from nmf333 mice fed a high fat diet.

In summary, this study provides evidence that p22phox dependent NADPH oxidases promote obesity induced cardiomyopathy by dysregulating the miRNA transcriptome including miR-1a, oxidative stress pathways, the UPR and programmed cell death. Targeting p22phox may provide therapeutic effects in obesity induced cardiovascular diseases and needs further investigation in experimental and clinical trials.

# 2 Zusammenfassung

Adipositas stellt weltweit ein bedeutendes Gesundheitsproblem dar, das in den letzten Jahrzehnten eine stark zunehmende Tendenz aufweist. Es besteht eine enge Assoziation zwischen Adipositas und metabolischen sowie kardiovaskulären Erkrankungen. Forschungsergebnisse haben gezeigt, dass Adipositas als unabhängiger Risikofaktor für die Entwicklung von Herzinsuffizienz anzusehen ist (Poirier et al., 2006). Fettleibigkeit erhöht nicht nur die Menge an reaktiven Sauerstoffspezies (ROS) in Fettzellen, sondern auch in Geweben des Herz-Kreislauf-Systems (Fernández-Sánchez et al., 2011; Furukawa et al., 2017).

NADPH-Oxidasen werden als wichtige Ursachen für die Bildung von ROS im Herz-Kreislauf-System angesehen und in Zusammenhang mit der Entstehung von verschiedenen Herzerkrankungen gebracht (Brown & Griendling, 2009; Petry et al., 2010). Ihr Beitrag zur Entwicklung kardiovaskulärer Komplikationen, insbesondere einer Kardiomyopathie, bei Adipositas ist jedoch nicht gut verstanden.

Das Ziel dieser Studie war es, die Rolle von NADPH-Oxidasen bei mit Adipositas assoziierten Herzerkrankungen besser zu verstehen. Hierzu wurden Mäuse mit einer Punktmutation im Cyba-Gen (nmf333), das für die essenzielle NADPH-Oxidase-Untereinheit p22phox kodiert, und Wildtypmäuse einer Hochfettdiät für 20 Wochen ausgesetzt.

Dieses Regime führte bei Wildtypmäusen zur Entwicklung einer Adipositas-induzierten Kardiomyopathie, die durch erhöhten linksventrikulären Druck, Herzhypertrophie und Reduktion der linksventrikulären Ejektionsfraktion sowie pulmonalvaskulärem Remodelling gekennzeichnet war. NADPH-Oxidase-defiziente nmf333 Mäuse waren jedoch vor der Entwicklung einer Adipositas-induzierten Kardiomyopathie geschützt. Tatsächlich reduzierte das Fehlen von p22phox die ROS-Bildung nicht nur im adipösen Herzen, sondern auch in isolierten Kardiomyozyten, die mit der ungesättigten Fettsäure Natrium-Palmitat behandelt wurden.

Um die bei Adipositas-induzierter Kardiomyopathie dysregulierten Signalketten besser zu verstehen, führten wir eine mikro-RNA Sequenzierungsanalyse (miRNA-seq) an linken Ventrikeln von gesunden und adipösen Wildtyp- und NADPH-Oxidase-defizienten Mäusen durch. Wir identifizierten mikro-RNA-1a (miR1a) als spezifisch herunterregulierte mikro-RNA in adipösen Herzen von Wildtypmäusen, während diese Antwort in Herzen von adipösen nmf333-Mäusen nicht beobachtet wurde.

Entsprechend war die Expression von miR-1a-Zielgenen in Herzen von Wildtypmäusen erhöht, jedoch nicht in Herzen von nmf333-Mäusen nach Hochfettdiät. Die Analyse von Signalwegen, die aus der miRNA-seq generierten Daten durchgeführt wurden, deutete auf mehrere Stresswege hin, insbesondere in Bezug auf oxidativen Stress, ungefaltete Proteinantwort (UPR) sowie programmierten Zelltod, die durch Adipositas und p22phox dysreguliert wurden. Tatsächlich waren p22phox sowie die NADPH-Oxidase-Untereinheiten NOX2 und NOX4 nicht nur in Herzen, sondern auch in Lungen von Wildtypmäusen, die einer Hochfettdiät ausgesetzt waren, erhöht, jedoch nicht in nmf333-Mäusen. Entsprechend waren oxidative DNA-Schäden und Lipidperoxidation in Herzen und Lungen von Wildtypmäusen, nicht aber von nmf333-Mäusen, nach Hochfettdiät, erhöht, was bestätigt, dass nmf333-Mäuse gegen oxidative Stresswege in Herz und Lungen durch Hochfettdiät geschützt waren. Schließlich waren Marker für Stress des endoplasmatischen Retikulums (ER-Stress), für die UPR sowie für programmierten Zelltod in Herzen von Wildtypmäusen, nicht aber von nmf333-Mäusen, nach Hochfettdiät erhöht.

Zusammenfassend liefert diese Studie Beweise dafür, dass p22phox-abhängige NADPH-Oxidasen das miRNA Transkriptom einschließlich miR-1a, oxidative Stresswege, die UPR und den programmierten Zelltod dysregulieren und dadurch die Adipositas-induzierte Kardiomyopathie fördern. Die gezielte Beeinflussung von p22phox könnte eine therapeutische Option für die Behandlung von Adipositas-induzierten kardiovaskulären Erkrankungen darstellen und erfordert weitere Untersuchungen in experimentellen und klinischen Studien.

# 3 List of abbreviations and symbols

ANT – adenine nucleotide translocator

ATF4 – activating transcription factor 4

ATF6 – activating transcription factor 6

BCKDH – branched-chain α-ketoacid dehydrogenase

BDM – 2,3-butanedione monoxime

BH – Benjamini Hochberg

BiP – binding immunoglobulin protein

BM – body mass

BMI – body mass index

BSA – bovine serum albumin

CaMKII – Ca2+/calmodulin-dependent protein kinase II

CAT – catalase

CHOP – C/EBP homologous protein

CMH – 1-hydroxy-methoxycarbonyl-2,2,5,5-tetramethyl-pyrrolidine hydrochloride

Ctr – control

DAPI – 4', 6-diamidino-2-phenylindole

DD – death domain

DDR – DNA damage response

DE – differential expression

DES – desferroxamine

DED – death effector domain

DETC – diethyldithiocarbamate

DHE – dihydroethidium

DISC – death-inducing signaling complex

DMSO – dimethyl sulfoxide

DMII – diabetes mellitus type two

DNA – deoxyribonucleic acid

DUOX – dual oxidase

EDN1 – endothelin 1

EDTA – ethylenediaminetetraacetic acid

EF – ejection fraction

eIF2α – eukaryotic translation initiation factor 2A

EPR – electron paramagnetic resonance

ER – endoplasmic reticulum

FADD – fas associated death domain

FAD+ – flavin adenine dinucleotide

FADH – flavin adenine dinucleotide (half reduced)

FADH2 – flavin adenine dinucleotide (hydroquinone form)

FCS – fetal calf serum

FDR – false discovery rate

FFPE – formalin fixed paraffin embedded

FMN – flavin mononucleotide

FS – fractional shortening

GKT – GKT-137831

GRP78 – glucose regulated proteins 78

GRP94 – glucose regulated proteins 94

GTPx – glutathione peroxidase

HBSS – Hank's balanced salt solution

HFD – high fat diet

HFmEF – heart failure with mildly reduced ejection fraction

HFpEF – heart failure with preserved ejection fraction

HFrEF – heart failure with reduced ejection fraction

HGNC – HUGO Gene Nomenclature Committee

HIF – hypoxia-inducible factor

HMEC-1 – human microvascular endothelial cells

$H_2O_2$ – hydrogen peroxide

IL-1 – interleukin 1

IL-6 – interleukin 6

IL-12 – interleukin 12

IRE-1 – inositol-requiring enzyme 1

IVSd – intraventricular septum wall thickness (diastolic)

IVSs – intraventricular septum wall thickness (systolic)

KHB – Krebs-Hepes buffer

LV – left ventricle

LVEDD – left ventricular end diastolic diameter

LVESD – left ventricular end systolic diameter

LVH – left ventricular hypertrophy

LVP – left ventricular pressure

LVPWd – left ventricular posterior wall thicknes (diastolic)

LVPWs – left ventricular posterior wall thicknes (systolic)

MDA – malondialdehyde

MCP-1 – monocyte chemoattractant protein-1

miRNA – micro RNA

mRNA – messenger RNA

NAC – N-acetyl cysteine

NAD+ – nicotinamide adenine dinucleotide

NADH – nicotinamide adenine dinucleotide (reduced)

NADPH – nicotinamide adenine dinucleotide phosphate

NF-κB – nuclear factor 'kappa-light-chain-enhancer' of activated B-cells

ODH – octopine dehydrogenase

$O_2$ - dioxygen

$O_2$- – superoxide

OH- – hydroxyl radical

p-eIF2α – phosphorylated eukaryotic translation initiation factor 2A

PAH – pulmonary arterial hypertension

PAI-1 – plasminogen-aktivator-inhibitor-1

PARP – poly ADP ribose polymerase

PBS – phosphate buffered saline

PCD – programmed cell death

PCR – polymerase chain reation

PDH – pyruvate dehydrogenase

PDI – protein disulfide isomerase

PERK – protein kinase R (PKR)-like endoplasmic reticulum kinase

PH – pulmonary hypertension

PTPC - permeability transition pore complex

PVR – pulmonary vascular remodeling

Q – ubiquinone

QH2 – ubiquinol

Rac – Ras-related C3 botulinum toxin substrate

RNA – ribonucleic acid

ROS – reactive oxygen species

Rot – rotenone

RV – right ventricle

RVH – right ventricular hypertrophy

RVP – right ventricular pressure

SD – standard deviation

SDS-PAGE – sodium dodecyl sulfate polyacrylamide gel electrophoresis

SDH – succinate dehydrogenase

SEM – standard error of the mean

shRNA – short hairpin ribonucleic acid

siRNA – silencing ribonucleic acid

α-SMA – alpha smooth muscle actin

SOD – superoxide dismutase

SSB – single strand breaks

TBS – tris-buffered saline

TBS-T – tris-buffered saline-tween20

TNFα - tumor necrosis factor alpha

TRX – thioredoxin

UPR – unfolded protein response

VDAC – voltage dependent anion channel

WGA – wheat germ agglutinin

WHO – World Health Organization

XBP1 – X-box binding protein 1

4-HNE – 4-hydroxynonenal

8-OHdG – 8-hydroxy-2' -deoxyguanosine

β-MHC – myosin heavy chain beta

# 4 Introduction

## 4.1 Obesity

### 4.1.1 Epidemiology

Obesity results from excessive caloric intake, surpassing the needs of the human body over the long term, which leads to increased body fat storage. It is assessed by means of the body mass index (BMI), for which the World Health Organization (WHO) has defined thresholds classifying the disease in 3 levels: overweight, obesity and massive obesity (World Health Organization, 2021). Being overweight corresponds to a BMI between 25 and 30 kg/m$^2$, obesity corresponds to a BMI between 30 kg/m$^2$ and 40 kg/m$^2$, and massive obesity corresponds to a BMI exceeding 40 kg/m$^2$ (World Health Organization, 2021).

In 1997, the WHO classified obesity as a chronic disease, and defined overweight and obesity as ‘abnormal or excessive fat accumulation that presents a risk to health’. Its prevention is a public health problem in developed countries.

According to the WHO, from 1975 to 2016, the prevalence of overweight or obese children and adolescents aged 5–19 years increased more than four-fold from 4% to 18% globally, while in 2016 39% of adults aged 18 years and over were overweight and 13% obese. In total, over 1.9 billion adults aged 18 years and more were overweight and over 650 million obese. While obesity remains preventable, it is the leading public health problem in developed countries, with its associated diseases being leading causes of death in the western world (World Health Organization, 2021).

### 4.1.2 Etiology

The development of obesity underlies a multifactorial process, reaching from the amount of caloric intake and physical activity to genetic predispositions (Gadde et al., 2018). Even if the genetic background is likely to favour the development of obesity, it has been clearly shown that the rapid changes in eating habits and the promotion of sedentary activities in the last century have both contributed significantly to this increase in prevalence. Overall, we distinguish the constitutive stage of obesity where few

complications are observed and "disease obesity" which is accompanied by multiple complications. From a metabolic point of view, obesity is most often associated with insulin resistance, a stage which precedes the onset of type 2 diabetes. This insulin resistance is linked to the infiltration of tissues, especially muscles, by lipids due to a permanent and increased flow of plasma free fatty acids into these tissues. These metabolic disturbances are usually accompanied by mitochondrial skeletal muscle dysfunction, which has recently been proposed as the main causative factor responsible for metabolic pathologies associated with obesity (Esser et al., 2014; Grundy, 2002; McCracken et al., 2018). However, while molecular insight into the development of obesity is increasing, more and more evidence shows that ROS are major players in this pathology.

### 4.1.3 Disease burden

About twenty-five years ago, it was thought that high-income countries were the ones most at risk for the obesity epidemic. In these high-income nations, an inverse connection was identified between obesity and socioeconomic position, particularly in women (Molarius et al., 2000). This was the case when looking at obesity rates. In contrast, the prevalence of obesity was found to be very low in low- and middle-income nations, and it was found almost exclusively among people with relatively high socioeconomic level. However, obesity had also become a problem in lower socioeconomic groups, particularly among women in middle-income countries (Monteiro et al., 2004). As of 2012, the link between socioeconomic position and obesity in low-income nations remained positive for both men and women. This was the case regardless of gender. However, when it came to children and teenagers, obesity remained primarily a concern in low- and middle-income countries that had populations with relatively high socioeconomic level (Seidell & Halberstadt, 2015).

Overweight and obesity are the major cause of economic expenditures to individuals and the government, as well as health issues. Consequently, overweight and obesity impose significant expenditures on the health care system and create difficulties for the labor and economy of a nation. According to a survey published by the McKinsey Global Institute, obesity costs the global economy two billion dollars in 2012. The value of these expenses, which were 2.8 percent of the world's gross domestic product, includes health

care costs, lost productivity, and additional costs incurred to mitigate the effects of this issue (Yusefzadeh et al., 2019).

### 4.1.4 Cardiovascular effects of obesity

#### 4.1.4.1 Coronary artery disease

Atherosclerosis remains one of the leading global causes of death, ranging from ischemic stroke to ischemic heart disease as well as peripheral arterial disease. It is characterized by fatty streaks developing in the arterial wall, gradually developing into plaques. A rupture of those plaques leads to an occlusion of an artery, causing the above stated pathologies. Several studies have shown connection between obesity and atherosclerotic risk factors (Chen et al., 2015; Wing et al., 2013). Those risk factors include diabetes mellitus type 2, systemic hypertension, dyslipidaemia as well as chronic kidney disease. In line, there is a clear observational association between adiposity and atherosclerosis. A meta-analysis of prospective observational studies of nearly 1 million adults has shown that an increasing BMI linearly correlates with an increase of ischemic heart disease mortality as well as stroke mortality (each 1 $kg/m^2$ above 25 $kg/m^2$ BMI increases mortality by approximately 8%) (Herrington et al., 2016; Whitlock et al., 2009). Thereby, obesity and atherosclerosis are both chronic inflammatory conditions (Ross, 1999).

The increased risk of atherosclerosis goes hand in hand with an increased risk of coronary artery disease, as obesity has been shown to accelerate the progression of coronary atherosclerosis (McGill Jr et al., 2002). Two decades of obesity has been identified as independent risk factor for coronary artery disease (Manson et al., 1990). While a progression of coronary atherosclerosis can for a long time remain asymptomatic, it will at some point lead to an acute coronary syndrome (ACS). The ACS is divided in unstable angina, non-ST segment elevation myocardial infarction (NSTEMI) and ST segment elevation myocardial infarction (STEMI). In relation, a higher BMI has been linked to early NSTEMI and STEMI development (Das et al., 2011; Madala et al., 2008).

#### 4.1.4.2 Hypertension

Several studies have demonstrated a correlation between increased blood pressure and weight gain (Jiang et al., 2016). It has been demonstrated that obese patients are 3.5 times more likely to have hypertension, while 60% of hypertension is linked to fat accumulation (Landsberg et al., 2013; Seravalle & Grassi, 2017). The distribution of visceral fat is partially influenced by hereditary variables that also contribute to the rise in blood pressure levels in obese persons (Pausova et al., 2002; Seravalle & Grassi, 2017). Environmental factors may also play a role in visceral fat distribution and blood pressure elevation. These include alcohol consumption, cigarette smoking, the timing of pediatric obesity start, changes in daily behavior and alterations in the lipid profile. All these factors have been linked with impaired insulin sensitivity, an inflammatory state, and endothelial dysfunction which may contribute to the onset and progression of atherosclerosis (Kotsis et al., 2010; Seravalle & Grassi, 2017).

Although antihypertensive drugs, such as RAS blockers, β-blockers, and diuretic therapies, especially at high doses, are appropriate for obese hypertension patients, they cause severe adverse effects, such as hyperglycemia, hyperlipidemia, and hyperuricemia. Therapeutic treatments to obesity caused by hypertension required the control of component obesity. The treatment of obesity necessitates guidelines recommending significant lifestyle alterations aimed at weight loss, such as consuming a low-calorie diet (Jiang et al., 2016). This may involve limiting salt intake, consuming less saturated fats and cholesterol, consuming more water, fruits, fresh and raw vegetables, fish, lean meats, whole grains, engaging in moderate and consistent physical activity, and getting enough sleep (Cuspidi et al., 2018).

#### 4.1.4.3 Cardiac arrythmias

Cardiac arrhythmias are present among people of all age. They can be caused by structural heart defects, however, they might also occur in structurally normal hearts. Atrial fibrillation (AF) is the most common cardiac arrhythmia and continues to rise globally (Hindricks et al., 2020). AF is associated with many cardiovascular factors like systemic hypertension, mitral valve stenosis, hypertrophic cardiomyopathy, coronary artery disease, as well as lung diseases such as pneumonia or pulmonary embolism.

The link between obesity and cardiac arrhythmias has also been described in several studies (Wang et al., 2004). Most of the time, patients have multiple risk factors for AF, however, most of these risk factors are often associated with obesity. While large epidemiological studies have observed an association between atrial fibrillation and obesity, it appeared to be caused by an enlargement of the left atrium (Karasoy et al., 2013; Stritzke et al., 2009), A multitude of mechanisms have been shown to explain the association between AF and obesity, with inflammation, diastolic impairment and pericardial fat accumulation playing a major role.

#### 4.1.4.4 Obesity cardiomyopathy

Obesity cardiomyopathy refers to cardiac structural and hemodynamic alterations that lead to congestive heart failure. Structural changes include left and right ventricular remodelling and hypertrophy, left atrial remodelling and aortic valve stenosis. These changes can lead to atrial fibrillation, left ventricular systolic dysfunction and/or diastolic dysfunction up to heart failure.

Heart failure is a clinical syndrome characterized by characteristic symptoms such as breathlessness, ankle swelling and fatigue that may be accompanied by additional symptoms (e.g. elevated jugular venous pressure, pulmonary crackles and peripheral oedema) caused by a structural and/or functional cardiac abnormality, resulting in reduced cardiac output and/ or elevated intracardiac pressures at rest or during stress (Ponikowski et al., 2016). Heart failure is one of the major causes of death worldwide, with a prevalence of approximately 3% which is still increasing (Mozaffarian et al., 2015; Ponikowski et al., 2016). While there are many risk factors for heart failure including coronary artery disease, systemic hypertension, atrial fibrillation and valvular heart disease, it is well established that obesity increases the risk of heart failure even in the absence of the stated risk factors (Baena-Díez et al., 2010; Kenchaiah et al., 2002).

While historically, heart failure was based on left ventricular ejection fraction (LVEF), we nowadays distinguish heart failure with reduced EF (<40%) (HFrEF) from heart failure with preserved EF (>50%) (HFpEF). In between is a grey area defined as mid-range EF (HFmEF) (Ponikowski et al., 2016). The symptoms of both HFrEF and HFpEF are similar, however, the differentiation is important due to different aetiologies as well as therapeutic approaches. Around half of the patients with heart failure have a preserved

ejection fraction, associated with a diastolic dysfunction. These patients are likely to have increased left ventricular wall thickness as signs of increased filling pressure. However, the other half of patients with heart failure have a reduced ejection fraction, characterized by systolic dysfunction as well as dilated left ventricles (Ponikowski et al., 2016). With both forms underlying different pathophysiological mechanisms, pharmacological treatments for HFrEF have failed to be beneficial in patients with HFpEF (Yancy et al., 2013). Nevertheless, there are also epidemiological differences between HFrEF and HFpEF. While HFpEF has been shown to be more prevalent in women, it is also closely correlated to obesity with an estimation of 85% of patients being obese (Garg et al., 2013; Owan et al., 2006). For patients with HFrEF, however, the obesity prevalence is lower than 50% (Carbone et al., 2017; Horwich et al., 2011). Nevertheless, the mechanisms of obesity cardiomyopathy remain unclear.

#### 4.1.4.5 Pulmonary hypertension and right heart disease

Pulmonary hypertension is a life-threatening condition of increased blood pressure in the pulmonary arteries, arising from obliterative changes in small to midsized pulmonary arterioles, associated with occlusive arteriopathy causing high resistance to blood flow and increased right ventricular pressure. Arising from a multitude of pathophysiological mechanisms, the condition can lead to a variety of symptoms like dyspnoea, tachycardia, lower extremity oedema, palpitations, syncope or chest pain. Pulmonary hypertension is defined by a mean pulmonary arterial pressure of over 25 mmHg (Nazzareno et al., 2016). The WHO divides pulmonary hypertension into 5 groups: idiopathic pulmonary arterial hypertension (Group I), pulmonary hypertension secondary to left heart disease (Group II), pulmonary hypertension due to lung disease, chronic hypoxia (Group III), chronic arterial obstruction (Group IV), pulmonary hypertension with unclear or multifactorial mechanisms (Group V) (Simonneau et al., 2009). The incidence of idiopathic (primary) pulmonary arterial hypertension is around 4-6/million worldwide, with females having a higher incidence (McGoon et al., 2013). Secondary forms of pulmonary hypertension, however, are far more common.

Several studies have shown an increased prevalence of obesity in pulmonary hypertensive patients (Friedman & Andrus, 2012; Taraseviciute & Voelkel, 2006; Weatherald et al., 2018). Obesity might increase the risk of pulmonary hypertension

through the increased risk of heart disease, however, several possible direct effects of obesity on the development of pulmonary hypertension like local inflammation or oxidative stress are discussed (Aggarwal et al., 2013; Schinzari et al., 2017). A direct effect of pulmonary hypertension is right ventricular dysfunction induced by pressure overload in the right ventricle. Right ventricular dysfunction can underlie various other pathologies including ischemic heart disease, arrhythmias, valvular heart disease or sepsis. As obesity has been associated with right ventricular dysfunction, underlying mechanisms might be volume overload, increased ventricular pressure or even direct hormonal effects on the myocardium (Wong et al., 2006).

## 4.2 Reactive oxygen species and oxidative stress

### 4.2.1 Oxidative stress

Oxidative stress has been proposed as a potential mechanism linking obesity to cardiovascular disease (Ceriello & Motz, 2004). Although recent evidence suggests a causal role for oxidative stress in cardiovascular diseases, insulin resistance as well as atherosclerosis, the underlying mechanisms remain controversial. Whether oxidative stress is caused by obesity itself, as consequence of obesity-related conditions or both has not yet been elucidated. Several pathways associated with obesity like low grade inflammation, a procoagulatory state or higher ROS levels with increased lipid and protein oxidation might all act interchangeably (Van Gaal et al., 2006). ROS have been shown to play a major role in the development of cardiovascular diseases as well as micro- and macrovascular complications of the metabolic syndrome (Folli et al., 2011; Hutcheson & Rocic, 2012; Lassègue & Griendling, 2010). While oxidative stress is a hallmark of the metabolic syndrome, several studies have attempted to dissect the contribution of its individual components of the increased ROS production. Increased oxidative stress has been observed in obese children without other components of the metabolic syndrome (Hutcheson & Rocic, 2012; Montero et al., 2012). Also weight loss in patients with metabolic syndrome has been shown to decrease ROS load, however, an isolated attribution of ROS to obesity or other components of the metabolic syndrome has not been made to date (Hutcheson & Rocic, 2012; Rector et al., 2007).

However, oxidative stress has been demonstrated to be a major player in the development of insulin resistance (Houstis et al., 2006). Increased levels of ROS contributed to the development of insulin resistance in an obesity mouse model which was inhibited by ROS scavengers (Haber et al., 2003; Hildebrandt et al., 2004; Houstis et al., 2006). In support, overexpression of catalase in rats preserved insulin sensitivity in rodents fed a high fat diet (Anderson et al., 2009). A considerable attention has come to ROS induced β-cell damage. Indeed, an increased sensitivity to oxidative stress and apoptosis has been discussed in pancreatic β-cells, while glucose-dependent insulin secretion itself caused oxidative stress (Fridlyand & Philipson, 2004). However, while most evidence suggests a correlation between ROS levels and insulin sensitivity, others have shown that ROS are obligatory signals for glucose-induced insulin secretion (Leloup et al., 2009). In addition, causal evidence for the enhancement of insulin signalling by ROS in vivo has also been reported (Loh et al., 2009). Nevertheless, mechanistic insights into the processes connecting ROS to insulin resistance and obesity remain incomplete.

### 4.2.2 Types of ROS

The ground-state oxygen is a paramagnetic biradical with two unpaired electrons in its outer electron layer, occupying separate π orbitals with parallel spins. This type of electronic configuration is called 'triplet state'. In order to create a chemical bond, paired electrons need to have opposite spins, however, most of nonradical organic molecules have pairs of electrons with antiparallel spins. Three out of four electrons in this process will have parallel spins, meaning that only one bond with opposite spins can be produced. Consequently, oxygen can only accept one electron at a time during redox reactions. Nevertheless, this might be overcome by creating oxygen radicals. These radicals can potentially be harmful for the organism by leading to lipid peroxidation, protein denaturation and also DNA damage (Bartsch & Nair, 2006).

Singlet oxygen ($^1O_2$) is created when a triplet state oxygen molecule absorbs enough energy to reverse the spin of one of its electrons. Both electrons will have opposite spins while being in the same orbital or separate orbitals. It is the lowest excited state of an oxygen molecule. Since the spin restriction is removed, the oxidizing capacity of $^1O_2$ is higher compared to ground-state $O_2$. It is far more reactive towards organic compounds.

Since the electrons have opposite spins, the singlet oxygen is able to create chemical bonds with non-radical organic molecules having pairs of electrons with opposite spins. Superoxide anion ($O_2^-$) is produced by reduction of triplet oxygen by an electron, occurring widely in nature. The electron pairs with one of the triplet oxygen's free electrons in the π orbital, leading to a negative charge. It has both reductive and oxidant properties. The reactivity of superoxide is controversial, while some have reported superoxide as relatively reactive (Gülçin et al., 2010; Naqui et al., 1986), others claim it is not highly reactive (Nordberg & Arnér, 2001). Two major sources are responsible for superoxide production in biological systems: the mitochondrial respiratory chain as a by-product of respiration and the nicotinamide adenine dinucleotide phosphate oxidase (NADPH oxidase) as a key player in the immune defense system.
Hydroxyl radicals ($OH^-$) are produced by reducing $O_2$ with three electrons, leading to a bond break of the two oxygen molecules. It is a very reactive molecule with a high oxidative potential.

### 4.2.3 Sources of ROS and antioxidants

#### 4.2.3.1 NADPH oxidases

NADPH oxidases are transmembrane multiprotein enzyme complexes which reduce $O_2$ to $O_2^-$ (Lambeth, 2004). NADPH oxidases were first discovered in neutrophils, where they are responsible for the respiratory burst. Their central part is the transmembrane cytochrome b558 which is composed of the catalytic subunit gp91phox, now termed NOX2, and the essential protein p22phox, and the regulatory subunits p40phox, p47phox and p67phox as well as the GTPase Rac (Babior et al., 2002; Hordijk, 2006; Nauseef, 2004; Segal & JONES, 1978; Vignais, 2002). Upon stimulation, the cytosolic subunits translocate to the membrane. p47phox is phosphorylated which leads to a conformational change allowing an interaction with p22phox and electron transfer from NADPH to extracellular $O_2$ (Sumimoto et al., 1996).
The electron transfer happens in a series of actions involving the C-terminal cytosolic flavin adenin dinucleotide (FAD) and two transmembrane hemes. First, two electrons are transferred from NADPH to FAD, which has a higher affinity to NADPH than NADH (Clark et al., 1987; Nisimoto et al., 1999). Then, one electron is transferred from $FADH_2$ to the iron centre of the inner heme. Since the heme can only accept one electron at a

time, the first electron needs to be transferred to the outer heme before FADH can transfer its electron. While the transfer of both electrons to the inner heme is energetically favourable, the transfer to the outer heme is not. Therefore, $O_2$ must be bound to the outer heme in order to accept the electron (Cross & Segal, 2004; Doussière et al., 1996). The NOX2 gene is located on the X-chromosome (Bedard & Krause, 2007). In phagocytes, NOX2 is highly glycosylated whereas this is not the case in most non-phagocytic cells (Bedard & Krause, 2007).

NOX2 has initially been thought to be specific for phagocytic cells. However, NOX2 expression has subsequently been identified in various other cell types including cardiomyocytes (Bendall et al., 2002; Krijnen et al., 2003), adipocytes (Furukawa et al., 2017), pancreatic islet cells (Rebelato et al., 2012), endothelial cells (Buul et al., 2005; Gorlach et al., 2000; Petry et al., 2006), and more (Bedard & Krause, 2007).

Over time, six additional NOX2 homologues have been discovered. NOX1, NOX3, NOX4 and NOX5, which is not expressed in rodents, are closer related to NOX2 than the dual oxidases DUOX1 and DUOX2. In addition to the structure, also the activation mechanisms vary between the family members.

NOX1 was the first homologue to be discovered, which has a ~60% amino acid identity with NOX2 (Bánfi et al., 2003; Suh et al., 1999) and conserved FAD and heme binding sites (Bataller et al., 2003). The NOX1 gene is located on the X-chromosome, and evidence suggests a molecular mass of 55-60 kDa. NOX1 activation requires p22phox and is preferentially regulated by NOXO1 and NOXA1, although it can also interact with p47phox and p67phox (Ambasta et al., 2004; Bánfi et al., 2003). While NOX1 mRNA is most abundantly expressed in colon epithelium (Bánfi et al., 2003; Szanto et al., 2005), it is also expressed in many other cell types. Those include vascular smooth muscle cells (Lassègue et al., 2001), endothelial cells (Ago et al., 2005), cardiomyocytes (Matsuno et al., 2012), prostate (Suh et al., 1999), hepatocytes (Bertram et al., 2015) and many more (Bedard & Krause, 2007).

NOX3 was discovered in 2000 shortly after NOX1 (Paffenholz et al., 2004). It has a ~56% amino acid identity with NOX2 and the human gene is located on chromosome 6. While the NOX3-p22phox complex has constitutive NADPH oxidase activity, the presence of p47phox, p67phox or NOXA1 and Rac1 enhances the production of superoxide. When p47phox is replaced with NOXO1, Rac1 becomes dispensable for the full activation of the NOX3 complex (Miyano & Sumimoto, 2007; Ueno et al., 2005; Ueyama et al., 2006). The highest expression of NOX3 is found in the inner ear (Bánfi

et al., 2004) although low levels can also be detected in fetal tissues (Bedard & Krause, 2007; Cheng et al., 2001; Kikuchi et al., 2000). NOX3 is involved in the biogenesis of otoconia/otolith, which are crystalline structures of the inner ear involved in the perception of gravity (Bánfi et al., 2004).

NOX4 has first been described in the kidney and only shares ~39% amino acid identity with NOX2 (Geiszt et al., 2000; Shiose et al., 2001). The gene is located on chromosome 11. Evidence suggests that NOX4 mainly produces $H_2O_2$ (Chen et al., 2008). The highest expression of NOX4 is found in the kidneys, although it has been detected in many other tissues including cardiomyocytes (Brewer et al., 2011), endothelial cells (Petry et al., 2006), thyroid tissue (Weyemi et al., 2010), neurons (Vallet et al., 2005), hepatocytes(Sancho et al., 2012), melanoma cells (Brar et al., 2002), haematopoietic stem cells (Piccoli et al., 2005) and more (Bedard & Krause, 2007). NOX4 is dependent on and stabilized by p22phox (Ambasta et al., 2004). However NOX4 does not require Rac nor cytosolic subunits for its activity (Martyn et al., 2006).

NOX5 is the most recently characterized subunit and was first described in 2001 by two groups simultaneously (Bánfi et al., 2001; Cheng et al., 2001). It is a 85kDa protein, which has nearly identical FAD and heme-binding sites to NOX2 (Biberstine-Kinkade et al., 2001; Cheng et al., 2001). However, there are some features that distinguish NOX5 from the other homologues. The gene is absent in rodents. NOX5 has four EF hands to allow $Ca^{2+}$ binding which is required for enzyme activation. NOX5 is not N-glycosylated and does not require p22phox nor other subunits for its activation. NOX5 activation involves conformational changes. It is the only isoform which has been crystalized (Bedard et al., 2012; Magnani et al., 2017; Touyz et al., 2019). NOX5 mRNA is expressed in various cells including endothelial cells (BelAiba et al., 2007), smooth muscle cells (Jay et al., 2008), cardiomyocytes (Dworakowski et al., 2006), and others (Bánfi et al., 2001; Cheng et al., 2001; Salles et al., 2005).

#### 4.2.3.2 Mitochondrial ROS

The electron transport chain is located in the inner membrane of the mitochondria, consisting of the transmembrane complexes I to IV as well as the electron transporters cytochrome c and ubiquinone. Energy gained through a chain of enzymatic electron transfers is used to pump $H^+$ through the inner mitochondrial membrane, creating a

gradient leading to ATP production by ATP synthase (complex V) (Junge & Nelson, 2015).

Complex I, also called NADH ubiquinone oxidoreductase, is composed of a flavin mononucleotide molecule (FMN) and an iron-sulfur (FeS) containing protein. FMN can accept two electrons from NADH, passing them through the intermediate of Fe-S-clusters to ubiquinone (Q) and reducing it to ubiquinol ($QH_2$). Ubiquinol then freely diffuses within the membrane. The continuous oxidation and reduction throughout the complex lead to a transport of four protons into the intermembrane space. Premature electron leakage to oxygen makes complex I a main site of ROS production (Turrens, 2003).

Complex II, also called succinate dehydrogenase, is composed of four subunits and oxidises succinate to fumarate by reducing FAD to $FADH_2$ (Bezawork-Geleta et al., 2017; Sun et al., 2005). Then, similar to complex I, the electrons are transferred to ubiquinone by the intermediate of the FeS-cluster. However, no protons are transported into the intermembrane space in this process. As part of the Krebs cycle, complex I connects metabolism and oxidative phosphorylation (Cecchini, 2003). Ubiquinone connects both complex I and II to complex III. It is lipid soluble and moves freely in the mitochondrial membrane, delivering electrons to complex III.

Complex III, referred to as cytochrome bc1 complex, transports electrons from $QH_2$ to cytochrome c. The complex is composed of a cytochrome b, 2 Fe-2S centres wrapped by a FeS protein and cytochrome c1 (Yang & Trumpower, 1986). There are two CoQ binding cites at the cytochrome b ends: one for $QH_2$ (Q0) and one for QH- (Qi) (Gao et al., 2003). In a series of transfers through the different components of complex III, electrons are moved from QH2 to cytochrome c in a process called Q-cycle. This process leads to transfer of protons into the intermembrane space (Mitchell, 1976).

Complex IV moves four electrons from four cytochrome c molecules to two $O_2$ molecules creating two $H_2O$ molecules. During this process, eight protons are moved into the intermembrane space, enhancing the $H^+$ gradient. The transmembrane electrochemical gradient of protons (Δμm), composed of an electrical (Δψm) and chemical (ΔpH) potential, is used by the F1F0 ATP synthase (complex V) to convert ADP and Pi to ATP in a process called oxidative phosphorylation (Mailloux, 2015).

Mitochondria are considered as main cellular ROS producers (Turrens, 2003). Around 1% of the electrons in the electron transfer chain leak under physiological conditions, reacting with oxygen and producing superoxide and hydrogen peroxide (Cadenas &

Davies, 2000). The transfer of electrons between prosthetic groups arises through a process called tunneling, which is influenced by the distance between the groups and difference in redox potential (Nicholls & Ferguson, 2002). The leakage of an electron in the electron transport chain is closely correlated to the same factors (Klinman, 2007). In mammals, 11 sites of $O_2^-$ and $H_2O_2$ have been discovered (Brand, 2016). Two different subgroups have been recognized depending on the source of the redox potential for producing $O_2^-$: the NADH/NAD group and the $QH_2$/Q group. The first one is composed of 4 enzymes: Complex I, generating only $O_2^-$, pyruvate dehydrogenase (PDH), branched-chain α-ketoacid dehydrogenase (BCKDH) and branched-chain octopine dehydrogenase (ODH) which all generate both $O_2$- and $H_2O_2$ (Starkov et al., 2004). On the other hand, the $QH_2$/Q isopotential group relies mostly on complex I, II, and III for reactive oxygen species production (Goncalves et al., 2014).

#### 4.2.3.3 Other cellular sources of ROS

Next to NADPH oxidases and the mitochondria, there are numerous other cytosolic or cell-organelle-bound sources of ROS. The xanthine oxidase for example, is acting as catalyst for the oxidation of hypoxanthine and xanthine in purine metabolism, leading to $O_2$- formation (Hille & Nishino, 1995). Other prominent examples are peroxisomes, lysosomes, lipoxygenases, cyclo-oxygenases, or nitric oxide synthases.

#### 4.2.3.4 Antioxidant systems

Antioxidant systems can be classified into enzymatic and non-enzymatic ROS scavengers. The main enzymatic scavengers are the superoxide dismutases (SOD), catalase (CAT), glutathione peroxidase (GTPx) and thioredoxin (TRX).
Superoxide dismutases are metalloproteins acting as oxidoreductases which catalyse the dismutation of superoxide anions $O_2$- into oxygen $O_2$ and hydrogen peroxide $H_2O_2$: $2\ O_2\text{-} + 2\ H^+ \longrightarrow O_2 + H_2O_2$. SODs belong to a multigene enzyme family composed of 3 different forms (Birben et al., 2012). The CuZn-SOD or SOD1 was the first one to be discovered and it is found in intracellular cytoplasmatic places. The Mn-SOD or SOD2 is localized in the mitochondrial matrix while the EC-SOD or SOD3 is primarily localized in the extracellular matrix. Since superoxide is the most abundantly produced ROS,

SODs play a crucial role in the cells' antioxidant defences (Birben et al., 2012; Mruk et al., 2002).

$H_2O_2$ is a harmful by-product of many physiological processes, produced for instance by SODs and other oxidases like xanthine oxidase, which is then reduced to $H_2O$ by catalase: $2\ H_2O_2 \longrightarrow O_2 + 2\ H_2O$. Catalase is a tetramer of four polypeptide chains located in the peroxisome. It contains four iron-containing heme groups that allow the enzyme to react with hydrogen peroxide (Birben et al., 2012; Fita & Rossmann, 1985).

The glutathione peroxidase (GTPx) was discovered in red blood cells. It not only catalyses the reduction of hydrogen peroxide to water and oxygen, but also the reduction of peroxide radicals to alcohols and oxygen (Wendel, 1981). It is a family of tetrameric enzymes localized in the cytosolic part of the cell. Seven different GTPxs have been identified in rodents and humans, some of them contain cysteine, others selenocysteine in their active site (Birben et al., 2012).

Non-enzymatic ROS scavengers include vitamin C, vitamin E, β-carotene and glutathione.

## 4.3 ROS and obesity

### 4.3.1 ROS and metabolic dysfunction

ROS are strongly linked to obesity and, thus, metabolic syndrome. Clinical and animal studies consistently implicate oxidative stress as the underlying mechanism mediating obesity- and diabetes-related health problems (Furukawa et al., 2017). Recent data suggest, that oxidative stress may be an early event in the pathophysiology of these chronic diseases, as opposed to being a result or innocent bystander (Roberts & Sindhu, 2009). The metabolic syndrome is a cluster of several medical conditions including insulin resistance, visceral obesity, hypertension and dyslipidaemia. Although it is generally accepted that insulin resistance is the primary pathogenic mechanism underlying the first level of metabolic changes in patients with metabolic syndrome, evidence has emerged demonstrating a close relationship between the metabolic syndrome, a state of chronic low level inflammation, and oxidative stress as second level abnormalities (Wellen & Hotamisligil, 2005).

Oxidative stress has been closely linked to insulin resistance. For example, $H_2O_2$ has been shown to induce glucose uptake in muscle and adipocytes, but also stimulates lipid synthesis and GLUT4 translocation in adipocytes (Bonomini et al., 2015; Higaki et al., 2008; May & de Haen, 1979). In animal models of obese mice, an increased $H_2O_2$ generation by adipose tissue has been shown to precede diabetes onset and concomitantly decreased mRNA levels of SOD, catalase, and glutathione peroxidase (Bonomini et al., 2015; Furukawa et al., 2017). The implications of ROS in human insulin resistance have been evidenced in several human studies as well (Campia et al., 2012). The metabolic activity of visceral fat tissue is an important mediator of obesity-related disease and thus metabolic syndrome. This metabolic activity consists of systemic oxidative stress and inflammation. Several studies have demonstrated that increased visceral adiposity increases systemic oxidative stress (Bonomini et al., 2015; Fujita et al., 2006).

Oxidative stress has been demonstrated to be caused by and to be a causative factor in the development of hypertension. Patients with hypertension have defective endogenous and exogenous anti-oxidant response, elevated plasma oxidative stress, and a dysregulated ROS production in response to various stimuli (Russo et al., 1998; Tse et al., 1994). Several neurohormonal systems, such as the renin-angiotensin-aldosterone system and the sympathetic nervous system, also contribute to oxidative stress, inflammation, and vascular immune dysfunctions (Bonomini et al., 2015). Increased oxidative stress, inflammation, and autoimmune vascular dysfunction in hypertension are the result of increased ROS production, an exaggerated sensitivity to ROS, and diminished antioxidant reserve (Bonomini et al., 2015; Dhalla et al., 2000; Tse et al., 1994).

Dyslipidaemia as a part of the metabolic syndrome has long been linked to insulin resistance as a causative factor. However, dyslipidaemias have been independently linked to oxidative stress. In an animal model, LDL receptor-deficient mice fed a diet rich in cholesterol had elevated LDL levels and oxidative stress (De Oliveira et al., 2011). In humans, several studies show a relationship between low HDL or high triglyceride levels and high oxidative stress, regardless of age, gender, or the existence of other components of the metabolic syndrome (Bonomini et al., 2015; Marques de Mattos et al., 2012; Zelzer et al., 2011).

### 4.3.2 ROS and cardiovascular disease

Atherosclerosis is a common precursor of cardiovascular diseases and is associated with endothelial dysfunction, excessive vascular inflammation, subendothelial lipoprotein retention and vascular remodelling. Several sources of ROS like NADPH oxidases and mitochondria as well as ROS-scavenging systems have been intensively investigated in the development of atherosclerosis.

The role of different NADPH oxidase isoforms in the development of atherosclerosis remains controversial. Animal models have shown that NOX1 deficient ApoE-/- mice were protected against hyperlipidaemia and vascular remodelling after high fat diet and even western diet (Forrester et al., 2018; Sobey et al., 2015). Similar results have been shown for NOX2 (Forrester et al., 2018; Judkins et al., 2010). Also NOX2 has been suggested to regulate oxLDL plasma levels (Cominacini et al., 2000). Recent data suggest that NOX4 can both act protective with regard to the development of atherosclerosis, as well as having a promoting effect. Some studies have shown that NOX4 promotes plaque instability and progression, while others showed a protective effect on plaque formation (Forrester et al., 2018).

Mitochondrial ROS production plays a significant role in atherosclerotic lesion pathogenesis. It has been shown to cause lesion progression and vascular complications in various human and animal studies (Forrester et al., 2018). However, the exact roles of the various ROS producing compounds in mitochondria still need further elucidation.

Similar to ROS production inhibition, ROS scavenging has been shown to protect against lesion development (Forrester et al., 2018).

Despite the amount of data demonstrating that reactive oxygen species have a causal role in atherosclerosis, mechanistic information on metabolic control and its function in ROS signaling are unclear.

## 4.4 Other stress pathways associated with obesity

### 4.4.1 ER stress and the UPR

The endoplasmic reticulum is the compartment through which secreted proteins must pass in order to reach their target (Palade, 1956). Proteins undergo a quality control which will lead either towards degradation in case of bad conformation, or to secretion to the Golgi body (Ellgaard & Helenius, 2003). The accumulation of unfolded proteins in the lumen of the endoplasmic reticulum leads to a process called unfolded protein response (UPR), which is started by the activation of three transmembrane proteins in the endoplasmic reticulum: PERK (PKR-like ER protein kinase), ATF6 (activating transcription factor 6) and IRE-1 (inositol requiring enzyme 1), and aims to increase the folding, maturing and degradation capacity of the endoplasmic reticulum. The UPR is a physiological response that plays a major role in cells with high secretory capacity like plasma cells or β-cells of the pancreas, but also in many stress responses like fat overload. Alterations in its quality or in its intensity are at the origin of many human pathologies such as certain types of diabetes or neurodegenerative diseases (Papa, 2012; Scheper & Hoozemans, 2015).

The purpose of the UPR response is to: (1) slow down overall protein synthesis to prevent the entry of other proteins into the ER lumen; (2) synthesize new chaperones to stimulate the folding process; (3) lead to the degradation of bad folded proteins; (4) trigger apoptosis if the previous processes fail (Hetz et al., 2020).

The translational response, via the PERK pathway activation is the first one that implements. It slows down the protein synthesis, by translation inhibition through PERK dimerization and autophosphorylation, to avoid additional influx of proteins in the ER. The protein thus activated phosphorylates the α-subunit of translation initiation factor eiF-2 (eukaryotic translation initiation factor 2) on the residue Ser51 preventing the formation of the pre-initiation complex translation and therefore the interaction of mRNAs with the 40S ribosome subunit (Harding et al., 1999). While mRNA translation is stopped for most of the proteins, ATF4 (activating transcription factor 4) protein synthesis is increased (Harding et al., 2000). AFT4 is involved in the activation of the apoptotic pathway by inducing the expression of the protein CHOP (CEBP homologous protein).

Next to the translational response, there also is a transcriptional response to stress of the ER activating a set of genes coding for chaperones as well as for other factors involved in protein degradation. This response is conveyed by the ATF6 and IRE1 proteins. During ER stress, the dissociation of BiP / GRP78 from ATF6 causes the latter to migrate from the ER to the Golgi where it undergoes double proteolytic cleavage by the proteases S1P and S2P (Ye et al., 2000). The amino-terminal domain of ATF6 then migrates to the nucleus to bind on ERSE sequences (ER stress response element). These sequences are present in the promoters of genes coding for major proteins in the endoplasmic reticulum such as the chaperones BiP / GRP78 and GRP94 (glucose regulated protein 78 and 94) which play a major role in protein folding, and protein disulfide isomerase (PDI) which catalyses the formation of disulfide bridges (Yoshida et al., 1998; Zhu & Lee, 2015). Activation of ATF6 thus increases the folding capacities of proteins in the ER. The dissociation of BiP / GRP78 causes oligomerization and induction of kinase activity of IRE1. The activated IRE1 leads to splicing of a transcription factor called XBP-1 (X-box binding protein 1) mRNA, making its translation possible. The XBP-1 then binds to ERSE sequences of promoters of targets of the UPR response. XBP-1 mainly activates the transcription of genes encoding the enzymes involved in the ERAD (endoplasmic-reticulum-associated protein) degradation pathway (Lee et al., 2003).

If all efforts to eliminate the excess unfolded proteins from the cell fail, the UPR leads to apoptosis, induced by the ER via three mechanisms. One of them involves CHOP which, by inhibiting the expression of Bcl2, promotes apoptosis of the cell (Szegezdi et al., 2006). The second involves the proapoptotic proteins Bak and Bax which undergo a conformational change during ER stress leading to an efflux of $Ca^{2+}$ in the cytosol which activates the $Ca^{2+}$-dependent protease m-calpain which in turn cleaves and activates procaspase 12. Caspase 12 induces an activation cascade of the caspase pathway leading to apoptosis via the effector caspases 3 and 7 (Szegezdi et al., 2003; Szegezdi et al., 2006). Finally, IRE-1, by forming a heterotrimeric complex with TRAF-2 and ASK-1 (apoptosis signal regulating kinase 1), activates c-Jun kinase (JNK) resulting in apoptosis (Chen & Brandizzi, 2013; Szegezdi et al., 2006).

While it has been shown that the UPR plays a major role in the development of dietary induced insulin resistance by mediating pancreatic β-cell apoptosis, it also plays an important role in insulin sensitive peripheral tissues like adipose tissue or skeletal muscle, thus having a pivotal role in the development of diabetes mellitus type II (DMII)

(Boden et al., 2008; Samuel & Shulman, 2012; Schenk et al., 2008; Song et al., 2008). ER-stress has also been shown to be either a cause or a consequence of cardiovascular diseases (Ren et al., 2021).

### 4.4.2 Apoptosis

Apoptosis is a form of programmed cell death which is triggered by different forms of cellular stress by ROS, hypoxia, lack of nutrients or accumulation of unfolded proteins to name a few. A highly regulated cascade of molecular events leads to apoptosis which is initiated by either the intrinsic or extrinsic pathway. Both pathways, by different signalling cascades, lead to an activation of initiator caspases, finally activating the executioner caspases (caspase 3 and caspase 7), which degrade the cells' proteins. Caspases are cysteine proteases that specifically hydrolyse their substrate at the C-terminus of an aspartate residue. They are translated as inactive pro-caspases, which need to undergo a pro-domain cleavage for their activation.

The extrinsic pathway is triggered by a signal outside the cell, involving transmembrane receptor-mediated interactions. Signalling proteins bind to so-called death receptors, members of the tumor necrosis factor (TNF) receptor gene superfamily, on the cell surface of the target protein (Locksley et al., 2001). They have an extracellular death domain, which transmits the death signal from outside to inside the cell. FasL/FasR, TNF-α/TNFR1 or Apo3L/DR3 are some examples of death domains (Ashkenazi & Dixit, 1998). For instance, the activation of FasR by its ligand leads to oligomerization and recruitment of a complex called DISC (Death-Inducing Signalling Complex) which is composed of the adapter molecules FADD (Fas Associated Death Domain) and the initiator procaspases 8 and 10. FADD binds via its own death domain (DD) to the DDs of Fas receptors by homotypic electrostatic bonds. After death domain (DD) aggregation, the receptor complex is internalized via the cellular endosomal machinery, allowing the adaptor molecule FADD to bind the death domain of Fas through its own death domain (Huang et al., 1996). FADD also contains a death effector domain (DED) which, through hydrophobic homotypic bonds, allows the recruitment of initiating caspases. The formation of this complex leads to the autocatalytic activation of caspase 8 which is then released into the cytosol in an active dimeric form (Kischkel et al., 1995). This allows the sequential activation of effector caspases, including caspase 3. The

initiator caspase 8 can activate the intrinsic pathway via the cleavage of the Bid protein and thus amplify the apoptotic signal.

As opposed to the extrinsic pathway, the intrinsic pathway of apoptosis is usually induced by signals internal to the cell involving non-receptor-mediated stimuli. The activation of this pathway relies mainly on the formation of permeability transition pores in the mitochondrial membrane by the opening of the PTPC (Permeability Transition Pore Complex), a multiprotein complex at the mitochondrial inner membrane. These pores are oligo-protein channels formed at the level of the outer membrane by the Voltage Dependent Anion Channel (VDAC) and on the inner membrane by the Adenine Nucleotide Translocator (ANT). This activation phase is accompanied by a decrease in the mitochondrial transmembrane potential, followed by the swelling of the mitochondrial matrix and an interruption in aerobic energy metabolism and oxidative stress. According to the models, there is rupture or opening of the mitochondria, releasing two groups of pro-apoptotic proteins in the cytosol (Saelens et al., 2004). Cytochrome c, Smac/DIABLO, and the serine protease HtrA2/Omi belong to the first group, activating the caspase-dependent pathway by interaction with Apaf-1 and caspase 9 to form a complex called apoptosome (Du et al., 2000; Hill et al., 2004). The second group consists of AIF, endonuclease G and CAD mainly causing DNA fragmentation (Joza et al., 2001). The regulation of this process is described to be under the control of complex and dynamic interactions between the pro- and anti-apoptotic members of the Bcl-2 family (Cory & Adams, 2002). The anti-apoptotic members (Bcl-2, Bcl-xL, Mcl-1) form heterodimers with the pro-apoptotic members Bax and Bak, counteract their activity and allow the stability of the mitochondria. When the mitochondria are activated, for example during an activation of FasR and through Bid, the latter interacts and directly activates Bax and Bak. This induces the loss of interaction between Bax, Bak and the anti-apoptotic members of the Bcl-2 family, their oligomerization, the formation of pores and the release of mitochondrial proteins. Once they have become cytosolic, mitochondrial pro-apoptotic factors will have specific targets and effects. However, most mechanisms have not been completely elucidated and still need further investigation (Adams & Cory, 1998; Chipuk et al., 2010; Reed, 1998).

Both the intrinsic and extrinsic pathway end in the execution pathway, led by the activation of effector caspases 3, 6 and 7. Caspase 3, the most important one is activated by initiator caspases and activates the endonuclease CAD. CAD then leads to

DNA fragmentation and chromatin condensation. Caspase 3 is also responsible for reorganization of the cell into apoptotic bodies (Porter & Jänicke, 1999).

### 4.4.3 Inflammation

It has been established that adipose tissue not only plays a role as storage, but also has an endocrine function by secreting adipokines (Ronti et al., 2006). These are cytokines produced by the adipose tissue like leptin, adiponectin, interleukin-6, TNF-α or plasminogen activator inhibitor 1 (PAI-1). Adipokines have emerged as crucial mediators in the development of cardiovascular diseases (Lau et al., 2017). A disruption of the physiological balance between anti- and pro-inflammatory adipokines in favour of the latter, is a hallmark of a disrupted adipose tissue metabolism (Nakamura et al., 2014). In caloric restriction anti-inflammatory adipokines increase in comparison to pro-inflammatory ones, while in caloric excess and adipocyte expansion, pro-inflammatory adipokines take the lead. Adiponectin is probably the best known and most abundant anti-inflammatory adipokine in human serum. It has been shown to reduce inflammatory processes by blocking NF-κB activation and negatively regulating macrophage function (Yamaguchi et al., 2005; Yokota et al., 2000). Pro-inflammatory adipokines like leptin or resistin can enhance the production of several pro-inflammatory cytokines like TNF-α, IL-6, IL-12 or IL-18 (Loffreda et al., 1998). They are also associated with increased cardiovascular risk and atherosclerosis (Drolet et al., 2008; Hasan-Ali et al., 2011). Additionally, an increased production of adipokines leads to an excess of unfolded proteins potentially leading to endoplasmic reticulum stress activating the unfolded protein response (Zha & Zhou, 2012).

It has been well accepted that obesity causes low grade inflammation not only by its cytokine activity, but also through a cellular component. Hypercaloric food intake leads to adipose tissue hyperplasia as well as hypertrophy (Spalding et al., 2008). This may lead to decreased vascularization subsequently leading to local hypoxia, which in turn promotes adipocyte apoptosis as well as macrophage recruitment (Chinetti-Gbaguidi & Staels, 2011; Pasarica et al., 2009). In line, studies have shown an accumulation of macrophages in adipose tissue around apoptotic adipocytes, forming stereotypic crown-like structures (Cinti et al., 2005; Lee, 2013). While macrophage recruitment has been associated with increased levels of MCP-1, they secrete various cytokines like TNF- α which are known to promote insulin resistance (Kanda et al., 2006). In both, insulin

resistance and obesity, the most prominent inflammation pathway comprising nuclear factor-κB (NF-κB) is activated, confirming the link between inflammation, obesity and diet induced insulin resistance (Juhan-Vague et al., 2003; Zeyda & Stulnig, 2009).

All in all, low grade inflammation caused by an excess fat storage has been associates with cardiovascular diseases (Ruiz-Núñez et al., 2016). However, considering the large number of adipokines, it is difficult to disentangle the exact pathogenetic mechanisms of low grade inflammation in cardiovascular disease.

In addition to a proinflammatory state, obesity is known to entail abnormalities in coagulation and fibrinolysis (De Pergola & Pannacciulli, 2002). There is a clear association between an elevated BMI and prothrombotic factors as well as impaired fibrinolysis, suggesting that obesity as a risk factor for cardiovascular diseases might be mediated in part by a prothrombotic state (Rosito et al., 2004). Several studies have highlighted the involvement of plasminogen activator inhibitor 1 (PAI-1) in this prothrombotic state (Landin et al., 1990; Loskutoff & Samad, 1998). An impaired fibrinolytic function, assessed by increased PAI-1 levels has been linked to elevated cardiovascular risk (Ridker et al., 1993). While obesity is part of the metabolic syndrome, insulin resistance might be a common pathway which could partly explain increased levels of thrombotic factors (Juhan-Vague et al., 1993). However, the low-grade inflammation is also associated with increased levels of PAI-1 as well as of other cytokines, supporting the theory that low grade inflammation also plays a role in the hypercoagulatory state of obesity.

# 5 Aims

Diet-induced obesity is a major thread to health in the Western world resulting in type 2 diabetes mellitus (T2DM), a proinflammatory state and diverse alterations of major organ functions including the cardiovascular system. Increased levels of reactive oxygen species (ROS), commonly termed oxidative stress, have been associated with obesity. Thus, ROS have been suggested to account for various obesity-induced organ dysfunctions although the exact underlying pathways have not been well elucidated.

The aim of this project is to evaluate the role of ROS-generating NADPH oxidases in the cardiovascular response to high fat diet induced obesity in vitro and in vivo.

Specifically, the following questions are addressed:

Which are the major sources of ROS in cardiomyocytes in response to the fatty acid palmitate?

Do NADPH oxidases affect the cardiovascular response to high fat diet?

Which molecular stress pathways are involved in the cardiovascular response to high fat diet and are they connected to NADPH oxidase activation?

Are cardiac miRNA profiles affected by a high fat diet?

Are cardiac miRNA profiles regulated by NADPH oxidases?

# 6 Materials and methods

## 6.1 Materials

### 6.1.1 Equipment

| Item | Product name | Company |
|---|---|---|
| Analytical balance | | Sartorius |
| Autoclave | KSG-116-2-ED KSG | KSG |
| Bunsen burner | Vulcan | Heraeus |
| Centrifuge 1 | Biofuge fresco | Heraeus |
| Centrifuge 2 | Biofuge stratos | Heraeus |
| Centrifuge 3 | Megafuge 1. OR | Heraeus |
| Deep-freezer (-80°C) 1 | Hera freeze | Heraeus |
| Deep-freezer (-80°C) 2 | | |
| Fluorescence microscope | IX50 | Olympus |
| Fluorescence microscope | Hg-Lamp U-RFL-T | Olympus |
| Fluorescence microscope | Camera Controller | Hamamatsu |
| Fluorescence microscope | Orbit | Improvision |
| Liquid-N2-Dewar | Locator 6 Plus | Thermolyne |
| Electron paramagnetic resonance | E-scan | Noxygen |
| Fridge (-20°C) | | Liebherr |
| Heating plate | CM1850 | Leica |
| Incubator 1 | | Heraeus |
| Incubator 2 | | WTC Binder |
| Isopropanol freezing box | | Thermofisher |
| Magnetic stirrer + heater | MR33001 | Heidolph |
| Microscope | HAL 100 | Zeiss |
| Mini-table-top-centrifuge | Capsulefuge PMC-060 | TOMY |
| Multifunction microplate reader | Tecan Safire | Tecan |
| pH Meter | pH 540 GLPU- | GLP WTW |

| | | |
|---|---|---|
| Shaker | Duomax 1030 IKA-Shaker MTS2 | Heidolph |
| Thermocycler | Rotor-Gene 6000 | Corbett |
| Water bath | Reax top | Heidolph |

### 6.1.2 Chemicals

| Compound | Company |
|---|---|
| Amidoblack | Roth |
| Bovine serum albumin (BSA) | Sigma |
| 1-hydroxy-methoxycarbonyl-2,2,5,5-tetramethyl-pyrrolidine hydrochloride (CMH) | Noxygen |
| Coumaric acid | Sigma |
| CYBR green qPCR mix | Thermofisher |
| 4’,6-diamidine-2-phenylindol (DAPI) | Invitrogen |
| Desferroxamine (DES) | Merck |
| Diethyldithiocarbamate (DETC) | Merck |
| Dihydroethidium (DHE) | Sigma |
| Dimethylsulfoxide (DMSO) | Roth |
| Ethanol | Merck |
| Ethidium bromide | Roth |
| Ethylene diamine tetraacetic acid (EDTA) | Roth |
| Formaldehyde 37% | Merck |
| Glycerol | Roth |
| Glycine | Roth |
| Hydrochloric acid | JT Baker |
| HEPES (4-(2-hydroxyethyl)-1-piperazineethanesulfonic acid) | Merck |
| Isopropanol | JT Baker |
| Luminol | Sigma |
| Lucigenin | Sigma |

| | |
|---|---|
| β –Mercaptoethanol | Roth |
| Methanol | Merck |
| Non-fat dry milk powder | Merck |
| Nitrocellulose membrane | BioRad |
| Nitrocellulose membrane | Fisher Scientific |
| PBS tablets | Gibco |
| PBS | |
| Protease inhibitor mix | Calbiochem |
| Ponceau S | Sigma |
| Rotiphorese Gel | Roth |
| SDS ultra pure | Roth |
| Sodium chloride | Roth |
| Sodium-Palmitate | Sigma |
| N,N,N',N'-Tetramethylethane-1,2-diamine (TEMED) | Roth |
| TBS | Sigma |
| Triton X-100 | Sigma |
| Tris | Roth |
| Tween 20 | |

### 6.1.3 Plastic ware

| Item | Company |
|---|---|
| Pipette tips (2, 5, 10, 25, 50 ml) | Sarstedt |
| Pipette filter tips (10,200, 1000 ul) | Sarstedt |
| Cell culture flasks (T75) | Greiner |
| Cell culture dish (6, 10 cm) | Sarstedt |
| Cell culture plates (6-, 12-, 96-well) | Greiner |
| Combi-tips | Sarstedt |
| Cryovials | Greiner |
| Falcon tubes (15 and 50 ml) | Sarstedt |
| Test tubes (1,5 and 2 ml) | Eppendorf |

| | |
|---|---|
| 8-well plate | Ibidi |

### 6.1.4 Primary antibodies

| Antibody | Company | Dilution |
|---|---|---|
| α-SMA | Agilent | 1:200 (IHC) |
| ATF4 | Abcam | 1:1000 |
| ATF6 | Cell Signaling | 1:1000 |
| β-actin | Santa Cruz | 1:1000 |
| BiP | Cell Signaling | |
| Caspase 3 | Cell Signaling | 1:1000 |
| Caspase 7 | Cell Signaling | 1:1000 |
| Caspase 12 | Cell Signaling | 1:1000 |
| HIF1α | Cell Signaling | 1:500 |
| NOX1 | Eurogentec | 1:1000 |
| NOX2 | Upstate | 1:1000 |
| NOX4 | Abcam | 1:1000 |
| p22phox | Abcam | 1:500 |
| p-eIF2α | Cell Signaling | 1:1000 |
| 4-HNE | Abcam | 1:1000 |
| 8-OHdG | Abcam | 1:200 (IHC) |

### 6.1.5 Secondary antibodies

| Antibody | Company | Dilution |
|---|---|---|
| Goat anti mouse HRP conjugated | Calbiochem | 1:10000 in 5% milk/TBST |
| Goat anti rabbit HRP conjugated | Calbiochem | 1:10000 in 5% milk/TBST |
| Rabbit anti goat HRP conjugated | Calbiochem | 1:10000 in 5% milk/TBST |
| Mouse IgG Alexa Fluor 488 | Invitrogen | 1:200 |
| Mouse IgG Alexa Fluor 594 | Invitrogen | 1:200 |
| Rabbit IgG Alexa Fluor 488 | Invitrogen | 1:200 |

| | | |
|---|---|---|
| Rabbit IgG Alexa Fluor 594 | Invitrogen | 1:200 |
| Goat IgG Alexa Fluor 488 | Invitrogen | 1:200 |
| Goat IgG Alexa Fluor 594 | Invitrogen | 1:200 |

### 6.1.6 Cell culture media and additives

| Item | Company |
|---|---|
| DMEM medium | Gibco |
| Epidermal growth factor 1 (EGF 1) | Invitrogen |
| Fetal calf serum (FCS) | Pan Biotech |
| HBSS | Gibco |
| Hydrocortisone | Sigma |
| MCDB 131-Medium | Gibco |
| L-arginine | Gibco |
| L-glutamine | PAA |
| Penicillin/streptomycin | Gibco |
| Phosphate buffered saline (PBS) | PAA |
| Trypsin-EDTA | Gibco |
| 2,3-Butanedione monoxime (BDM) | Sigma |

### 6.1.7 Kits

| Item | Company |
|---|---|
| Qiagen RNeasy Mini Kit | Qiagen |
| Qiagen Plasmid Maxi Kit | Qiagen |
| SuperScript$^{TM}$III Reverse Transcriptase | Invitrogen |
| Expand High FidelityPLUS PCR System | Roche |
| Phusion$^{TM}$ High-Fidelity DNA Polymerase | NewEngland Biolabs |

## 6.2 Methods

### 6.2.1 Animals

All mice were of genetic C57BL/ 6j background. Mice carrying a single point mutation in exon 5 of the Cyba gene (nmf333 mice), leading to the substitution of a tyrosine residue to histidine were originally obtained from Jackson Laboratories, Bar Harbor, MN (A.B6 $Tyr^{+}$- $Cyba^{nmf333}$/J). As previously described, while the p22phox protein is lost, mRNA levels are preserved (Petry et al., 2018). In all experiments, littermates from the same breeding pair were used as controls.

### 6.2.2 Animal model

At an age of 5-6 weeks, both wild type and nmf333 mice were divided into two groups. The first group was fed a normal chow diet (NFD), whereas the second group was fed a high fat diet (HFD) (reference E15741-34; ssniff Spezialdiäten, GmbH, Soest, Germany) for 20 weeks, where 60% of caloric intake came from fat. The high fat diet was constituted of 24.4% crude protein, 34.6% crude fat, 60% crude fibre, 5.5% crude ash, 0.1% starch, 9.4% sugar. All animal experiments were approved by the Regierung von Oberbayern (AZ 55.2.1.54-2532.94.2013).

### 6.2.3 Isolation of cardiomyocytes

Isolation of cardiomyocytes was performed as described (Kračun et al., 2020). In short, isolated murine hearts were washed and perfused with EDTA buffer (130 mM NaCl, 5 mM KCl, 0.5 mM $NaH_2PO_4$, 10 mM HEPES, 10 mM glucose, 10 mM BDM, 10 mM taurine, and 5 mM EDTA) and then with perfusion buffer (130 mM NaCl, 5 mM KCl, 0.5 mM $NaH_2PO_4$, 10 mM HEPES, 10 mM glucose, 10 mM BDM, 10 mM taurine, and 1 mM $MgCl_2$). The hearts were then digested with collagenase buffer (0.5 mg/ml collagenase 2, 0.5 mg/ml collagenase 4, and 0.05 mg/ml protease XIV). After the digestion, additional enzymatic reactions were stopped by adding perfusion buffer containing 5% FCS to the suspension. In a next step, undigested tissue was removed by passing the suspension through a 100 µm pore-size strainer. After sequential gravity settlement, myocytes were cultivated in DMEM medium supplemented with 10% FCS,

100 U/ml penicillin, 100 $\mu$g/ml streptomycin and 2,3-butanedione monoxime to prevent myocyte contractions.

### 6.2.4 Hemodynamic measurements

Hemodynamic measurements were performed as previously described (Kračun et al., 2020). In short, mice were anesthetized by isoflurane and the chest was shaved. Buprenorphine was administered for analgesia. Left (LVP) and right (RVP) ventricular systolic and diastolic pressure was determined hemodynamically by left transthoracic puncture. The measurements were performed with a 24G needle connected to a pressure amplifier (Isotec, Harvard Apparatus via Hugo Sachs Elektronik, March-Hugstetten) and recorded using HSE-HA HAEMODYN W software (Harvard Apparatus) for hemodynamic studies.

### 6.2.5 Echocardiography

Echocardiography was performed with a Vivid S6 Ultrasound System (General Electrics) and a 12i linear array transducer (12 MHz) as previously described (Kračun et al., 2020). Mice were anesthetized with an intraperitoneal injection of midazolam (4 mg/kg). The chest hair was shaved prior to measurement. Left ventricular end diastolic (LVEDD) and end systolic (LVESD) diameters and wall thicknesses were obtained from two-dimensional M-mode measurements in short axis view obtained from 3 separate cardiac cycles and then averaged. Left ventricular fractional shortening was derived using the equation FS = ((LVEDD-LVESD)/LVEDD)x100. Left ventricular ejection fraction was calculated using the Teichholz formula: EF (%) = 100 x (LVEDV – LVESV)/ LVEDV, with $LVEDV = (7 \times LVEDD^3)/(2.4 + LVEDD)$ and $LVESV = (7 \times LVESD^3)/(2.4 + LVESD)$.

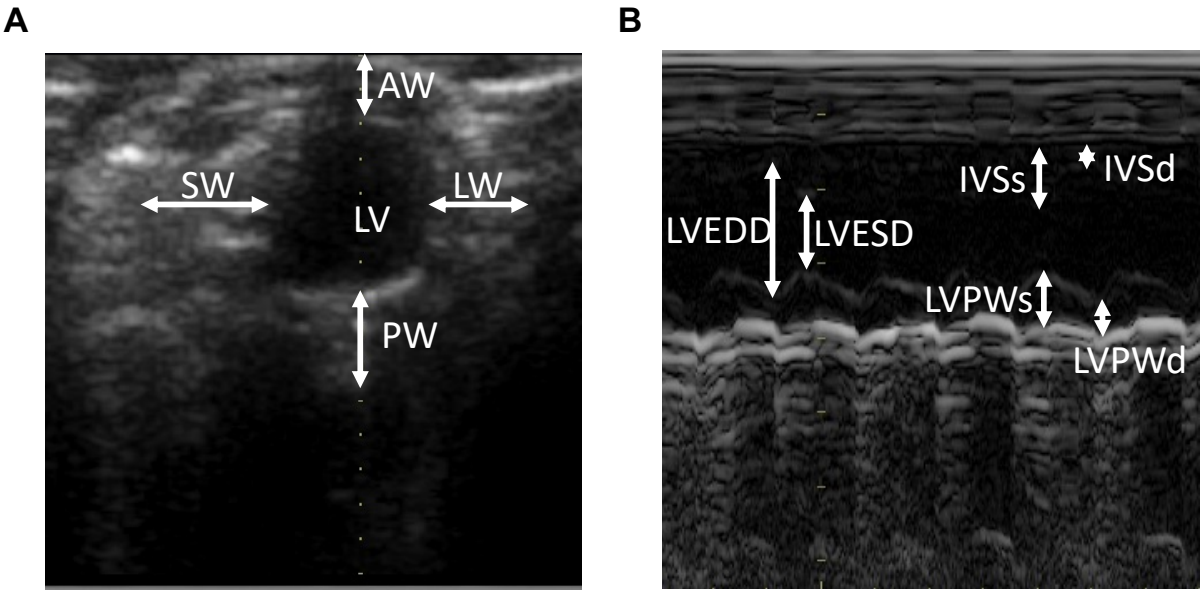


**Figure A. Representative echocardiography 2D images.** (A) Parasternal short axis view showing the left ventricular cavity (LV), the left ventricular anterior (AW) and posterior (PW) walls, the intraventricular septal wall (SW), and lateral wall (LW). (B) M-mode tracing with arrows indicating left ventricular end diastolic diameter (LVEDD), left ventricular end systolic diameter (LVESD), diastolic left ventricular posterior wall thickness (LVPWd), systolic left ventricular posterior wall thickness (LVPWs), diastolic intraventricular septum thickness (IVSd) and systolic intraventricular septum thickness (IVSs).

### 6.2.6 Cell culture

H9C2 cells were obtained from Prof. Moretti, Klinikum Rechts der Isar. They were maintained and grown in Dulbecco's modified Eagle's medium (DMEM) supplemented with 10% fetal calf serum (FCS), 100 U/ml penicillin and 100 µg/ml streptomycin. H9C2 cells are an immortalized myoblasts cell line derived from embryonic BDIX rat heart tissue (Kimes & Brandt, 1976). Experiments were performed with cells cultured in DMEM medium supplemented with 1% FCS. Cells were exposed to sodium-palmitate in different concentrations as indicated. H9C2 cells were maintained at 37 °C under the humidified atmosphere of 5% $CO_2$. Cells were placed in basal DMEM with 1% FCS without additives 16 h prior to stimulation.

### 6.2.7 Gene silencing

For gene silencing, H9C2 cells were transfected with short interfering RNAs (siRNA) as has been previously described (Kračun et al., 2020). In short, siRNA targeting p22phox

(SI03078523) was purchased from Qiagen. Negative control siRNA (5′-GACUACUGGUCGUUGAAGUdTdT-3′) was synthesized by Eurogentec.

### 6.2.8 Fatty acid stimulation

Sodium-palmitate (Sigma) was dissolved in 50% ethanol while stirring at 60°C to get a 200 mM sodium palmitate solution. It was then diluted 1:10 with a 20% bovine serum albumin in PBS solution of (20 mM).

### 6.2.9 Detection of hydrogen peroxide by Amplex Red assay

To detect the generation of hydrogen peroxide, a modified Amplex Red assay (Thermo Fisher) was used, as previously described (Kračun et al., 2020). In short, H9C2 cells grown on 96-well plates were incubated with 50 μM Amplex Red and 0.2 units/ml horseradish peroxidase for 15 min, followed by measurement of the $H_2O_2$-dependent oxidation of Amplex Red by fluorescence (excitation = 550 nm, emission = 590 nm) using a multiplate fluorescence reader (Tecan).

### 6.2.10 Wheat germ agglutinin staining

Hearts were fixed in a 10% formalin solution for 48 h, embedded in paraffin (FFPE) and sectioned at 2.5 μm thickness. To assess cardiomyocyte size in the right (RV) and left (LV) ventricle, FFPE cardiac tissue sections were stained with rhodamine-coupled wheat germ agglutinin (WGA; Biozol) to mark cell boundaries. For each heart, the cross sectional area of 15 longitudinally oriented cardiomyocytes, were measured in four high power fields with 40x magnification using a fluorescence microscope (OLYMPUS) and analysed with cellSens Dimension imaging software (OLYMPUS).

### 6.2.11 Immunohistochemistry

Lungs and hearts were fixed in a 10% formalin solution for 48 h, embedded in paraffin (FFPE) and sectioned at 2.5 μm thickness. Heat-induced antigen retrieval was performed at pH 8.0 for 20 min. Sections were blocked in 3% BSA in PBS to block non-specific sites. The sections were incubated with the primary antibody at a dilution factor

of 1:1000 overnight at 4.0°C. A mouse α-smooth-muscle actin antibody (α–SMA, Agilent) was used to detect α–SMA actin-positive vessels in lung tissue and a mouse-monoclonal 8-hydroxy-2-deoxyguanosine (8OhdG) antibody (Abcam) was used to assess high fat diet induced left ventricular oxidative DNA damage. Secondary goat anti-rabbit antibody conjugated with Alexa Fluor 488 (Invitrogen) was applied for 2 h at room temperature in a dark chamber. Sections were counterstained with 4',6-Diamidino-2-phenylindole (DAPI, 1:10000, Enzo) for 5 min, mounted with anti-fade mounting medium (DAKO) and measured using a fluorescence microscope (OLYMPUS) and analysed with cellSens Dimension imaging software (OLYMPUS). In each lung, α–SMA-positive vessels of four high power fields in 10x magnification were counted (<30 µm). For quantification of 8-dOHG staining, 40-60 nuclei were circled per sample and grey value intensity (GVI) per nucleus was measured using cellSens Dimension imaging software (OLYMPUS).

### 6.2.12 Quantitative real-time PCR analysis

RNA was extracted as previously described (Chalupsky et al., 2015). cDNA was synthesized using SuperScript III RT (Invitrogen), according to the manufacturer's instructions. Real-time PCR analysis was performed using Perfecta CYBR Green FastMix (VWR) in a Rotor-Gene 6000 System (Corbett Life Science), normalized with β-actin. Quantification was performed using REST analysis software based on ∆CT calculation. Polymerase chain reaction (PCR) was performed with the following primers: spXBP1 5′-TGA GTC CGC AGC AGG TG-3′ (sense), (antisense); β-MHC 5′- CTA CAG GCC TGG GCT TAC CT -3′ (sense), 5′-TCT CCT TCT AGA CTT CCG-3′ (antisense); Hand2 5′-GGC TCC GTT CTG AGG ACT TC-3′ (sense), 5′-CTT ACC ACA CGG GAG TGT CC-3′ (antisense); CDK9 5′-AGA GAC ATT CCT GGA CGC AG-3′ (sense), 5′-AGT GTC CTG GCT GAC CAA AC-3′ (antisense); Bcl-2 5'-GAA CTG GGG GAG GAT TGT GG-3' (sense), 5'-GCA TGC TGG GGC CAT ATA GT-3' (antisense); EDN1 5'-TGT GTC TAC TTC TGC CAC CT-3' (sense), 5'-CCC TGA GTT CTT TTC CTG CTT-3' (antisense); β-actin 5′-CTA AGG CCA ACC GTG AAA AG-3′ (sense), 5′-ACA GCC TGG ATG GCT ACG-3′ (antisense).

### 6.2.13 Western blot analysis

Western blot analysis was performed using standard procedures as previously described (Kračun et al., 2014). LV tissue was homogenized in Cell Lysis Buffer (Cell Signaling). Prior to use, Complete Mini$^{TM}$ protease inhibitor (Roche) and $Na_3VO_4$ were added to the buffer. Extracted protein was fractionated using 8-12% TRIS-gels and transferred to a nitrocellulose transfer membrane. The membrane was blocked for 2 h in TBS containing 5% non-dry milk and 0.3% Tween20. Membranes were incubated overnight at 4$^{o}$C using antibodies against Nox2 (Upstate), Nox1, p-eIF2α, BiP, caspase 12 (All Cell Signaling), 4-HNE, Nox4, p22phox, ATF6, ATF4, HIF1α (All Abcam) and β-actin (Santa Cruz). Horseradish peroxidase-conjugated goat anti-rabbit, mouse anti-goat or rabbit anti-mouse immunoglobulin G (1:10000 in 5% milk of 5% BSA) were used as secondary antibodies. Luminol-enhanced chemiluminescence was performed for protein visualization. Densitometric analyses for quantification of the western blots were performed using ImageJ software.

### 6.2.14 Superoxide anion radical measurements by electron paramagnetic resonance

Electron paramagnetic resonance (EPR) measurements were performed to determine superoxide production in isolated adult cardiomyocytes and H9C2 cells (electron paramagnetic resonance, Escan; Noxygen, Elzach, Germany). EPR was connected to a gas mixing unit to allow adjustment of oxygen concentrations in the measuring cuvette as previously described. Isolated adult cardiomyocytes and H9C2 cells were washed with PBS and harvested in Krebs-Hepes buffer pH 7.35 (KHB: 99 mM NaCl, 4.69 mM KCl, 2.5 mM $CaCl_2$, 1.2 mM MgSO4, 25 mM NaHCO3, 1.03 mM $KH_2PO4$, 5.6 mM glucose, 20 mM Na-HEPES), supplemented with 5 μM diethyldithiocarbamate (DETC), 25 μM desferroxamine (DES), and 100 μM superoxide-specific spin probe 1-hydroxy-methoxycarbonyl-2,2,5,5-tetramethyl-pyrrolidine hydrochloride (CMH; Noxygen). Cell suspensions were placed in a glass capillary and spectra were recorded inside the temperature-controlled (37$^{o}$C) electron paramagnetic resonance spectrometer. Superoxide production rate was calculated by using linear regression and normalized to protein content.

### 6.2.15 Small RNA sequencing

Total RNA from the left ventricle was isolated using the peqGOLD Total RNA Kit (VWR). Library was created using the NEBNext Small RNA library kit for Illumina. Sequencing was performed using an Illumina miniSeq (Illumina) with default settings. Cleaning, trimming, size selection and mapping was performed using the Chimira web tool for small RNA sequencing data (Vitsios & Enright, 2015) using default settings. Due to low total library size one sample was removed from each group. The remaining counts were uploaded to the Galaxy web platform using the public server UseGalaxy Europe (UseGalaxy.eu) for differential expression analysis (Jalili et al., 2020). For DE analysis the EdgeR method was used with the Galaxy Version 3.24.1 (Liu et al., 2015; Robinson et al., 2010). Trimmed mean of M values (TMM) was the method used to normalize library sizes, eBayes was used with robust settings. Differentially expressed miRNAs with a p-value <0.05 were considered as significant and further analysed. Principal component analysis and heatmaps were generated using the integrated Differential Expression and Pathway analysis (iDEP) version 0.91 (Ge et al., 2018). Volcano plot was generated using Prism (Graphpad).

### 6.2.16 miRNA validation

Validation of miRNA expression was performed as described (Zhang et al., 2019). Briefly, total RNA was reverse transcribed using the miscript II RT kit (Qiagen) and quantitative PCR was performed with the miScript Precursor Assay (Qiagen) and the Perfecta SYBR Green FastMix (VWR) in a Rotor-Gene 6000 (Corbett Life Science). Quantification was performed by using REST analysis software based on deltaCT calculation (Pfaffl et al., 2002).

### 6.2.17 Target prediction and pathway overrepresentation analysis

To predict miRNA targets, the miRWalk 3.0 atlas of predicted and validated miRNA-target interaction was used with default settings. Identified miRNA-target pairs with a p-value < 0.05 were accepted for further analysis. For overrepresentation analysis, murine genes were converted into human HGNC symbols via the Ensemble version 100 and Biomart (Smedley et al., 2015; Yates et al., 2020) and the Mouse Genome Database

(MGD) at the Mouse Genome Informatics website (URL:http://www.informatics.jax.org), the Jackson Laboratory, Bar Harbor, Maine (Bult et al., 2019) and an overrepresentation analysis for diseases using the TopFun tool from the ToppGene Suite (Chen et al., 2009) was used with pValue Method set to probability density function and BH method for FDR correction and minimal gene limit set to 1. Enriched diseases with a FDR<0.05 were considered significant.

### 6.2.18 Statistical analysis

All experimental data have been received from independent experiments. The sample size (number of independent experiments) required to reach an experimental power $(1-\beta) \geq 0.8$ at a p-value threshold of 0.05 was calculated by power analysis using the power-t.test function in R 2.15 (The R foundation). Independent sample preparations from different cellular batches or animals adjusted to the required sample size were then used. Values are presented as mean ± SD. For qPCR analysis, REST analysis was used. For other statistical analysis GraphPad Prism software (GraphPad Software, La Jolla, CA) was used. Results were compared by One-Way ANOVA followed by Tukey's Multiple Comparison Test or by Student´s t-test.

# 7 Results

## 7.1 NADPH oxidases increase superoxide production induced by palmitate

To test the link between cardiac ROS and obesity, an in vitro model was established. H9C2 cells were stimulated with different concentrations of sodium-palmitate for 3 hours (Fig. 1A). Sodium-palmitate stimulation increased superoxide generation as measured by EPR using CMH as a spin trap with a significant response starting at 200 nM (Fig. 1A). In order to determine an adequate stimulation time, H9C2 cells were stimulated for 0.5 h, 1 h, 2 h, 4 h and 8 h with a concentration of 200 nM of sodium-palmitate (Fig. 1B). Superoxide generation was significantly increased after 4 h of stimulation. Therefore, we chose to perform further experiments with a sodium-palmitate concentration of 200 nM for 4 h.

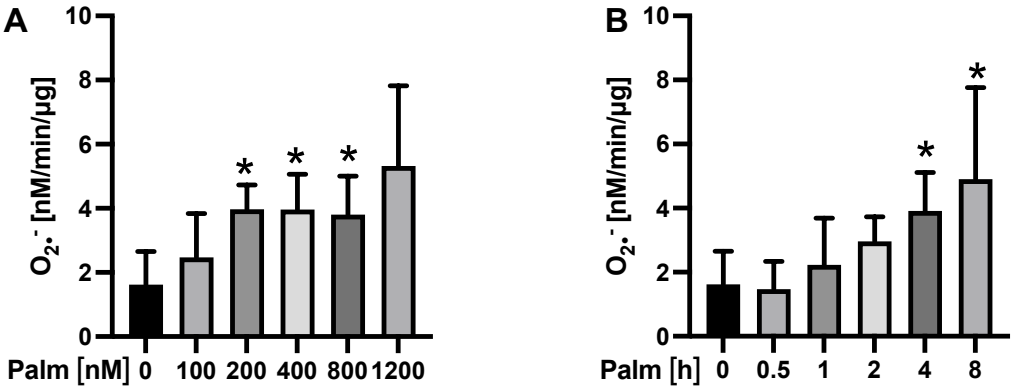


**Figure 1. Dose and time response of sodium-palmitate induced superoxide production in cardiomyocytes.** (A) H9C2 cells were stimulated with 100 nM, 200 nM, 400 nM, 800 nM and 1200 nM of sodium-palmitate (Palm) for 3 h and superoxide generation was determined by EPR using CMH ($n$ = 5; *$p$ < 0.05, *vs.* Ctr (0 nM)). (B) H9C2 cells were stimulated with 200 nM Palm for 0.5 h, 1 h, 2 h, 4 h and 8 h and superoxide generation was determined by EPR using CMH ($n$ = 5; *$p$ < 0.05, *vs.* Ctr (0 h)). One-way ANOVA followed by Tukey's post-hoc test for multiple comparisons was used in all cases.

In order to show the specificity of CMH for superoxide detection, H9C2 cells were stimulated with sodium-palmitate in the presence of either polyethylene glycol-

superoxide dismutase (PEG-SOD) or PEG-catalase or both (Fig. 2A). Indeed, the EPR signal was inhibited by 95-98% in the presence of PEG-SOD (alone or together with PEG catalase), while addition of PEG catalase alone had no effect – thus proving the specificity of the method for superoxide detection (Fig. 2A). Since superoxide can be rapidly transformed to hydrogen peroxide, we also determined $H_2O_2$ levels in H9C2 cardiomyoblasts by Amplex red assay (Fig. 2B). Similar to the results obtained by EPR, sodium-palmitate increased Amplex red mediated fluorescence in H9C2 cells (Fig. 2B). Addition of PEG-catalase (alone or with PEG-SOD) decreased the signal, while addition of PEG-SOD alone had little effect (Fig. 2B). To test the effect of sodium-palmitate on mature cardiomyocytes, cardiomyocytes were isolated from wild type mice and stimulated with 200 nM of sodium-palmitate for 4 h (Fig. 2C). Sodium-palmitate stimulation increased superoxide generation as measured by EPR using CMH (Fig. 2C). Next, the sources of superoxide generation following sodium-palmitate stimulation were examined. To this end, isolated cardiomyocytes were treated with the mitochondria-targeted ROS scavenger MitoQ (100 μm), the NADPH oxidase inhibitor GKT-137831 (50 μM) or the NOX2 inhibitor Gp91-dstat (Fig. 2D/E). Compared to control conditions, application of MitoQ, GKT-137831 and Gp91-dstat decreased sodium-palmitate-induced superoxide generation suggesting that palmitate increases both mitochondrial as well as NADPH oxidase mediated superoxide generation (Fig. 2D/E). Additionally, H9C2 myoblasts were depleted of NOX4, which has been reported as a source of hydrogen peroxide (Nauseef, 2008). Compared to control cells, sodium-palmitate induced hydrogen peroxide levels were significantly reduced in NOX4-depleted cells (Fig. 2F).

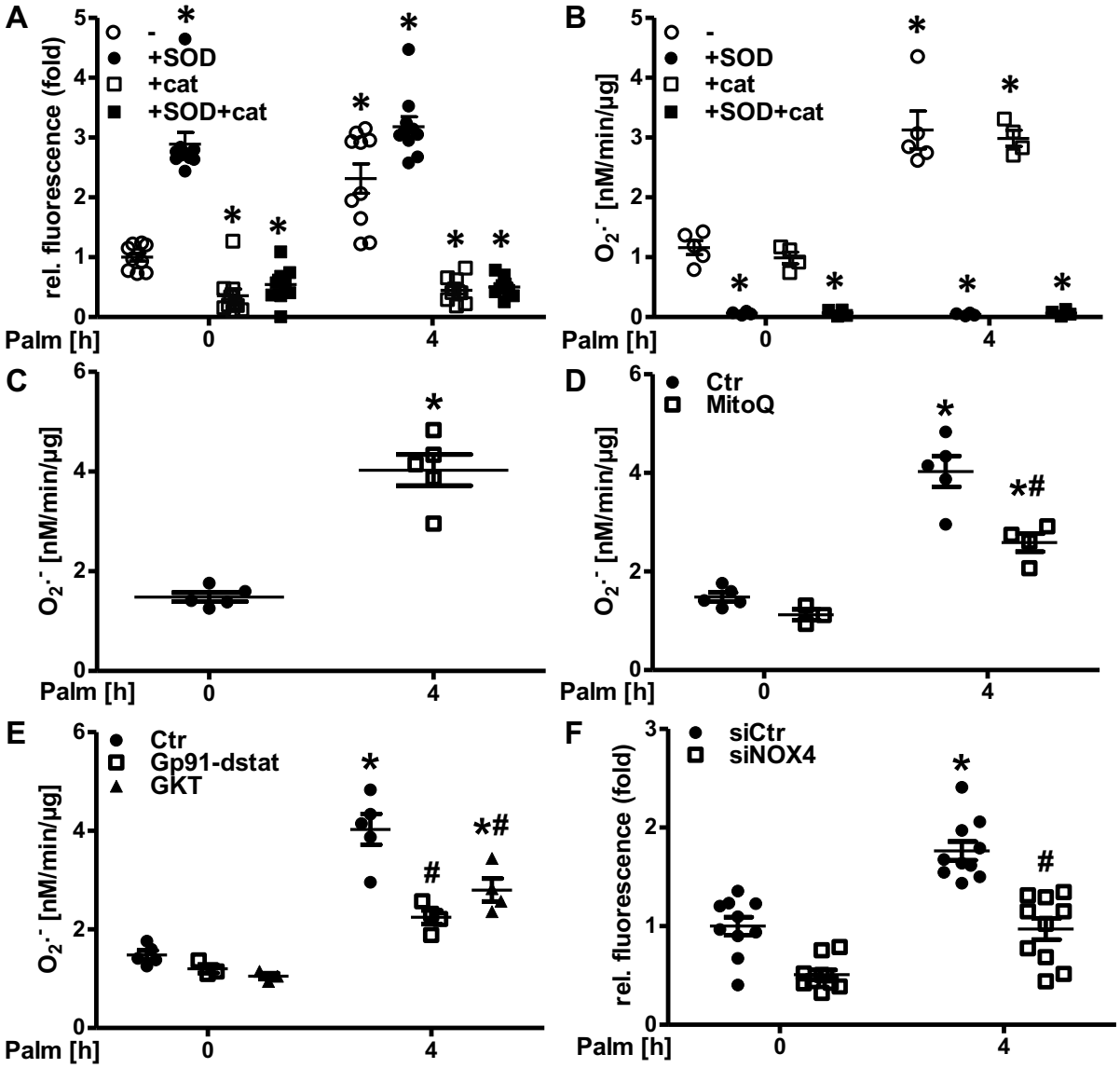


**Figure 2. Sodium-palmitate induces superoxide production promoted by NADPH oxidases.** (A/B) H9C2 cells were treated with 400 nM sodium palmitate (Palm) for 4 h. Polyethylene glycol (PEG) superoxide dismutase (SOD) or PEG catalase (cat) or both (SOD + cat) were added prior to measuring (A) superoxide production rate by EPR using CMH ($n$ = 4-5; *$p$ < 0.05 *vs.* Palm 0 h) or (B) hydrogen peroxide levels by Amplex red assay ($n$ = 10; *$p$ < 0.05 *vss.* Palm 0 h). (C-E) Cardiomyocytes isolated from wild type mice were stimulated with 200 nM of Palm for 4 h and superoxide generation was determined by EPR using CMH (C) without prior inhibitor treatment ($n$ = 5; *$p$ < 0.05, *vs.* Ctr (0 h)) or (D) after treatment 1 h prior to 400 nM Palm stimulation with the mitochondria targeted scavenger MitoQ (100 µM) ($n$ = 4-5; *$p$ < 0.05 *vs.* CtrPalm 0 h; #$p$ < 0.05 *vs.* CtrPalm 4 h) or (E) after treatment 1 h prior to 400 nM Palm stimulation with the Nox2 inhibitor gp91-dstat or the NADPH oxidase inhibitor GKT-137831 (GKT, 50 µM) ($n$ = 4-5; *$p$ < 0.05 *vs.* CtrPalm 0 h; #$p$ < 0.05 *vs.* CtrPalm 4 h). (F) H9C2 cells were silenced for NOX4 using RNAi or transfected with siCtr and exposed to palmitate for 4 h. Hydrogen peroxide levels were measured by Amplex red assay ($n$ = 10; *$p$ < 0.05 *vs.* siCtrCtr; #$p$ < 0.05 *vs.* siCtrPalm). One-way ANOVA followed by Tukey's post-hoc test for multiple comparisons was used in all cases.

## 7.2 High fat diet promotes obesity and heart mass increase dependent on p22phox

CD57BL6j (wild type) mice were chronically treated with a high fat diet (HFD, 60% of caloric intake from fat) for a period of 20 weeks. HFD feeding significantly increased body mass in wild type mice, as shown by the body mass gain related to tibia length as a measure of obesity (Tab. 1). Hearts, lungs, kidneys and skeletal muscles were weighed (Tab. 1). HFD caused an increase in heart mass in wild type mice, as indexed by the heart mass vs. tibia length ratio, indicating cardiac hypertrophy (Tab. 1). Other organs, however, showed no significant mass increase.

| | WT-NFD | nmf333 NFD | WT HFD | nmf333 HFD |
|---|---|---|---|---|
| BW/TL (mg/mm) | 1.14 ± 0.06 | 1.10 ± 0.08 | 1.43* ± 0.19 | 1.36* ± 0.13 |
| Heart/TL (mg/mm) | 5.85 ± 0.41 | 5.51 ± 0.21 | 6.35* ± 0.39 | 5.83# ± 0.63 |
| LV/TL (mg/mm) | 4.81 ± 0.50 | 4.58 ± 0.23 | 5.46* ± 0.24 | 4.61# ± 0.42 |
| RV/TL (mg/mm) | 1,12 ± 0.18 | 0.98 ± 0.11 | 1.04 ± 0.06 | 0.93 ± 0.10 |
| Lung/TL (mg/mm) | 2.67 ± 0.52 | 3.20 ± 0.99 | 2.67 ± 0.87 | 4.02 ± 1.15 |
| Quad.L/TL (mg/mm) | 7.64 ± 0.47 | 7.31 ± 1.40 | 6.36 ± 1.04 | 5.94 ± 0.55 |
| Quad.R/TL (mg/mm) | 8.60 ± 0.81 | 7.45 ± 0.52 | 8.70 ± 0.67 | 7.62 ± 0.77 |
| Kidney/TL (mg/mm) | 7.72 ± 0.91 | 7.03 ± 0.76 | 8.62 ± 0.90 | 7.78 ± 0.54 |

**Table 1. Effects of high fat diet on organ mass.** Table shows organ mass and ratio of organ mass to tibia length (TL). Two-tailed Student's *t*-test was used in all cases ($n$ =8-15; *$p < 0.05$, *vs.* WTNFD; #$p < 0.05$ *vs.* WTHFD). BW = body weight; LV = left ventricle; RV = right ventricle; Quad.L = left quadriceps; Quad.R = right quadriceps.

To assess the effect of NADPH oxidases in our in vivo model, CD57BL6j (wild type) mice and mice lacking p22phox protein and thus functional NADPH oxidases due to a mutation in the *Cyba* gene (nmf333) were chronically treated with a high fat diet (HFD, 60% of caloric intake from fat) for a period of 20 weeks. Nmf333 mice fed with HFD significantly increased body mass similarly to wild type littermates (Tab. 1). However, while HFD caused an increase in heart mass in wild type mice, as indexed by the heart

mass vs. tibia length ratio, indicating cardiac hypertrophy, nmf333 mice were protected (Tab. 1).

## 7.3 High fat diet increases expression of NADPH oxidases

HFD increased p22phox protein levels in the heart from wild type mice while p22phox was almost absent in hearts from nmf333 mice under control and HFD conditions (Fig. 3A/B). To test whether HFD would affect protein levels of NADPH oxidases, Western blot analyses were performed for p22phox, NOX1, NOX2 and NOX4.

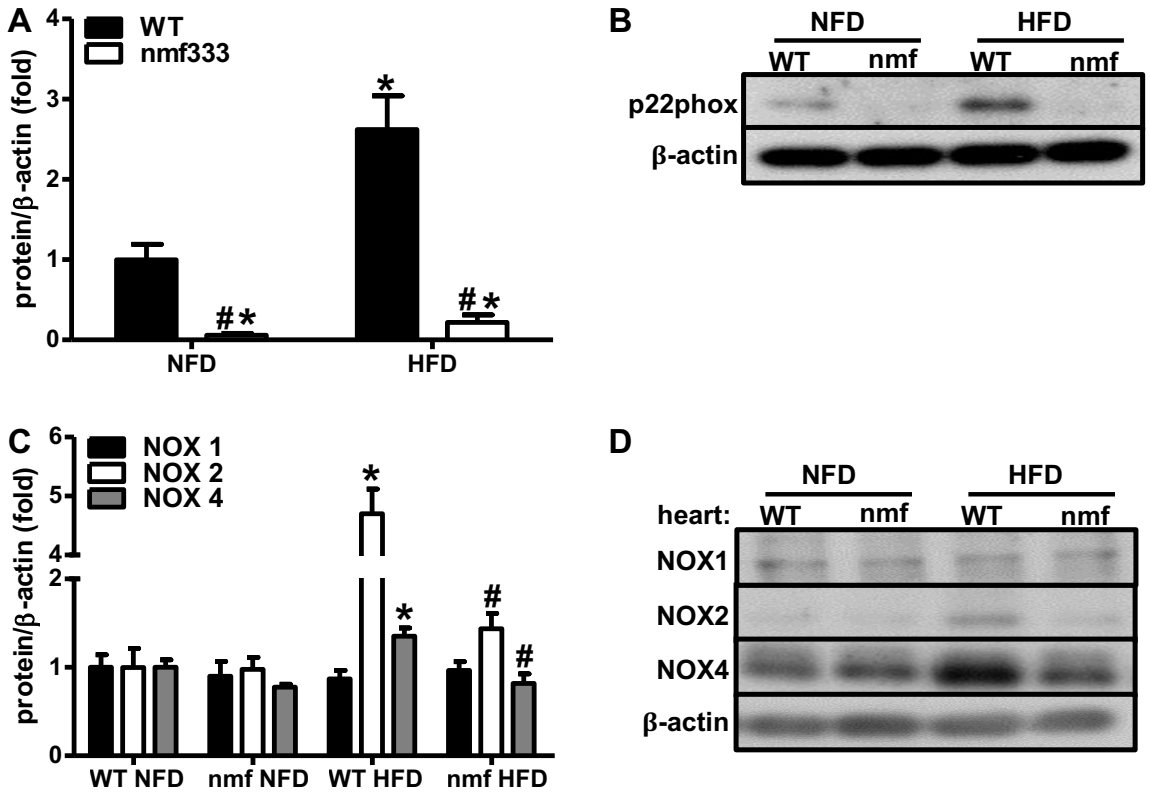


**Figure 3. HFD increases NADPH oxidase protein expression.** C57BL/6j wild type mice (WT) and mice deficient in p22phox due to a point mutation in the *Cyba* gene (nmf333) were fed a high fat diet (HFD) for 20 weeks. Littermates were fed a regular chow (NFD) for 20 weeks. (A/B) Western blot analyses were performed in heart samples using an antibody against p22phox. β-actin served as loading control. (A) Statistical analysis was performed ($n$ =6; $^{*}p < 0.05$, *vs.* WTNFD; $^{\#}p < 0.05$ *vs.* WTHFD). (B) Representative blots are shown. (C/D) Western blot analyses were performed in murine heart tissues using antibodies against NOX1, NOX2 and NOX4. β-actin served as a loading control ($n$ = 6,$^{*}p < 0.05$ *vs.* WTCtr; #$p$ <

0.05 *vs.* WTHFD). (D) Representative blots are shown. One-way ANOVA followed by Tukey's post-hoc test for multiple comparisons was used in all cases.

NOX2 and NOX4 protein levels were increased in wild type HFD mice, while they remained unchanged in p22phox deficient nmf333 mice (Fig. 3C/D). NOX1 protein levels remained unchanged regardless of both diet and genotype (Fig. 3C/D).

## 7.4 p22phox promotes left ventricular hypertrophy and increases left ventricular pressure in response to high fat diet

As cardiac hypertrophy can develop as a result of hypertension, hemodynamic measurements were performed to determine LV pressure. Hemodynamic measurements showed that HFD in wild type mice increased left ventricular systolic pressure (Fig. 4A). Consequently, HFD fed mice showed an increase in left ventricular mass and enlarged cardiomyocytes in the left ventricle indicative of left ventricular hypertrophy (Fig. 4B-D). However, mice lacking p22phox were protected against HFD-induced hypertension and left ventricular hypertrophy (Fig. 4A-D). In support of these findings, mRNA levels of the cardiac hypertrophy marker β-heavy myosin chain (β-MHC), were significantly increased in the left ventricles from wild type mice fed a HFD, but not from nmf333 mice (Fig. 4E).

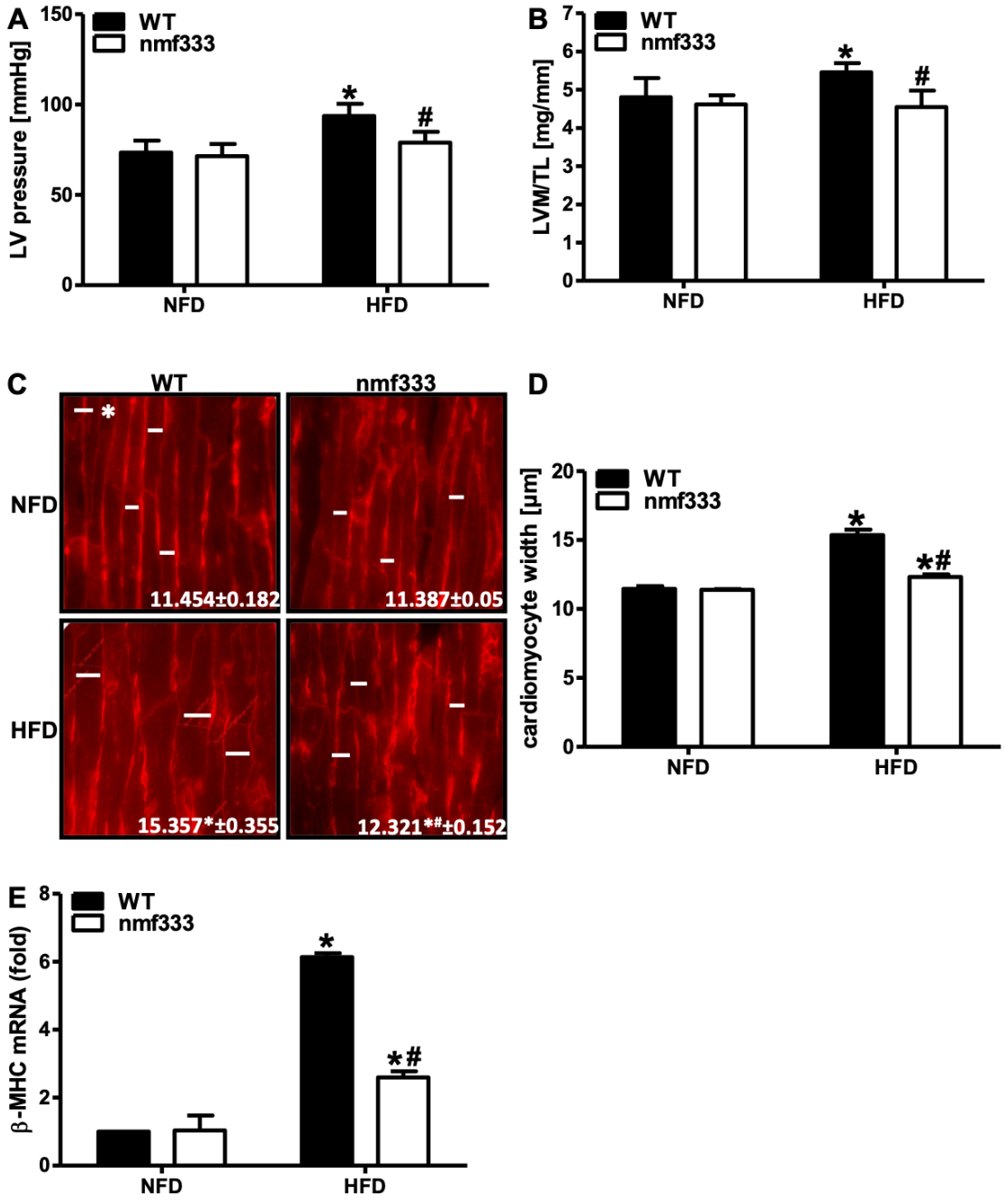


**Figure 4. p22phox promotes left ventricular pressure and left ventricular hypertrophy in response to high fat diet.** C57BL/6j wild type mice (WT) and mice deficient in p22phox due to a point mutation in the *Cyba* gene (nmf333) were fed a high fat diet (HFD) for 20 weeks. Littermates were fed a regular chow (NFD) for 20 weeks. (A) Left ventricular (LV) pressure was determined hemodynamically ($n$ = 3-4; $^{*}p < 0.05$ *vs.* WTNFD; $^{\#}p < 0.05$ *vs.* WTHFD). (B) Mass of left ventricle and septum (LVM) was evaluated and LVM/TL (tibia length) ratio was determined ($n$ =8-10; $^{*}p < 0.05$, *vs.* WTNFD; $^{\#}p < 0.05$ *vs.* WTHFD). (C/D) Formalin-fixed paraffin embedded (FFPE) sections from the left ventricle were stained with wheat germ agglutinin. (C) Representative stainings are shown. Scale bar with asterisk represents 10 µm. (D) LV cardiomyocyte diameters were determined in four high power fields per section. ($n$ = 3–5; $^{*}p < 0.05$, vs. WTNFD; $^{\#}p < 0.05$ *vs.* WTHFD). (E) RT-qPCR was performed using gene-specific primers for **β**-MHC

or for 18S rRNA for normalization ($n = 3$*$p < 0.05$ *vs.* WTNFD; $^{\#}p < 0.05$ *vs.* WTHFD). One-way ANOVA followed by Tukey's post-hoc test for multiple comparisons was used for (A-D) and REST analysis was used for (E).

## 7.5 p22phox promotes left ventricular dysfunction in response to high fat diet

To further evaluate the functional consequences of HFD feeding for the left ventricle, echocardiography was performed (Fig. 5-6). HFD feeding in wild type mice resulted in increased left-ventricular end-systolic and end-diastolic diameter (Fig. 5A-C). Moreover, fractional shortening (FS) was decreased in HFD fed mice compared to control mice (Fig. 5C-D). Similar results were obtained for ejection fraction (EF) that was approximated using the Teichholz formula (EF (%) = 100 x (LVEDV – LVESV)/ LVEDV, with LVEDV = (7 x LVEDD 3 )/(2.4 + LVEDD) and LVESV = (7 x LVESD 3 )/(2.4 + LVESD), pointing to heart failure with reduced ejection fraction (HFrEF) in wild type HFD mice. However, p22phox deficient mice were protected against HFD-induced left ventricular dysfunction and HFrEF (Fig. 5).

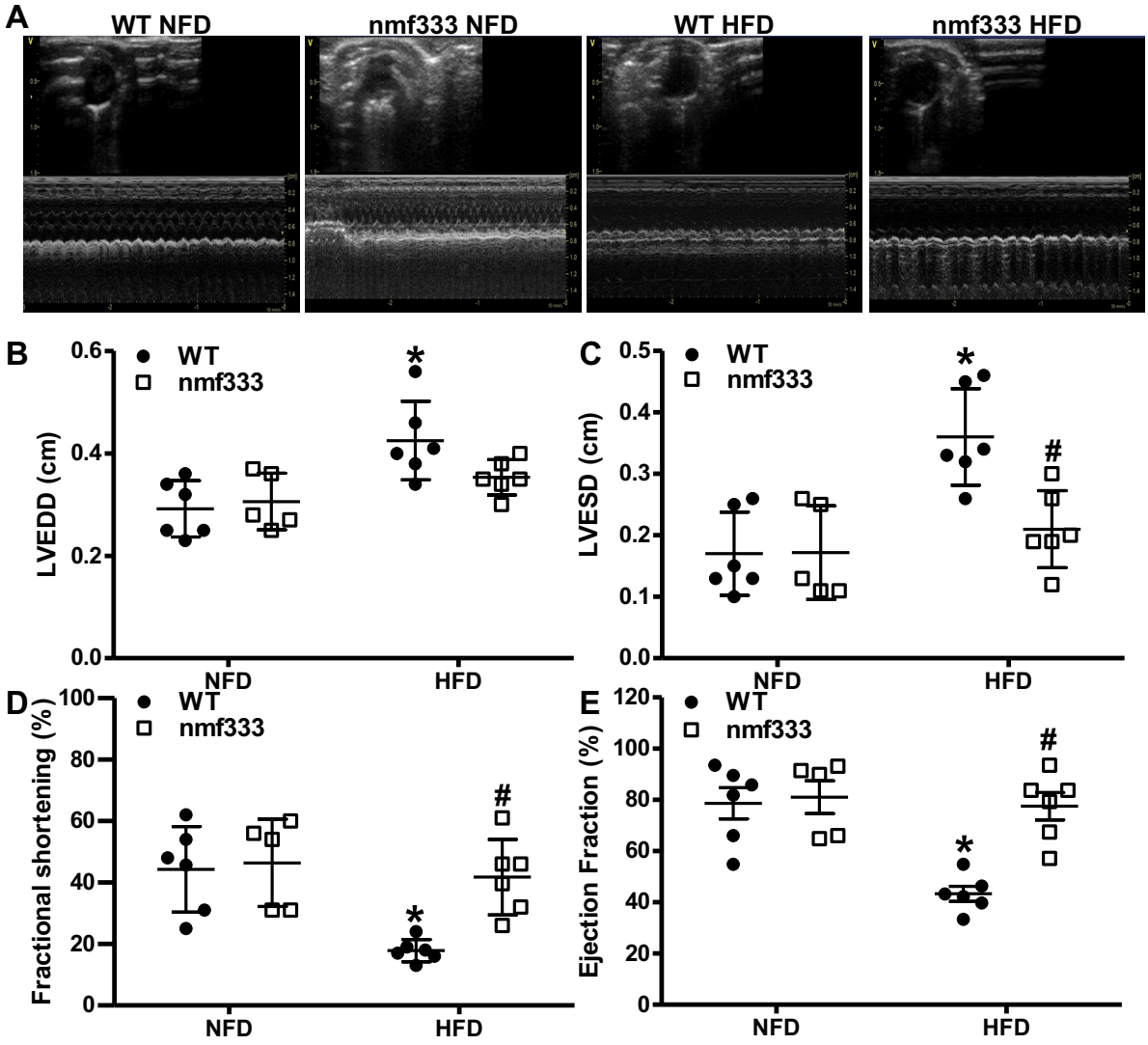


**Figure 5. p22phox promotes left ventricular dysfunction in response to high fat diet.** C57BL/6j wild type mice (WT) and mice deficient in p22phox due to a point mutation in the *Cyba* gene (nmf333) were fed a high fat diet (HFD) for 20 weeks. Littermates were fed a regular chow (NFD) for 20 weeks. Echocardiography of the left ventricle was performed in M-mode. (A) Representative tracings are shown. (B) Left ventricular end-diastolic diameters (LVEDD) were measured. (C) Left ventricular end-systolic diameters (LVESD) were measured. (D) Fractional shortening (FS) was calculated using the following formula: (LVEDD-LVESD)/LVEDD. (E) Ejection fraction (EF) was approximated using Teichholz formula ($n$ = 5-6, $^{*}p < 0.05$ WTNFD *vs.* nmf333NFD; $^{**}p < 0.05$ WTNFD *vs.* WTHFD; $^{\#}p < 0.05$ WTHFD *vs.* nmf333HFD). One-way ANOVA followed by Tukey's post-hoc test for multiple comparisons was used in all cases.

Nmf333 mice had a lower heart rate compared to wildtype mice, however, without reaching statistical significance (Fig. 6A). There was also no difference in diastolic left ventricular posterior wall thickness (LVPWd), nor in diastolic intraventricular septum wall thickness (IVSd) (Fig. 6B/C).

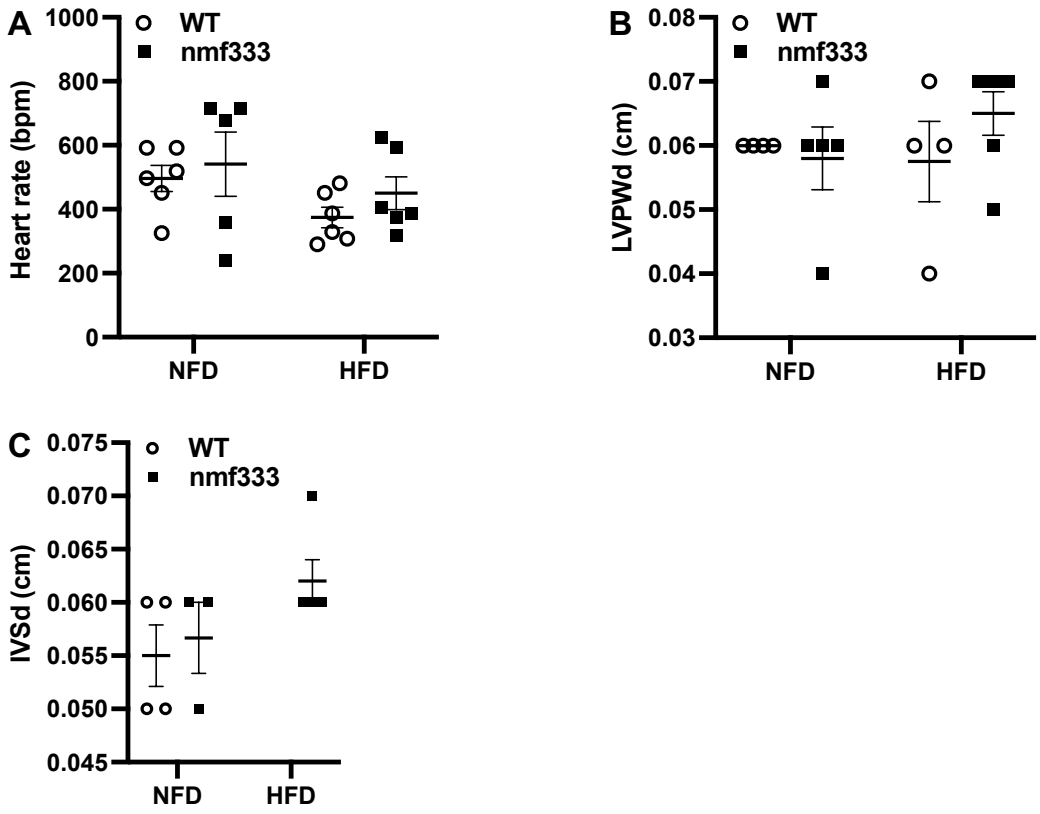


**Figure 6. p22phox promotes left ventricular dysfunction.** C57BL/6j wild type mice (WT) and mice deficient in p22phox due to a point mutation in the *Cyba* gene (nmf333) were fed a high fat diet (HFD) for 20 weeks. Littermates were fed a regular chow (NFD) for 20 weeks. (A) Heart rate (HR) was determined using echocardiography ($n$ = 5-6; $^{*}p < 0.05$ *vs.* WTNFD; $^{\#}p < 0.05$ *vs.* WTHFD). (B) Diastolic left ventricular posterior wall thickness (LVPWd) and (C) diastolic intraventricular septum wall thickness (IVSd) were determined using echocardiography. One-way ANOVA followed by Tukey's post-hoc test for multiple comparisons was used in all cases.

## 7.6 p22phox promotes pulmonary vascular remodeling in response to high fat diet

Left heart disease (HFrEF and HFpEF) as well as obesity have been associated with pulmonary hypertension and pulmonary artery disease (Miller et al., 2013). Since our in vivo model showed signs of HFrEF, we assessed whether HFD would lead to vascular remodeling in the lungs. Formalin fixed paraffin embedded (FFPE) lung sections were stained with an antibody against α-smooth muscle actin (α-SMA) to visualize pulmonary vascular remodeling (Fig. 7A/B). Indeed, wild type mice fed a HFD showed an increased number of small muscularized vessels (<30 μm) in lungs indicative of pulmonary

vascular remodeling (Fig. 7A/B). In line with our previous results, nmf333 mice fed HFD showed no signs of pulmonary vascular remodeling (Fig. 7A/B).

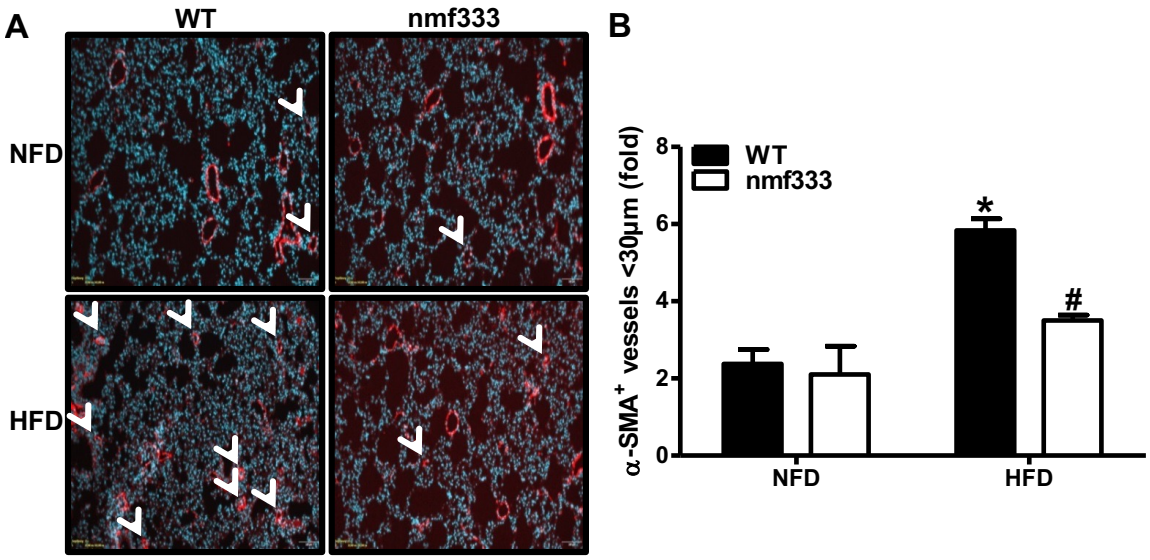


**Figure 7. p22phox promotes pulmonary vascular remodeling in response to high fat diet.** C57BL/6j wild type mice (WT) and mice deficient in p22phox due to a point mutation in the *Cyba* gene (nmf333) were fed a high fat diet (HFD) for 20 weeks. Littermates were fed a regular chow (NFD) for 20 weeks. Formalin-fixed paraffin embedded (FFPE) lung sections were stained with primary antibodies against (A) α-smooth muscle actin (α-SMA) and visualized with secondary goat anti-rabbit antibody conjugated with Alexa Fluor 488. Nuclei were visualized with DAPI. Representative stainings are shown. α-SMA-positive small- and medium-sized arterioles (<30 $\mu$m) were counted and related to the total number of arterioles of the same diameter in four high power fields per lung section ($n$ = 5; $^{*}p < 0.05$, *vs.* WTNFD; $^{\#}p < 0.05$ *vs.* WTHFD). One-way ANOVA followed by Tukey's post-hoc test for multiple comparisons was used.

## 7.7 HFD increases NADPH oxidase protein levels in the lung

To test whether HFD would also affect NADPH oxidase protein levels in the lung, Western blot analysis was performed. p22phox protein levels also increased in obese wild type mice, while they were poorly expressed in nmf333 mice (Fig. 8A/B). In addition, exposure to HFD increased levels of NOX2 and NOX4 protein in lung tissue from wild type HFD mice, while they remained unchanged in p22phox deficient mice (Fig. 8C/D). NOX1 protein levels remained unchanged regardless of both diet and genotype (Fig. 8C/D).

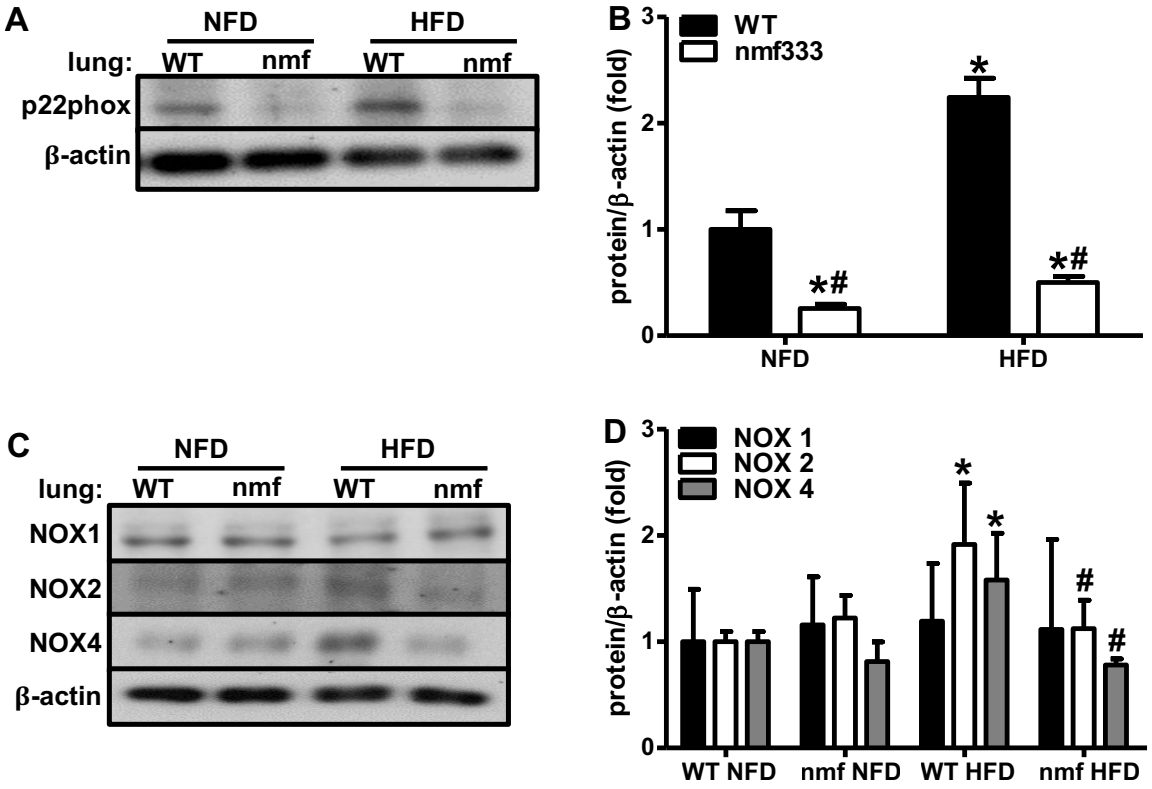


**Figure 8. HFD increases protein levels of NADPH-oxidases in lungs.** C57BL/6j wild type mice (WT) and mice deficient in p22phox due to a point mutation in the *Cyba* gene (nmf333) were fed a high fat diet (HFD) for 20 weeks. Littermates were fed a regular chow (NFD) for 20 weeks. (A/B) Western blot analyses were performed in lung (A) using an antibody against p22phox. β-actin served as loading control. (B) Representative blots are shown. (C/D) Western blot analyses were performed on murine lung tissues using antibodies against NOX1, NOX2 and NOX4. β-Actin served as a loading control. Representative blots are shown (D). Statistical analyses were performed ($n = 6$; $^{*}p < 0.05$, *vs.* WTNFD; $^{\#}p < 0.05$ *vs.* WTHFD). One-way ANOVA followed by Tukey's post-hoc test for multiple comparisons was used in all cases.

## 7.8 p22phox promotes right ventricular hypertrophy in response to HFD

To evaluate the consequences of HFD on right ventricular pressure, hemodynamic measurements of the right ventricle (RV) were performed. While there was a tendency towards increased right ventricular pressure in obese wild type mice compared to control mice and HFD fed nmf333 mice, the measurements did not reach statistical significance (Fig. 9A). However, cardiomyocyte size was increased in HFD fed wildtype but not

nmf333 mice, indicating right ventricular hypertrophy although the overall RV mass normalized to the tibia length showed no difference between the groups (Fig. 9B/C).

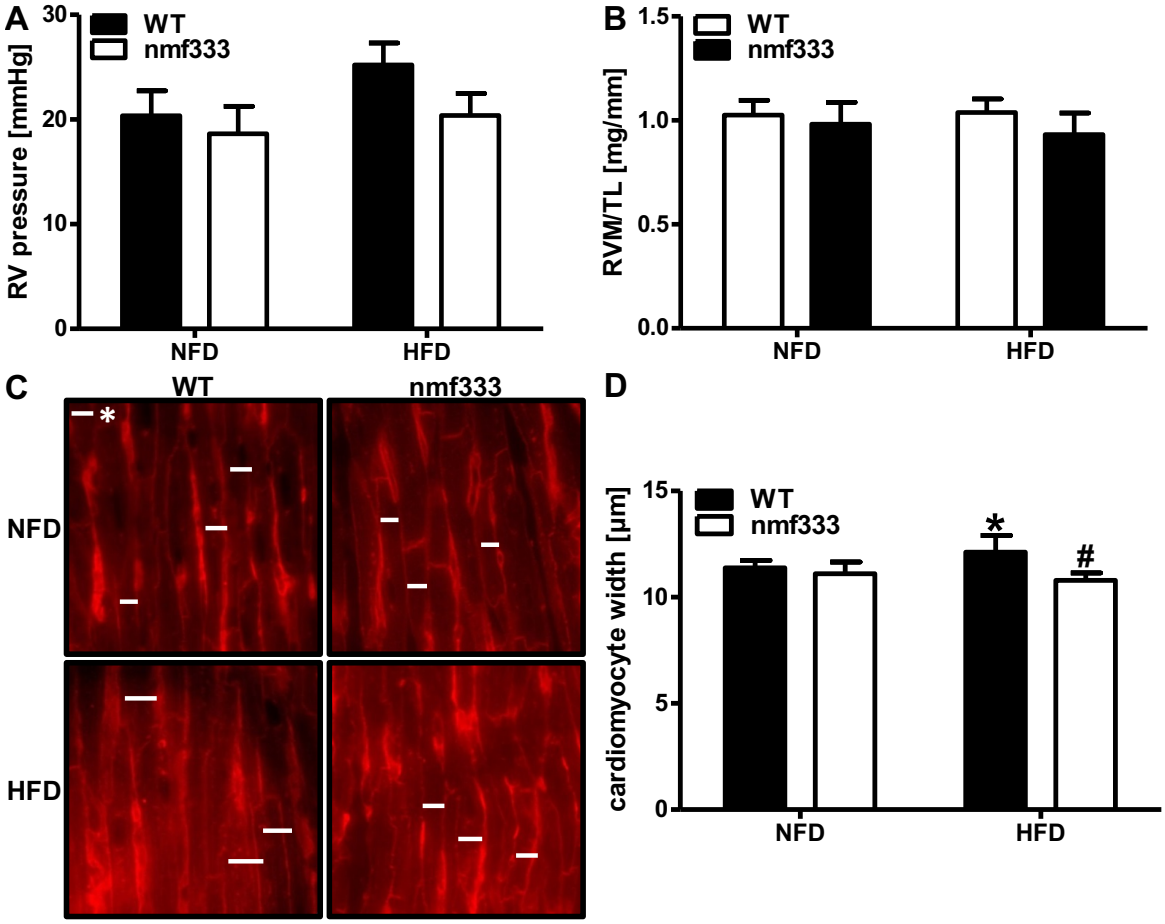


**Figure 9. p22phox promotes RV cardiomyocyte hypertrophy in response to HFD.** C57BL/6j wild type mice (WT) and mice deficient in p22phox due to a point mutation in the *Cyba* gene (nmf333) were fed a high fat diet (HFD) for 20 weeks. Littermates were fed a regular chow (NFD) for 20 weeks. (A) Right ventricular (RV) pressure was determined hemodynamically ($n$ = 3-4; *$p < 0.05$ *vs.* WTNFD; $^{\#}p < 0.05$ *vs.* WTHFD). (B) Mass of the right ventricle (RVM) was evaluated, and related to TL. RVM/TL ratio was determined ($n$ =8-10; *$p < 0.05$, *vs.* WTNFD; $^{\#}p < 0.05$ *vs.* WTHFD). (C/D) Formalin-fixed paraffin embedded (FFPE) sections from the right ventricle were stained with wheat germ agglutinin. (C) Representative stainings are shown. Scale bar with asterisk represents 10 $\mu$m. (D) RV cardiomyocyte diameters were determined in four high power fields per RV section. ($n$ = 3–5; *$p < 0.05$, vs. WTNFD; $^{\#}p < 0.05$ *vs.* WTHFD). One-way ANOVA followed by Tukey's post-hoc test for multiple comparisons was used in all cases.

## 7.9 p22phox modulates left ventricular miRNA profiles in response to high fat diet

To further investigate regulatory pathways and biological processes involved in the induction of cardiovascular dysfunction following HFD feeding, a RNAseq analysis for small regulatory RNAs (miRNAs), was performed in left ventricular tissues. 18 miRNAs downregulated and 14 miRNAs upregulated were identified in left ventricles of HFD wild type mice compared to the corresponding NFD littermates (Fig. 10A). In nmf333 HFD mice, 9 miRNAs were downregulated, and 30 miRNAs were upregulated (Fig. 10A). As indicated by the principal component analysis (PCA) plots, the heart miRNA transcriptomes exhibited clear diet differences in WT mice (Fig. 10C). In addition, heart transcriptomes from HFD mice showed clear genotype differences (Fig. 10D).

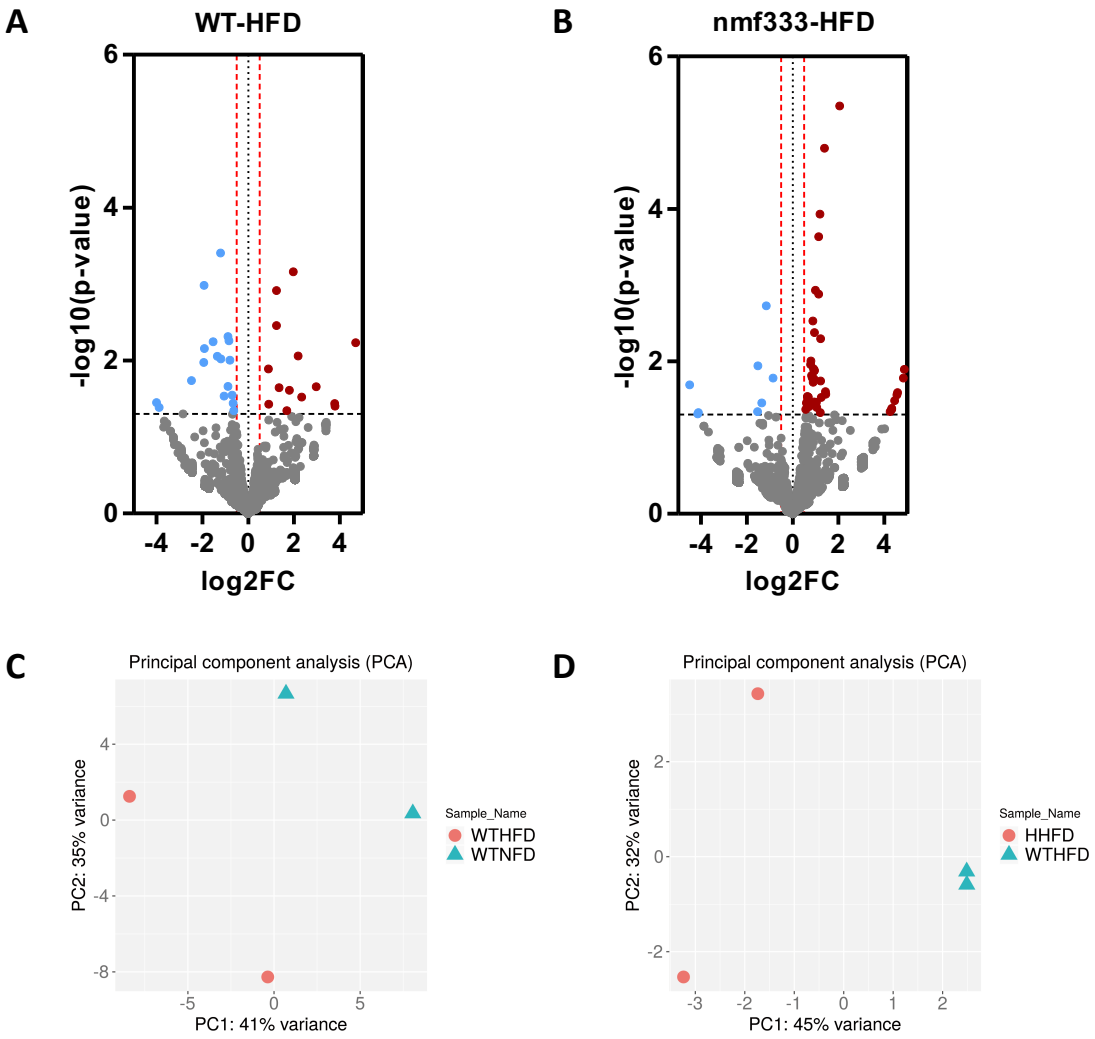


**Figure 10**. **p22phox modulates left ventricular miRNA profiles in response to high fat diet.** C57BL/6j wild type mice (WT) and mice deficient in p22phox due to a point mutation in the *Cyba* gene (nmf333) were fed a high fat diet (HFD) for 20 weeks. Littermates were fed a regular chow (NFD) for 20 weeks. miRNA profiles of the left ventricle were determined by RNAseq. (A/B) Volcano plots show miRNA profiles for WT (A) and nmf333 (B) hearts after high fat diet. Blue: miRNAs with log2FC≤0.5 and p≤0.05, red: log2FC≥0.5 and p≤0.05; grey: unregulated miRNAs. C) Principal component analysis of miRNA-seq samples for wild type mice fed a NFD (WTNFD - blue) or HFD (WTHFD - red) (n = 2). D) Principal component analysis of miRNA-seq samples for wild type (WTHFD - blue) and nmf333 (HHFD - red) mice fed a high fat diet (n = 2).

To find pathways affected by HFD and NADPH oxidases, a functional gene list enrichment analysis was performed with potential target genes of the dysregulated miRNAs. Genes implicated in cardiovascular processes, proliferation, cell death and fat/glucose metabolism (Fig. 11A/B) were found, in addition to genes implicated in ROS signaling and stressor pathways as targets of downregulated miRNAs in wild type HFD fed mice (Fig. 11A) and upregulated miRNAs in nmf333 fed HFD mice (Fig. 11B).

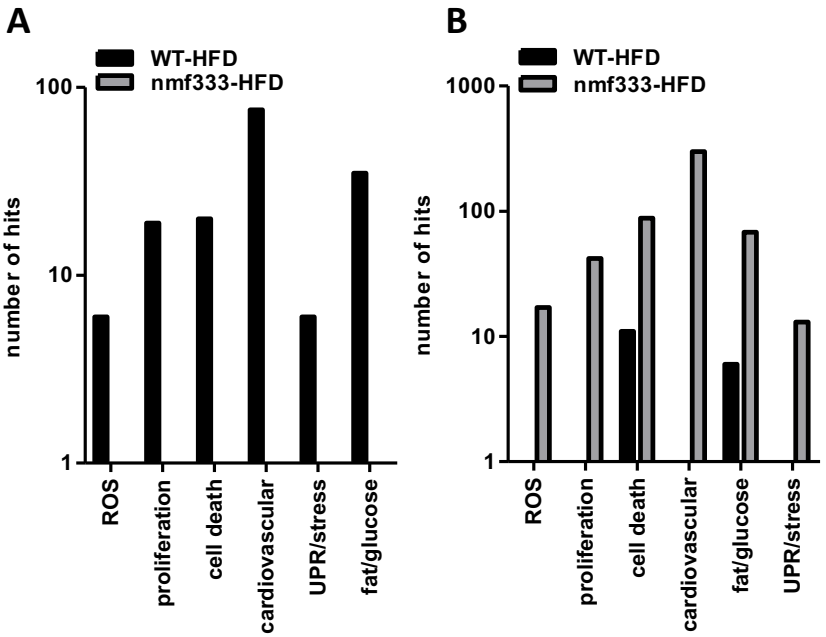


**Figure 11. p22phox affects the functional enrichment of target genes of dysregulated miRNAs.**
C57BL/6j wild type mice (WT) and mice deficient in p22phox due to a point mutation in the *Cyba* gene (nmf333) were fed a high fat diet (HFD) for 20 weeks. Littermates were fed a regular chow (NFD) for 20 weeks. Potential targets of upregulated (A) or downregulated (B) miRNAs for the comparisons WT-HFD vs WT-NFD and nmf-HFD vs nmf-HFD were used for an over-representation analysis using ToppGene analysis tool. Graphs show total number of terms significantly overrepresented (FDR<0.05) and connected to the mentioned categories.

Among the dysregulated miRNAs, miR-1a was reciprocally regulated, downregulated in hearts from wild type HFD mice and upregulated in hearts from nmf333 HFD mice. In line, validation by qPCR analyses confirmed this reciprocal regulation in hearts from wild type and nmf333 mice after HFD feeding (Fig 12A). To further validate this finding, the expression of target genes of miR-1a was investigated. HFD increased the expression of Heart and neural crest-derived transcript 2 (HAND2), cyclin dependent kinase 9 (CDK9), endothelin 1 (EDN1) and B-cell lymphoma 2 (Bcl-2) in left ventricles from wild type mice, but not from nmf333 mice (Fig. 12B). In HFD treated wild type mice, gene ontology (GO) biological processes involved in oxidative stress and the response to unfolded proteins could be found on targets affected by miR-1a (Fig. 12C). In nmf333 mice exposed to HFD, similar biological processes, such as response to oxidative stress and response to endoplasmatic reticulum (ER) stress, were enriched for targets of upregulated miRNAs including miR-1a (Fig. 12D). Based on these oppositely regulated

biological processes we reasoned that redox stress, endoplasmic reticulum stress and unfolded protein response might be affected in the left ventricles by HFD.

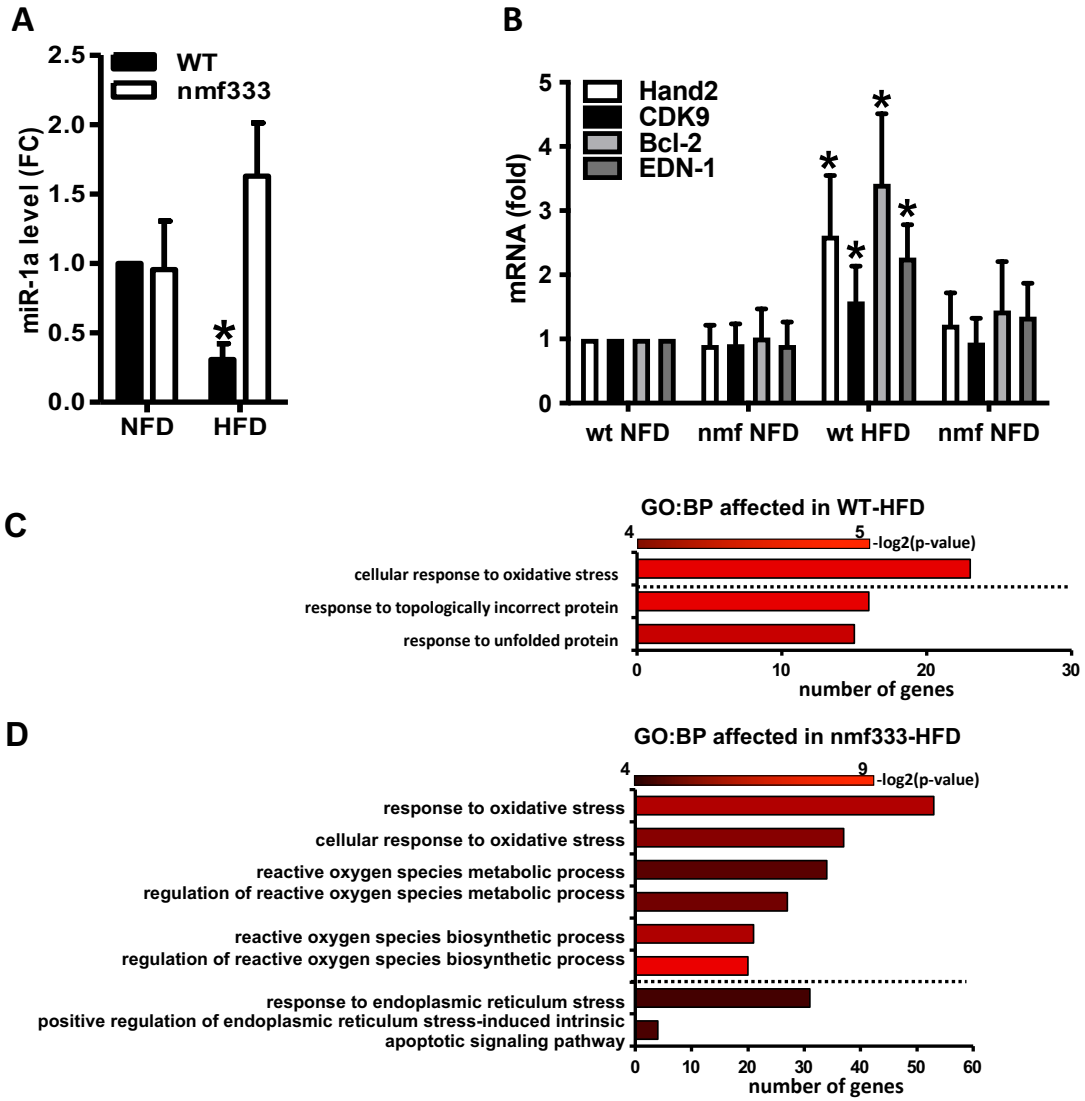


**Figure 12**. **p22phox affects expression of miR-1a and its target genes in the left ventricle in response to HFD**

C57BL/6j wild type mice (WT) and mice deficient in p22phox due to a point mutation in the *Cyba* gene (nmf333) were fed a high fat diet (HFD) for 20 weeks. Littermates were fed a regular chow (NFD) for 20 weeks. (A/B) RT-PCR analysis for miR-1a (A) and its targets HAND1, CDK9, EDN-1 and Bcl-2 (B) were performed. Data plotted as fold change compared to wildtype WT HFD (n=3-4; *p<0.05 HFD vs NFD; #p<0.05 nmf333 vs WT, SEM). (C/D) Enriched (FDR<0.05) Gene Ontology Biological Processes (GO:BP) connected to ROS or UPR for targets of downregulated miRNAs (p<0.05) in WT HFD (C) or for targets of upregulated miRNAs (p<0.05) in nmf333-HFD (D). Graph shows numbers of targets genes involved; color represents -log2 (p-value).

## 7.10 p22phox promotes left ventricular oxidative stress in response to high fat diet

To validate the biological processes dysregulated by miR-1a, oxidative stress was determined in left ventricles. Heart sections were stained for the oxidative DNA damage marker, 8-hydroxy-2-deoxyguanosine (8OHdG) (Fig. 13A/B). 8OHdG staining was increased in hearts from HFD fed wild type mice, while this response was markedly lower in hearts from HFD fed nmf333 mice (Fig. 13A/B). In line, Western blot analyses were performed on left ventricular tissue lysates with an antibody against the lipid peroxidation by-product 4-hydroxynonenal (4-HNE) (Fig. 13C/D). Indeed, 4-HNE levels were increased in hearts from HFD fed wild type mice, while this response was markedly lower in hearts from HFD fed nmf333 mice (Fig. 13C/D).

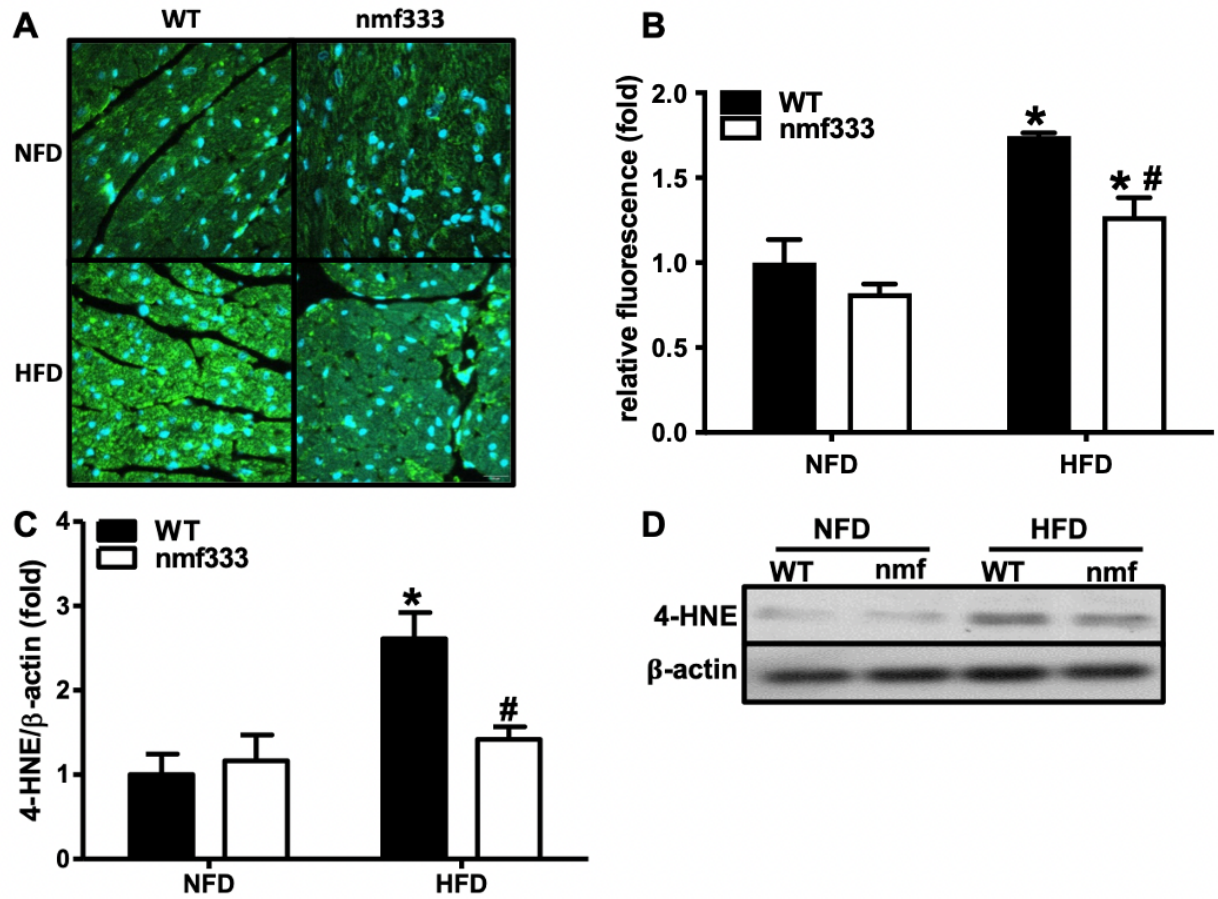


**Figure 13. p22phox promotes ROS induced DNA damage and left ventricular lipid peroxidation in response to high fat diet.** C57BL/6j wild type mice (WT) and mice deficient in p22phox due to a point mutation in the *Cyba* gene (nmf333) were fed a high fat diet (HFD) for 20 weeks. Littermates were fed normal chow (NFD). (A/B) Formalin-fixed paraffin embedded (FFPE) lung sections were stained with a primary antibody against 8-hydroxy-2-deoxyguanosine (8OHdG) and visualized with a secondary goat anti-rabbit antibody conjugated with Alexa Fluor 488. Nuclei were visualized with DAPI. Representative stainings are shown (A). Fluorescence intensity was measured in four high power fields per heart section ($n = 4$; $^{*}p < 0.05$, vs. WTNFD; $^{\#}p < 0.05$ *vs.* WTHFD) (B). (C/D) Western blot analyses were performed from heart tissue lysates using an antibody against 4-hydroxynonelal (4-HNE). β-Actin served as a loading control ($n = 3$, $^{*}p < 0.05$ WT NFD; $^{\#}p < 0.05$ *vs.* WT HFD) (C). Representative blots are shown (D). One-way ANOVA followed by Tukey's post-hoc test for multiple comparisons was used in all cases.

## 7.11 p22phox promotes oxidative stress in lungs in response to high fat diet

Similar to heart tissue, oxidative stress markers were evaluated in lung tissue in both wild type and nmf333 mice following HFD. 8OHdG staining was increased in lungs from HFD fed wild type mice, while this response was markedly lower in lungs from HFD fed

nmf333 mice (Fig. 14A/B). In line, Western blot analyses were performed on lung lysates with an antibody against the lipid peroxidation byproduct 4-hydroxynonenal (4-HNE) (Fig. 14C/D). Indeed, 4-HNE levels were increased in lungs from HFD fed wild type mice, while this response was markedly lower in lungs from HFD fed nmf333 mice (Fig. 14C/D).

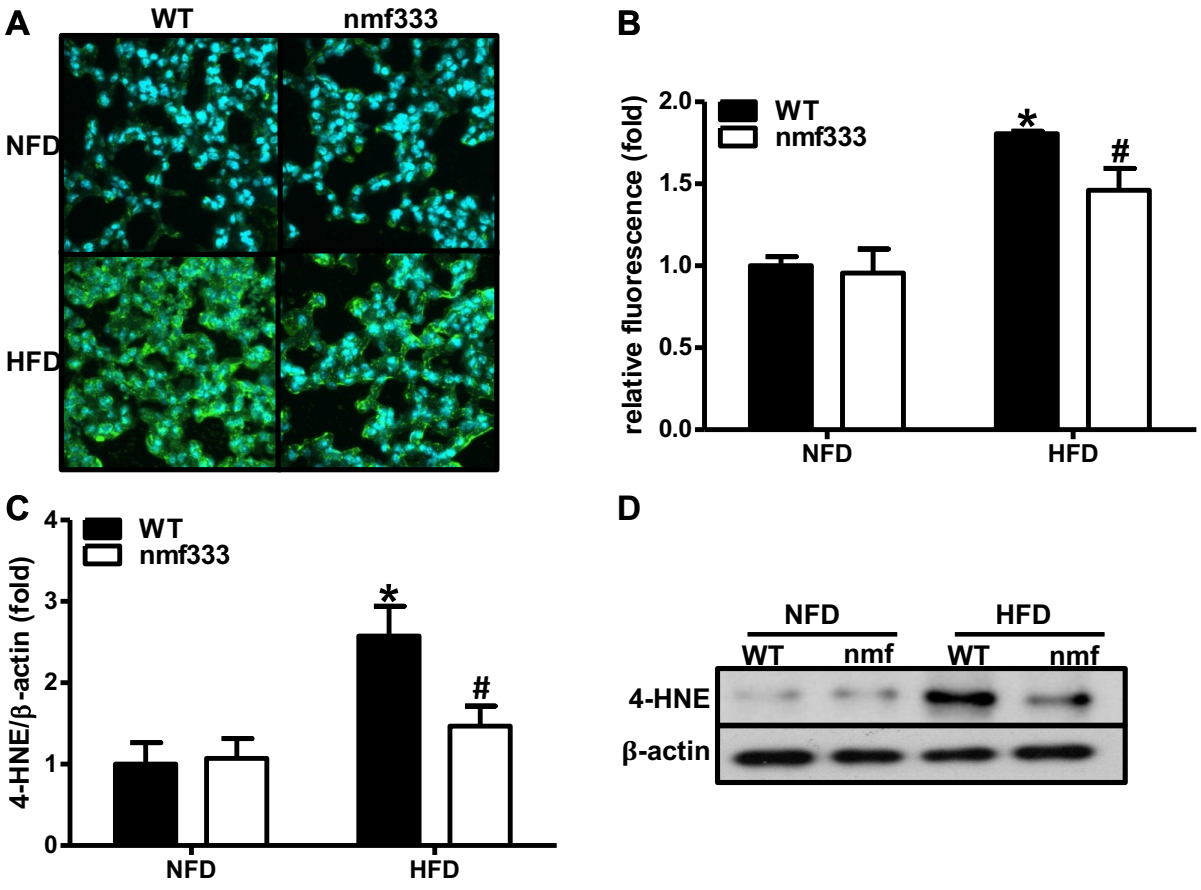


**Figure 14. p22phox promotes pulmonary lipid peroxidation and ROS-induced DNA damage in response to high fat diet.** C57BL/6j wild type mice (WT) and mice deficient in p22phox due to a point mutation in the *Cyba* gene (nmf333) were fed a high fat diet (HFD) for 20 weeks. Littermates were fed normal chow (NFD). (A/B) Formalin-fixed paraffin embedded (FFPE) lung sections were stained with an antibody against 8-hydroxy-2-deoxyguanosine (8OHdG) and visualized with a secondary goat anti-rabbit antibody conjugated with Alexa Fluor 488. Nuclei were visualized with DAPI. Representative stainings are shown (A). Fluorescence intensity was measured in four high power fields per heart section ($n = 4$; $^{*}p < 0.05$, vs. WTNFD; $^{\#}p < 0.05$ *vs.* WTHFD) (B). (C/D) Western blot analyses were performed from lung tissue lysates using an antibody against 4-hydroxynonelal (4-HNE). β-Actin served as a loading control ($n = 4$, $^{*}p < 0.05$ WT NFD; $^{\#}p < 0.05$ *vs.* WT HFD) (C). Representative blots are shown (D).

## 7.12 p22phox promotes the unfolded protein response in response to high fat diet

Since the results from the miRNAseq analysis pointed to an induction of the unfolded protein response (UPR) in the left ventricle from wild type HFD mice, Western blot analyses were performed for UPR markers in heart and lung tissues from wild type and nmf333 mice. In both heart (Fig. 15A/B) and lung (Fig. 15C/D) tissues from wild type HFD fed mice, but not from nmf333 HFD mice, protein levels of the downstream effectors of the PERK branch, activation transcription factor 4 (ATF4) and phosphorylated eukaryotic translation initiation factor 2-α (p-eIF2α), were increased. Activation transcription factor 6 (ATF6) as well as binding immunoglobulin protein (BiP) protein levels were also increased in heart and lung tissues from HFD fed wild type, but not nmf333 mice as shown by Western blot analyses. Similarly, mRNA levels of spliced X-box binding protein 1 (spXBP1), a downstream effector of the IRE-1 branch, were increased in both heart and lung tissues from wild type HFD fed mice, but not from nmf333 HFD fed mice (Fig. 15E/F). In contrast, none of these proteins or mRNA levels were significantly upregulated in nmf333 HFD mice (Fig. 15A-D).

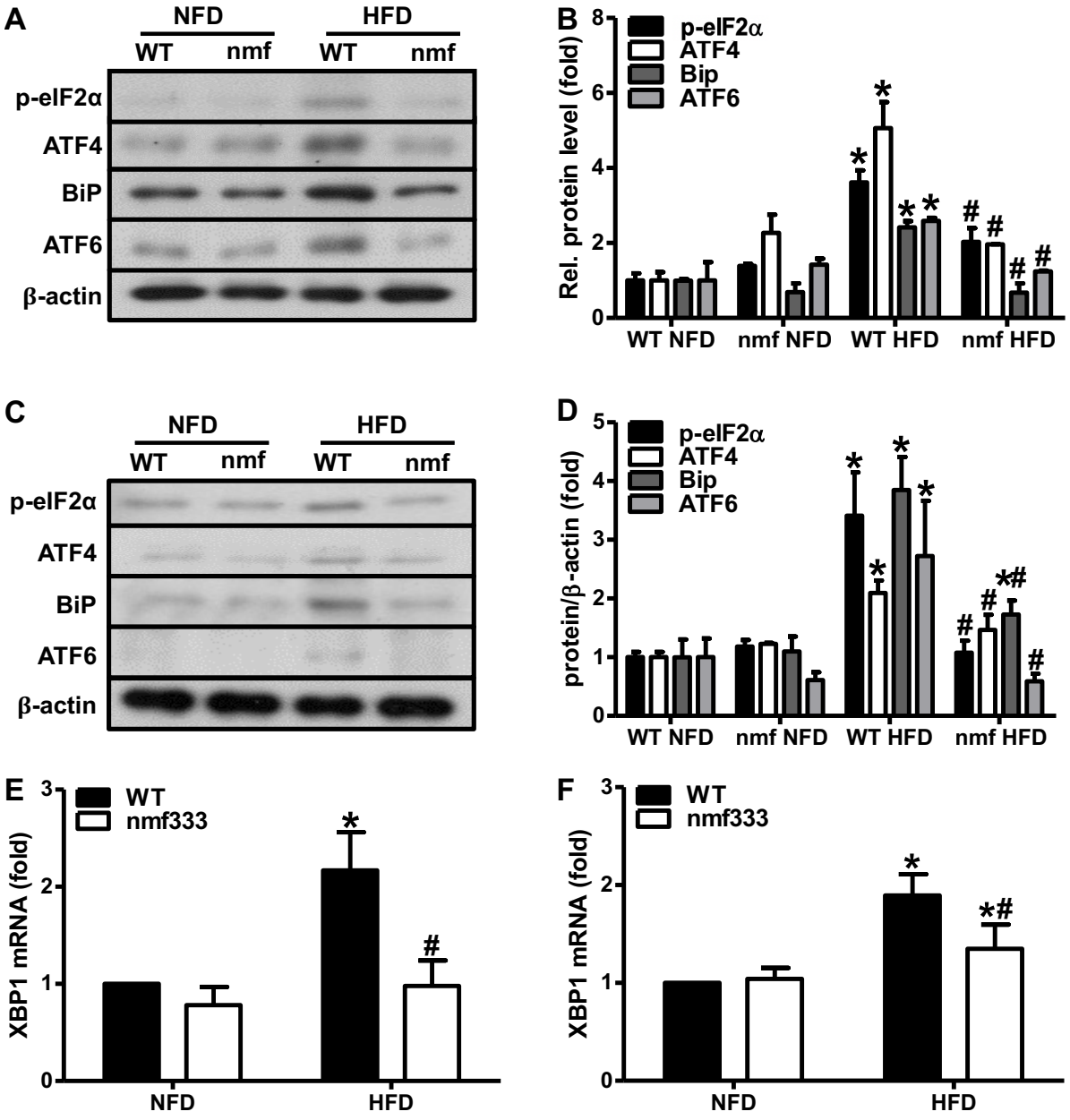


**Figure 15. p22phox promotes the unfolded protein response in hearts and lungs in response to high fat diet.** C57BL/6j wild type mice (WT) and mice deficient in p22phox due to a point mutation in the *Cyba* gene (nmf333) were fed a high fat diet (HFD) for 20 weeks. Littermates were fed normal chow (NFD). (A-D) Western blot analyses were performed on murine heart (A/B) and lung (C/D) tissues using antibodies against Binding immunoglobulin protein (BiP), activating transcription factor 6 (ATF6), activating transcription factor 4 (ATF4). β-Actin served as a loading control ($n = 6$,*$p < 0.05$ *vs.* WTCtr; #$p < 0.05$ *vs.* WTHFD). Representative blots are shown. (E/F) RT-qPCR was performed on heart (E) and lung (F) RNA using gene-specific primers for spliced Xbox binding protein 1 (spXBP1) or for 18S rRNA for normalization ($n = 3$,*$p < 0.05$ *vs.* WTNFD; $^{\#}p < 0.05$ *vs.* WTHFD). One-way ANOVA followed by Tukey's post-hoc test for multiple comparisons was used in all cases.

## 7.13 p22phox promotes apoptosis in hearts and lungs in response to high fat diet

Caspase-12 is an endoplasmic reticulum (ER) resident caspase that is cleaved and activated specifically during ER stress (UPR), but not by death receptor- or mitochondrial-mediated apoptotic signals and may function to mediate the onset of ER stress associated apoptosis (Szegezdi et al., 2006; Zhang et al., 2016). Hence, the levels of caspase 12 were evaluated to substantiate the role of the UPR in HFD. Indeed, cleavage of caspase 12 was increased in heart tissues from wild type HFD fed mice, but not from nmf333 HFD fed mice (Fig. 16 C/D).

As caspase 3 cleavage is a marker for apoptosis, the levels of the cleaved effector caspases 3 were evaluated as a measure of the potentially ongoing apoptosis. Cleaved caspase 3 levels were increased in heart tissues from wild type HFD fed mice, but not from nmf333 HFD fed mice (Fig. 16 C/D).

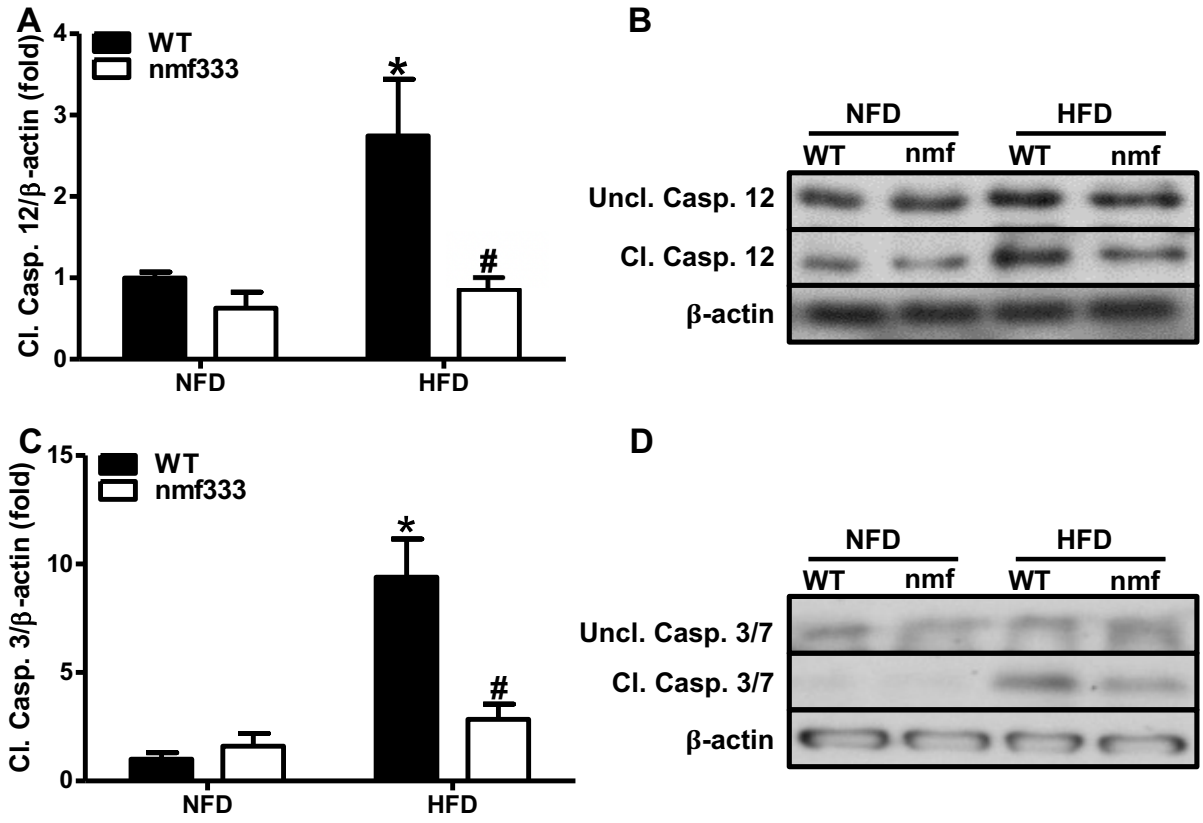


**Figure 16. p22phox promotes cardiac apoptosis in response to high fat diet.** C57BL/6j wild type mice (WT) and mice deficient in p22phox due to a point mutation in the *Cyba* gene (nmf333) were fed a high fat diet (HFD) for 20 weeks. Littermates were fed normal chow (NFD). Western blot analyses were performed on murine heart tissues using antibodies against Cleaved Caspase-3 (A/B) and Cleaved Caspase 12 (C/D). β-Actin served as a loading control ($n = 6$,*$p < 0.05$ *vs.* WTCtr; #$p < 0.05$ *vs.* WTHFD). Representative blots are shown. One-way ANOVA followed by Tukey's post-hoc test for multiple comparisons was used in all cases.

Similarly, the levels of cleaved caspase 12 and cleaved caspase 3 were elevated in the lungs from HFD fed wild type mice, but not from HFD fed nmf333 mice (Fig. 17 A-D) indicating that ER stress associated apoptosis depends on p22phox in the cardiopulmonary system in response to HFD.

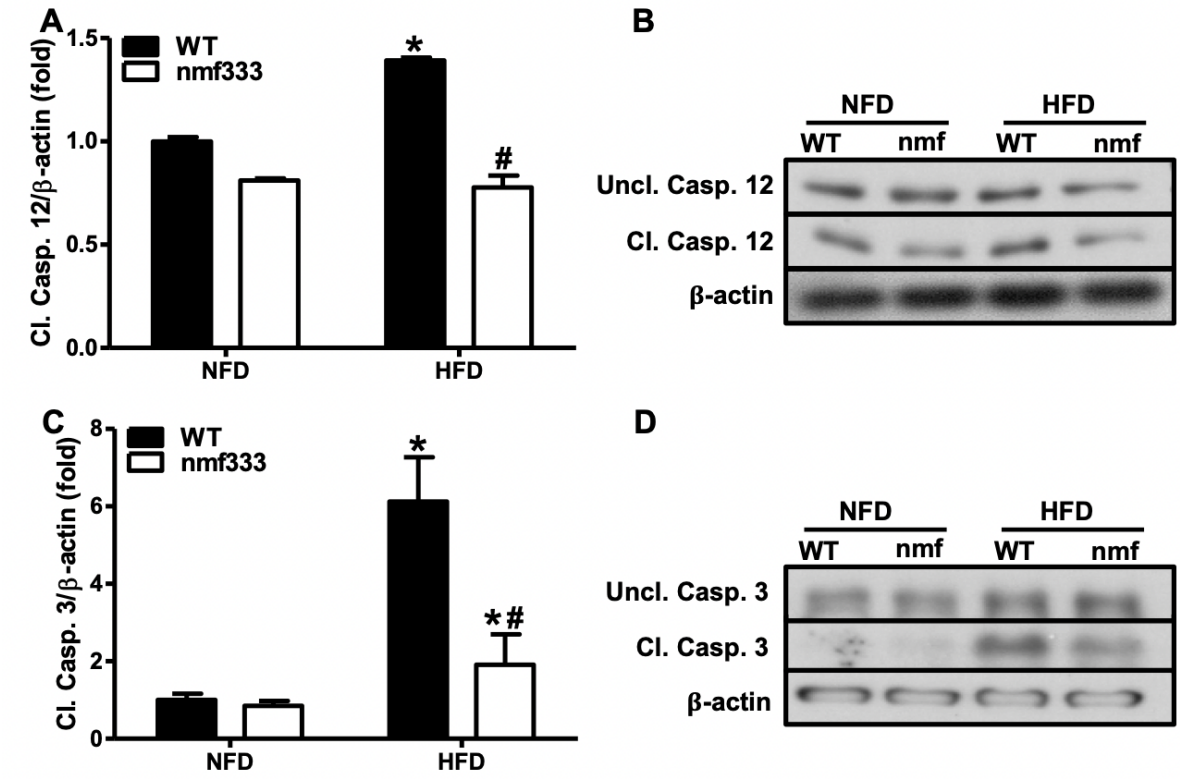


**Figure 17. p22phox promotes pulmonary apoptosis in response to high fat diet.** C57BL/6j wild type mice (WT) and mice deficient in p22phox due to a point mutation in the *Cyba* gene (nmf333) were fed a high fat diet (HFD) for 20 weeks. Littermates were fed normal chow (NFD). Western blot analyses were performed on murine lung tissues using antibodies against Cleaved Caspase-3 (A/B) and Cleaved Caspase 12 (C/D). β-Actin served as a loading control ($n = 3$,*$p < 0.05$ *vs.* WTCtr; #$p < 0.05$ *vs.* WTHFD). Representative blots are shown. One-way ANOVA followed by Tukey's post-hoc test for multiple comparisons was used in all cases.

# 8 Discussion

## 8.1 Obesity phenotype and cardiopulmonary impact

High fat diet and subsequent obesity are well known to impair cardiac metabolism, leading to heart disease, often referred to as metabolic or obesity cardiomyopathy (Dirkx et al., 2011; Perrotta et al., 2019). It is characterized by left ventricular enlargement, cardiomyocyte hypertrophy and dysfunction which can manifest as heart failure with preserved ejection fraction (HFpEF) or heart failure with reduced ejection fraction (HFrEF), also classified as diastolic and systolic dysfunction (Alpert et al., 2014; de Divitiis et al., 1981; Obokata et al., 2017).

In this study, we successfully established a murine model of obesity cardiomyopathy by exposing mice to HFD for 20 weeks. In fact, wild type mice developed an enlarged left ventricle with significant cardiomyocyte hypertrophy and left ventricular dysfunction manifested by increased left ventricular pressure and reduced ejection fraction.

In line with our findings, previous studies reported that rodents treated with high fat diet developed an increased left ventricular pressure, left ventricular remodeling and dysfunction (Christoffersen et al., 2003; Kaufman et al., 1991; Panchal et al., 2011). Several pathophysiologic mechanisms might explain the relationship between obesity and left ventricular hypertrophy. Those include metabolic changes in arterial walls leading to increased resistance in the peripheral vasculature, systemic hypertension, increased intravascular volume, nocturnal hypoxia in the context of obstructive sleep apnea, or production of myocardial growth substances by pericardial fat (Avelar et al., 2007; Corry & Tuck, 1999; Cuspidi et al., 2014). Systemic hypertension and consequently increased afterload might aggravate the effects of obesity on left ventricular hypertrophy (Schunkert, 2002). However, this effect was not confirmed in a study of mild hypertensive patients with obesity (Lauer et al., 1992). While systemic hypertension might enhance obesity induced left ventricular hypertrophy, the effects were also observed in the Birmingham Study after adjusting for age and blood pressure (Lauer et al., 1991). Thus, also direct hypertrophic effects of fat overload on cardiomyocytes, as have been observed in our study in sodium palmitate treated cardiomyocytes, have been reported and cannot be ruled out (Xue et al., 2019).

Obesity has been reported to clearly increase the risk of heart failure (Kenchaiah et al., 2002). In our study we could show that HFD treatment resulted in the development of HFrEF since fractional shortening and subsequently ejection fraction were significantly reduced.

While the association of obesity and HFpEF was confirmed by several studies, its association with HFrEF remains a controversy (Klapholz et al., 2004; Litwin, 2010; Obokata et al., 2017). A recent study underlines a greater population-attributable risk of obesity to HFpEF than HFrEF among women (Eaton et al., 2016). Later, a study of 22,681 participants showed that obesity and associated cardiometabolic traits conferred a higher risk of HFpEF than HFrEF and that obesity among women in particular seemed to predispose to future HFpEF (Savji et al., 2018). No association, however, has been described between LV function and the severity of obesity.

On a pathophysiologic level, the differences between HFpEF and HFrEF have been investigated in several human and mouse studies. HFrEF is usually associated with eccentric remodelling, normal wall thickness and left ventricular dilation, while HFpEF primarily leads to concentric hypertrophy, supported by an increased cardiomyocyte size in HFpEF compared to HFrEF (Gurusamy & Das, 2009; Simmonds et al., 2020; Tsutsui et al., 2011; van Heerebeek et al., 2006; Zile et al., 2011). However, different aetiologies might contribute to distinct types of hypertrophies in HFpEF and HFrEF. On a molecular level, insulin-like growth factor 1 (IGF-1) was reduced in HFrEF compared to HFpEF in a human study, while IGF-1 was protective against cardiomyocyte hypertrophy and oxidative stress in a murine heart failure model (Faxén et al., 2017; Simmonds et al., 2020; Vinciguerra et al., 2010). In addition, metabolic differences have been found between HFpEF and HFrEF, especially in fatty acid oxidation which is reduced in HFrEF and increased in HFpEF (De Jong & Lopaschuk, 2017).

While the development of HFrEF seems to be surprising in our model it might well be that HFpEF might have developed in an earlier stage. During the prolonged time course of high fat diet, ejection fraction might have diminished, possibly due to the development of further risk factors for HFrEF such as LV pressure overload, ischemic injury and cardiac remodeling, hypertension or even chronic kidney disease (Noll et al., 2020). In fact, our data show increased expression of cardiac remodelling markers. In support of our data, studies in rodents also described reduced ejection fraction in response to prolonged HFD (Carbone et al., 2015; Yu et al., 2021).

In line, transition of HFpEF to HFrEF has been reported, as HFpEF might in some cases be a temporary stage of ejection fraction maintenance during the initial trajectory of some diseases ultimately leading to the HFrEF phenotype (Noll et al., 2020; Savarese et al., 2019). This notion is supported by our echocardiographic data, pointing towards a concentric hypertrophy, which is more frequently associated with HFpEF. Since our mice, however, have a reduced EF, it might have developed from HFpEF with concentric hypertrophy.

In this study, we also investigated the effects of obesity on the right heart as several studies reported pulmonary vascular remodelling and pulmonary arterial hypertension in obese patients (Friedman & Andrus, 2012; Weatherald et al., 2018). Pathophysiologically, pulmonary arterial hypertension has been linked to vascular inflammation, oxidative stress and insulin resistance which all occur in obese patients. Moreover, obesity can cause cardiac (LVH, HFpEF, HFrEF) and pulmonary (obstructive sleep apnea, obesity hypoventilation syndrome, chronic thrombo-embolic pulmonary disease) conditions as substrates for pulmonary hypertension (Ayinapudi et al., 2018; Chin & Rubin, 2008; Hotamisligil, 2017; Lai et al., 2014).

HFD fed wild type mice showed signs of right ventricular hypertrophy as right ventricular cardiomyocyte diameter was increased although right ventricular mass did not show a significant increase in obese mice. Since the right ventricle is smaller than the left one and more difficult to separate, the inconsistency of our findings could be explained by small measurement errors, or by an insufficient sample size.

We further observed a slight increase in right ventricular pressure in obese wild type mice, however, not to a significant extent. A study by Chahal et al. including 4127 participants showed that obese and overweight participants had greater RV, larger RV end-diastolic volume, larger RV stroke and lower RV ejection fraction than lean participants (Chahal et al., 2012). Pathophysiologically, these findings might be explained by increased RV afterload, increased blood volume, hormonal effects, or direct obesity-related myocardial effects (Chahal et al., 2012). While several studies reported increased right ventricular pressure and hypertrophy in HFD fed mice (Gonçalves et al., 2021; Meng et al., 2017), it has been reported that not all mouse strains present with this pathophysiology after HFD feeding (Agrawal et al., 2019). Thus, the mouse strain used in this study might not have been susceptible to right ventricular dysfunction following HFD.

However, we could show that obese mice developed pulmonary vascular remodelling as has been described previously in mice fed a HFD for 20 weeks (Kelley et al., 2014; Mair et al., 2019).
As our mouse strain seems to be less susceptible to develop right ventricular dysfunction following HFD it might thus be that HFD feeding was not long enough to induce full left to right ventricle transition that would result in a fully developed pulmonary hypertensive phenotype.

## 8.2 NADPH oxidase derived ROS generation in high fat diet and promotion of cardiovascular phenotype

High fat diet and obesity have been reported to promote a state of oxidative stress in several organs including the cardiovascular system (McMurray et al., 2016).
In our study we could demonstrate that HFD induced oxidative stress not only in the heart as has been described previously in several animal models (Matsuda & Shimomura, 2014), but also in the lungs.
Our study in isolated cardiomyocytes showed that sodium-palmitate treatment primarily induced ROS generation by NADPH oxidases. This is in line with previous studies showing an increased ROS production in H9C2 cells via NOX2 (Jaishy et al., 2015; Yang et al., 2019) or NOX4 (Geng et al., 2019) after sodium-palmitate exposition.
In our animal model we could also show increased levels of p22phox, NOX2 and NOX4 in heart and lungs from HFD treated mice while NOX1 protein levels were not elevated. In line, a recent study showed increased left ventricular NOX2 protein levels in high fat diet induced LVH (Bhatti & Li, 2020). Other studies showed elevated levels of p22phox and NOX4 in obese hearts (Ge et al., 2019; Geetha et al., 2015). While NOX1 levels were elevated in diabetic cardiomyopathy as well as in the vasculature and in the kidney in diabetic rats (Thompson et al., 2017), and deletion of NOX1 prevented concentric diabetic cardiomyopathy (Xu et al., 2021; Zhang et al., 2022) and improved microvascular function in obese db/db mice (Thompson et al., 2017), expression and role of NOX1 in obesity cardiomyopathy remain to be further elucidated.
In order to investigate the role of NADPH oxidases in obesity cardiomyopathy, we used nmf333 mice which lost p22phox due to the Y121H mutation in the CYBA gene (Nakano et al., 2008). It has been demonstrated that NOX1, NOX2 and NOX4 interact with

p22phox to form a functionally active enzyme (Ambasta et al., 2004; Nakano et al., 2008; Yu et al., 1998). A loss of function of the p22phox protein in the nmf333 mouse model subsequently leads to a loss of function of NOX1 and NOX2 dependent NADPH oxidases while the function of NOX4 seems to remain preserved (von Löhneysen et al., 2008).

Upon HFD treatment body weight gain was not significantly lower in p22phox deficient mice than in wildtype mice. In contrast, smooth muscle specific knock out of p22phox as well as deletion of p22phox in the hypothalamus have been reported to prevent weight gain upon 6 weeks or 10 weeks treatment with HFD, respectively (Lob et al., 2017; Youn et al., 2014). While the reasons for this discrepancy are not fully elucidated, our study clearly shows that p22phox deficient mice were protected against the development of obesity cardiomyopathy since they did not develop left ventricular hypertrophy, remodelling and heart failure.

While this is to our knowledge the first study demonstrating a functional role of p22phox in obesity cardiomyopathy, it has been previously shown that NOX2 knock out mice were protected against high fat diet induced LVH (Bhatti & Li, 2020) and LV dysfunction (Hafstad et al., 2020) suggesting that p22phox might contribute to obesity cardiomyopathy via NOX2.

In line, several studies underline a role of p22phox and NOX2 in vascular and metabolic consequences of high fat diet (De Figueiredo et al., 2015; Joseph et al., 2019; Sukumar et al., 2013; Youn et al., 2014). Also insulin signaling in cardiomyocytes was reported to be mediated by NOX2 and NOX4 derived ROS (Steinhorn et al., 2017).

In support we showed that cardiac NOX4 protein levels were upregulated after high fat diet, while this response was prevented in p22phox deficient mice. As p22phox deficient mice were protected against obesity cardiomyopathy these data suggest that NOX4 might also contribute to cardiac dysfunction in obesity. Although no loss in NOX4 function has been reported in nmf333 mice (von Löhneysen et al., 2008), it might well be that the loss of ROS production in nmf333 hearts also decreased NOX4 levels as NOX4 expression has been shown to be redox sensitive (Colston et al., 2005; Pendyala & Natarajan, 2010).

While to our knowledge there are no studies on the role of NOX4 in obesity cardiomyopathy several studies investigated the role of NOX4 in different responses to high fat diet. NOX4-deficient mice displayed latent adipose tissue accumulation and

were susceptible to diet-induced obesity and early onset insulin resistance (Trayhurn et al., 2009).

NOX4 deficiency was further reported to promote atherosclerosis in high fat diet fed ApoE$^{-/-}$ mice or LDL receptor deficient mice (Langbein et al., 2016; Schürmann et al., 2015). In contrast, another group reported that NOX4 deficiency in adipocytes protected from high fat diet induced insulin resistance (Den Hartigh et al., 2017). In contrast, other studies reported that NOX4 promotes cardiac dysfunction in models of cardiac overload (Kuroda et al., 2010; Zhang et al., 2018). However, whether NOX4 has protective or damaging effects in the development of cardiac dysfunction, and more specifically in obesity induced cardiac dysfunction, remains unclear (Morawietz, 2011, 2018).

## 8.3 miRNA1-a and its targets are dysregulated in vivo dependent on NADPH oxidases

In our study, miRNA-seq analysis performed on left ventricular tissues showed differentially regulated miRNA profiles between wild type and p22phox deficient mice, as well as between normal chow and HFD fed mice. Verified by qPCR, our data indicated that miR-1a was downregulated in HFD treated wild type mice, whereas miR-1a levels remained unchanged in the normal chow groups. miRNAs of the miR-1a precursor family have pivotal roles in development and physiology of muscle tissues including the heart (Mishima et al., 2007). While miR-1 is known to play an important role in heart diseases such as hypertrophy, myocardial infarction, and arrhythmias (Cai et al., 2010; Silvestri et al., 2009; Zorio et al., 2009), recent data show that miR-1 is closely associated with hypertrophic development in cardiac tissue (Care et al., 2007; Karakikes et al., 2013; Q. Li et al., 2010). Mechanistically, reduced levels of miR-1a have been shown to induce cardiac hypertrophy, while overexpression of miR-1a proved to be protective (Care et al., 2007; Sayed et al., 2007). In line, in our study LVH was associated with decreased levels of miR-1a.

Furthermore, known miR-1a target genes were upregulated in LVH induced by HFD in our study: Heart and neural crest-derived transcript 2 (HAND2) has been described to promote cardiac hypertrophy, adult and embryonic heart failure (Srivastava et al., 1997; Thattaliyath et al., 2002) and plays an important role in cardiogenesis by promoting

ventricular cardiomyocyte expansion (Zhao et al., 2005) as well as in angiotensin-II-induced cardiac hypertrophy (Yu et al., 2019).

Cyclin-dependent kinase 9 (CDK9) has been shown to induce cardiac hypertrophy (Sano et al., 2002) and heart failure (Sano et al., 2004), and has been identified as a possible therapeutic target in heart failure and cardiac hypertrophy. While CDK9 has been described as a target of miR-1a (Takaya et al., 2009), it has also been reported that upregulation of CDK9 precedes miR-1 overexpression during cardiac differentiation in embryonic stem cells (Tarhriz et al., 2018).

B-cell lymphoma 2 (Bcl-2) is an important regulator of programmed cell death (Zhai et al., 2015), and has been linked to end stage heart failure (Latif et al., 2000).

Endothelin 1 (EDN1) is important for the regulation of endothelial function and has been associated with LV hypertrophy (Castro et al., 2007).

While this is to our knowledge the first report linking obesity-induced cardiac pathologies to miR-1a dysregulation, it has recently been shown that miR-1a expression is reduced in skeletal muscle of obese mice and treatment with miR-1a improved insulin resistance in skeletal muscle (Rodrigues et al., 2021). These findings support the notion that dysregulation of miR-1a and its target genes might contribute to obesity cardiomyopathy in our model system. Importantly, while miR-1a levels were not affected in untreated p22phox deficient mice, downregulation by obesity was completely abolished in these mice. In line, high fat diet induced upregulation of mir-1a target genes was prevented in p22phox deficient mice. This suggests that miR-1a is regulated by p22phox and might be susceptible to ROS in the context of obesity subsequently promoting the development of cardiac hypertrophy and dysfunction. Interestingly, a recent study showed that miR-1a is susceptible to oxidation in a redox sensitive model of cardiac hypertrophy and that oxidized miR-1a is able to promote cardiac hypertrophy (Seok et al., 2020). Thus, oxidation of miR-1a by p22phox-dependent ROS might be an important mechanism in promoting obesity cardiomyopathy, and modulation of miR-1a levels might be a future therapeutic approach in the development of obesity-induced cardiac dysfunction. However, further studies are needed to identify precise mechanisms.

## 8.4 High fat diet promotes UPR via NADPH oxidases

Analysis of our miRNA sequencing data further suggested that p22phox-dependent downregulation of miR-1a might affect various pathways known to promote the consequences of obesity in the heart including ROS signalling, ER stress/UPR and apoptosis (Cai et al., 2010; Cai & Kang, 2001, 2003; Ren et al., 2021).

As discussed above, our findings showed that ROS levels and lipid peroxidation are enhanced in obesity cardiomyopathy in a p22phox-dependent manner.

ROS are closely linked to ER stress and are fundamental elements of acute and chronic UPR signaling (Ozgur et al., 2018). The relationship between endoplasmic reticulum stress, activation of the UPR, and ROS has been described in several studies (Eletto et al., 2014). Excessive ROS production has been shown to increase the load of unfolded proteins, leading to UPR (Alfadda & Sallam, 2012).

High fat diet and subsequent obesity have been associated with several pathophysiologic mechanisms which might lead to ER stress. Those include hyperglycemia, hyperlipidemia or pressure overload (Toth et al., 2007; Xu et al., 2012). All of them can lead to ROS production promoting the accumulation of unfolded proteins (Minamino et al., 2010). Indeed, we observed increased levels of surrogate markers for oxidative stress like 4-HNE and 8-OHdG in hearts and lungs of HFD-treated mice. In line, cardiomyocytes showed increased superoxide production after sodium-palmitate stimulation.

We have substantiated the importance of UPR in hearts and lungs since phosphorylation of eIF2α was induced in HFD WT mice in comparison to control littermates. Furthermore, both ATF4- and ATF6-branches of the UPR pathway were induced in hearts and lungs dependent on p22phox. In addition, we have observed increased levels of XBP1 in hearts and lungs from obese wild type mice. In support, ER stress in the heart was observed in mice fed a HFD for 42 weeks (Che et al., 2018).

Importantly, p22phox deficient mice did not develop ER stress in hearts and lungs in response to HFD. This is in line with previous studies demonstrating that p22phox promotes ER stress and the UPR in heart and lungs exposed to hypoxia (Petry et al., 2018). On the other hand, ER stress has been shown to induce p22phox-dependent ROS production, indicating a positive feedback mechanism (Petry et al., 2018).

A similar cross talk has been described for NOX2 in the kidney (G. Li et al., 2010) and 7-ketocholesterol induced ER-stress in aortic smooth muscle cells via activation of both NOX2 and NOX4 (Pedruzzi et al., 2004).

It has been suggested that a significant portion of ROS production under ER stress condition is attributable to NOX4 (Santos et al., 2009). Similarly, we observed a significant increase in NOX4 protein levels. While a detrimental effect of NADPH oxidases including NOX4 has been widely accepted, previous studies also reported protective effects by NOX4 activation (Schröder et al., 2012). NOX4 has been shown to interact with the ER, allowing for an enhanced stress signaling response and cell survival (Santos et al., 2016). In contrast, several other studies have also suggested protective NOX4 effects against ER stress in murine hearts in various pathologies (Hansen et al., 2018; Matsushima et al., 2013; Zhang et al., 2010).

Although the mechanisms linking the different NOXes to UPR still need further understanding, our results underline a crucial role of p22phox-dependent NADPH oxidases in cardiac and pulmonary ER-stress induced by HFD feeding.

In line, ER stress and the UPR have been discussed to be prominent mechanisms in cardiac and pulmonary vascular remodeling in response to obesity and high fat diet (Amen et al., 2019; Shah et al., 2017). Recent studies have linked ER-stress/UPR to the metabolic syndrome including obesity, insulin resistance, and to heart failure (Mohan et al., 2019; Ochoa et al., 2018). The UPR has been discovered as key player in metabolic and lipid homeostasis (Achard & Laybutt, 2012), while it also contributed to the development of insulin resistance (Samuel & Shulman, 2012).

In line with our study increased levels of ER stress marker proteins GRP78/BiP, p-PERK, ATF6 and CHOP were found in the atrial myocardium from mice exposed to HFD and GRP78/BiP and CHOP levels were elevated in atrial biopsies from overweight patients (Zhang et al., 2020). Another study showed increased levels of the ER stress markers Bip, p-eIF2α and pPERK in the hearts from ob/ob mice (Ceylan-Isik et al., 2011). EDN1 which has been linked to the UPR response in hepatocarcinoma (Lu et al., 2014), was also dysregulated by p22phox in obesity cardiomyopathy in our study.

In addition, cardiac UPR has been investigated in heart failure and cardiac dysfunction models. PERK phosphorylation and ATF6, but not IRE-1α-XBP1, were shown to play important roles in ER stress-mediated diabetic cardiomyopathy in non-obese type 2 DM (Lakshmanan et al., 2013). STZ-induced diabetes also increased CHOP and caspase 12 levels in the heart (Xu et al., 2009).

In line, caspase 12 levels were also increased in the hearts of HFD fed wild type but not nmf333 mice. ER stress activates caspase 12, which is released to the cytoplasm initiating the proapoptotic cascade involving caspases 3 and 7 (Szegezdi et al., 2003). In support, p22phox-dependent activation of caspases 3 and 7 was observed in hearts and lungs from HFD fed mice. In support, high fat diet has been previously shown to induce apoptosis in several organs including the heart, and ROS have been implicated in this process (Dirkx et al., 2011). Furthermore, apoptosis has been considered an early event in the development of metabolic cardiomyopathy (Gürtl et al., 2009) and has been identified in patients with heart failure (Kang & Izumo, 2000). Although apoptosis in failing hearts might be associated with loss of some cardiomyocytes leading to heart dysfunction (Kumar et al., 2002; NEVIÈRE et al., 2001), the exact link between apoptosis and heart failure, in particular in the context of obesity, remains to be elucidated.

Surprisingly, p22phox also promoted the induction of the anti-apoptotic protein Bcl-2 in hearts from HFD fed mice in our study. Bcl2 has been described to reduce caspase 12 cleavage and thereby to abrogate caspase 3 cleavage and apoptosis (Donovan & Cotter, 2004). However, it has also been reported that under states of oxidative stress, overexpression of Bcl-2 functions as a redox sink to prevent excessive formation of ROS (Jang & Surh, 2003). Thus, elevated levels of Bcl2 might be the result of a compensatory answer towards NADPH oxidase activation in the obese heart.

Taken together, the findings in this study showed that p22phox-dependent NADPH oxidases mediate high fat diet induced ROS generation leading to downregulation of miR-1a in the heart, the induction of ER stress and the UPR and finally to apoptosis (Fig. 18). These pathways might contribute to the development of left ventricular hypertrophy and dysfunction, eventually also affecting the pulmonary vasculature and the right heart. Thus, targeting p22phox-dependent NADPH oxidases might serve as an interesting therapeutic target in obesity-induced cardiomyopathy.

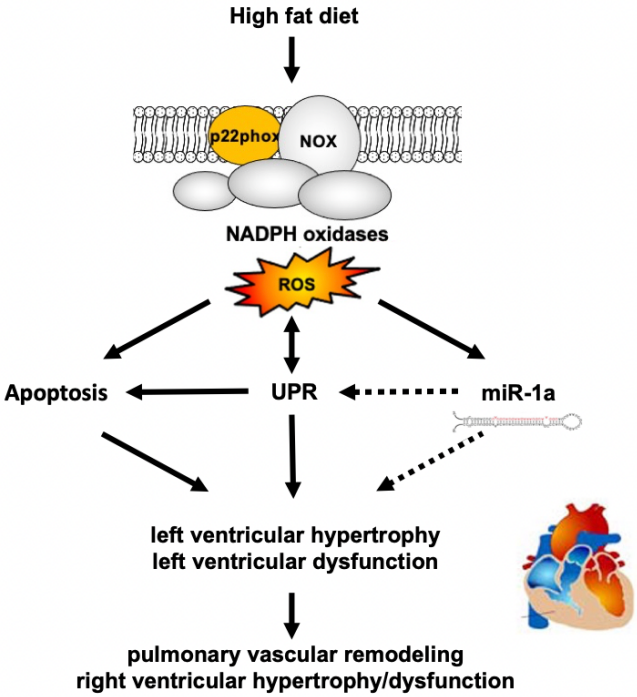


**Figure 18. p22phox-dependent NADPH oxidases mediate high fat diet induced cardiomyopathy.** NADPH oxidase dependent ROS generation leads to downregulation of miR-1a in the heart, as well as to ER stress, UPR and apoptosis. These pathways might result in obesity cardiomyopathy with left ventricular dysfunction and pulmonary vascular remodelling.

# 9 Acknowledgements

I would like to acknowledge and give my warmest thanks to the people that have supported me over the course of this doctoral program. Your support, guidance and advice have helped me get through the lows and made the highs feel even more special. I would like to express my gratitude to my supervisor, Dr. Damir Kračun, for his guidance and support throughout my research. I also extend my sincere thanks to Dr. Andreas Petry and Prof. Agnes Görlach for their valuable insights, guidance and expertise.

Last but certainly not least, I would like to express my deepest gratitude to my parents, relatives and friends for their continuous support and understanding during these last years. I would like to thank my parents for their love, support, and encouragement throughout my academic journey. Their belief in me and my abilities has been a constant source of motivation, and I am deeply grateful for all that they have done for me. I could not have completed this thesis without their unwavering support. Thank you to my Mom for all her efforts to make this process as smooth as possible for me, my Dad for his infinite optimism and faith in me, my brothers for their support and help whenever and wherever, and Liz, my safe haven.

# 10 Literature


Achard, C. S., & Laybutt, D. R. (2012). Lipid-induced endoplasmic reticulum stress in liver cells results in two distinct outcomes: adaptation with enhanced insulin signaling or insulin resistance. *Endocrinology*, *153*(5), 2164-2177.

Adams, J. M., & Cory, S. (1998). The Bcl-2 protein family: arbiters of cell survival. *Science*, *281*(5381), 1322-1326.

Aggarwal, S., Gross, C. M., Sharma, S., Fineman, J. R., & Black, S. M. (2013). Reactive oxygen species in pulmonary vascular remodeling. *Comprehensive Physiology*, *3*(3), 1011-1034.

Ago, T., Kitazono, T., Kuroda, J., Kumai, Y., Kamouchi, M., Ooboshi, H., Wakisaka, M., Kawahara, T., Rokutan, K., & Ibayashi, S. (2005). NAD (P) H oxidases in rat basilar arterial endothelial cells. *Stroke*, *36*(5), 1040-1046.

Agrawal, V., Fortune, N., Yu, S., Fuentes, J., Shi, F., Nichols, D., Gleaves, L., Poovey, E., Wang, T. J., & Brittain, E. L. (2019). Natriuretic peptide receptor C contributes to disproportionate right ventricular hypertrophy in a rodent model of obesity-induced heart failure with preserved ejection fraction with pulmonary hypertension. *Pulmonary circulation*, *9*(4), 2045894019878599.

Alfadda, A. A., & Sallam, R. M. (2012). Reactive oxygen species in health and disease. *Journal of Biomedicine and Biotechnology*, *2012*.

Alpert, M. A., Omran, J., Mehra, A., & Ardhanari, S. (2014). Impact of obesity and weight loss on cardiac performance and morphology in adults. *Progress in cardiovascular diseases*, *56*(4), 391-400.

Ambasta, R. K., Kumar, P., Griendling, K. K., Schmidt, H. H., Busse, R., & Brandes, R. P. (2004). Direct interaction of the novel Nox proteins with p22phox is required for the formation of a functionally active NADPH oxidase. *Journal of Biological Chemistry*, *279*(44), 45935-45941.

Amen, O. M., Sarker, S. D., Ghildyal, R., & Arya, A. (2019). Endoplasmic reticulum stress activates unfolded protein response signaling and mediates inflammation, obesity, and cardiac dysfunction: therapeutic and molecular approach. *Frontiers in pharmacology*, *10*.

Anderson, E. J., Lustig, M. E., Boyle, K. E., Woodlief, T. L., Kane, D. A., Lin, C.-T., Price, J. W., Kang, L., Rabinovitch, P. S., & Szeto, H. H. (2009). Mitochondrial H 2 O 2 emission and cellular redox state link excess fat intake to insulin resistance in both rodents and humans. *The Journal of clinical investigation*, *119*(3), 573-581.

Ashkenazi, A., & Dixit, V. M. (1998). Death receptors: signaling and modulation. *science*, 1305-1308.

Avelar, E., Cloward, T. V., Walker, J. M., Farney, R. J., Strong, M., Pendleton, R. C., Segerson, N., Adams, T. D., Gress, R. E., & Hunt, S. C. (2007). Left ventricular hypertrophy in severe obesity: interactions among blood pressure, nocturnal hypoxemia, and body mass. *Hypertension*, *49*(1), 34-39.

Ayinapudi, K., Singh, T., Motwani, A., Le Jemtel, T. H., & Oparil, S. (2018). Obesity and pulmonary hypertension. *Current hypertension reports*, *20*(12), 1-8.

Babior, B., Lambeth, J., & Nauseef, W. (2002). The neutrophil NADPH oxidase. *Archives of biochemistry and biophysics*, *397*(2), 342-344.

Baena-Díez, J. M., Byram, A. O., Grau, M., Gómez-Fernández, C., Vidal-Solsona, M., Ledesma-Ulloa, G., González-Casafont, I., Vasquez-Lazo, J., Subirana, I., & Schroder, H. (2010).

Obesity is an independent risk factor for heart failure: Zona Franca Cohort study. *Clinical cardiology*, *33*(12), 760-764.

Bánfi, B., Clark, R. A., Steger, K., & Krause, K.-H. (2003). Two novel proteins activate superoxide generation by the NADPH oxidase NOX1. *Journal of Biological Chemistry*, *278*(6), 3510-3513.

Bánfi, B., Malgrange, B., Knisz, J., Steger, K., Dubois-Dauphin, M., & Krause, K.-H. (2004). NOX3, a superoxide-generating NADPH oxidase of the inner ear. *Journal of Biological Chemistry*, *279*(44), 46065-46072.

Bánfi, B., Molnár, G., Maturana, A., Steger, K., Hegedûs, B., Demaurex, N., & Krause, K.-H. (2001). A Ca2+-activated NADPH oxidase in testis, spleen, and lymph nodes. *Journal of Biological Chemistry*, *276*(40), 37594-37601.

Bartsch, H., & Nair, J. (2006). Chronic inflammation and oxidative stress in the genesis and perpetuation of cancer: role of lipid peroxidation, DNA damage, and repair. *Langenbeck's Archives of Surgery*, *391*(5), 499-510.

Bataller, R., Schwabe, R. F., Choi, Y. H., Yang, L., Paik, Y. H., Lindquist, J., Qian, T., Schoonhoven, R., Hagedorn, C. H., & Lemasters, J. J. (2003). NADPH oxidase signal transduces angiotensin II in hepatic stellate cells and is critical in hepatic fibrosis. *The Journal of clinical investigation*, *112*(9), 1383-1394.

Bedard, K., Jaquet, V., & Krause, K.-H. (2012). NOX5: from basic biology to signaling and disease. *Free Radical Biology and Medicine*, *52*(4), 725-734.

Bedard, K., & Krause, K.-H. (2007). The NOX family of ROS-generating NADPH oxidases: physiology and pathophysiology. *Physiological reviews*, *87*(1), 245-313.

BelAiba, R. S., Djordjevic, T., Petry, A., Diemer, K., Bonello, S., Banfi, B., Hess, J., Pogrebniak, A., Bickel, C., & Görlach, A. (2007). NOX5 variants are functionally active in endothelial cells. *Free Radical Biology and Medicine*, *42*(4), 446-459.

Bendall, J. K., Cave, A. C., Heymes, C., Gall, N., & Shah, A. M. (2002). Pivotal role of a gp91phox-containing NADPH oxidase in angiotensin II-induced cardiac hypertrophy in mice. *Circulation*, *105*(3), 293-296.

Bertram, K., Valcu, C.-M., Weitnauer, M., Linne, U., & Görlach, A. (2015). NOX1 supports the metabolic remodeling of HepG2 cells. *PloS one*, *10*(3), e0122002.

Bezawork-Geleta, A., Rohlena, J., Dong, L., Pacak, K., & Neuzil, J. (2017). Mitochondrial complex II: at the crossroads. *Trends in biochemical sciences*, *42*(4), 312-325.

Bhatti, S. N., & Li, J.-M. (2020). Nox2 dependent redox-regulation of Akt and ERK1/2 to promote left ventricular hypertrophy in dietary obesity of mice. *Biochemical and Biophysical Research Communications*, *528*(3), 506-513.

Biberstine-Kinkade, K. J., DeLeo, F. R., Epstein, R. I., LeRoy, B. A., Nauseef, W. M., & Dinauer, M. C. (2001). Heme-ligating Histidines in Flavocytochromeb 558 IDENTIFICATION OF SPECIFIC HISTIDINES IN gp91 phox. *Journal of Biological Chemistry*, *276*(33), 31105-31112.

Birben, E., Sahiner, U. M., Sackesen, C., Erzurum, S., & Kalayci, O. (2012). Oxidative stress and antioxidant defense. *World Allergy Organization Journal*, *5*(1), 9-19.

Boden, G., Duan, X., Homko, C., Molina, E. J., Song, W., Perez, O., Cheung, P., & Merali, S. (2008). Increase in endoplasmic reticulum stress–related proteins and genes in adipose tissue of obese, insulin-resistant individuals. *Diabetes*, *57*(9), 2438-2444.

Bonomini, F., Rodella, L. F., & Rezzani, R. (2015). Metabolic syndrome, aging and involvement of oxidative stress. *Aging and disease*, *6*(2), 109.

Brand, M. D. (2016). Mitochondrial generation of superoxide and hydrogen peroxide as the source of mitochondrial redox signaling. *Free Radical Biology and Medicine*, *100*, 14-31.

Brar, S. S., Kennedy, T. P., Sturrock, A. B., Huecksteadt, T. P., Quinn, M. T., Whorton, A. R., & Hoidal, J. R. (2002). An NAD (P) H oxidase regulates growth and transcription in melanoma cells. *American Journal of Physiology-Cell Physiology*, *282*(6), C1212-C1224.

Brewer, A. C., Murray, T. V., Arno, M., Zhang, M., Anilkumar, N. P., Mann, G. E., & Shah, A. M. (2011). Nox4 regulates Nrf2 and glutathione redox in cardiomyocytes in vivo. *Free Radical Biology and Medicine*, *51*(1), 205-215.

Brown, D. I., & Griendling, K. K. (2009). Nox proteins in signal transduction. *Free Radical Biology and Medicine*, *47*(9), 1239-1253.

Bult, C. J., Blake, J. A., Smith, C. L., Kadin, J. A., & Richardson, J. E. (2019). Mouse genome database (MGD) 2019. *Nucleic acids research*, *47*(D1), D801-D806.

Buul, J. v., Fernandez-Borja, M., Anthony, E., & Hordijk, P. (2005). Expression and localization of NOX2 and NOX4 in primary human endothelial cells. *Antioxidants & redox signaling*, *7*(3-4), 308-317.

Cadenas, E., & Davies, K. J. (2000). Mitochondrial free radical generation, oxidative stress, and aging. *Free Radical Biology and Medicine*, *29*(3-4), 222-230.

Cai, B., Pan, Z., & Lu, Y. (2010). The roles of microRNAs in heart diseases: a novel important regulator. *Current medicinal chemistry*, *17*(5), 407-411.

Cai, L., & Kang, Y. J. (2001). Oxidative stress and diabetic cardiomyopathy. *Cardiovascular toxicology*, *1*(3), 181-193.

Cai, L., & Kang, Y. J. (2003). Cell death and diabetic cardiomyopathy. *Cardiovascular toxicology*, *3*(3), 219-228.

Campia, U., Tesauro, M., & Cardillo, C. (2012). Human obesity and endothelium-dependent responsiveness. *British journal of pharmacology*, *165*(3), 561-573.

Carbone, S., Lavie, C. J., & Arena, R. (2017). Obesity and heart failure: focus on the obesity paradox. Mayo Clinic Proceedings,

Carbone, S., Mauro, A. G., Mezzaroma, E., Kraskauskas, D., Marchetti, C., Buzzetti, R., Van Tassell, B. W., Abbate, A., & Toldo, S. (2015). A high-sugar and high-fat diet impairs cardiac systolic and diastolic function in mice. *International journal of cardiology*, *198*, 66-69.

Care, A., Catalucci, D., Felicetti, F., Bonci, D., Addario, A., Gallo, P., Bang, M.-L., Segnalini, P., Gu, Y., & Dalton, N. D. (2007). MicroRNA-133 controls cardiac hypertrophy. *Nature medicine*, *13*(5), 613.

Castro, M., Rodríguez-Pascual, F., Magán-Marchal, N., Reguero, J., Alonso-Montes, C., Moris, C., Alvarez, V., Lamas, S., & Coto, E. (2007). Screening of the endothelin1 gene (EDN1) in a cohort of patients with essential left ventricular hypertrophy. *Annals of human genetics*, *71*(5), 601-610.

Cecchini, G. (2003). Function and structure of complex II of the respiratory chain. *Annual review of biochemistry*, *72*(1), 77-109.

Ceriello, A., & Motz, E. (2004). Is oxidative stress the pathogenic mechanism underlying insulin resistance, diabetes, and cardiovascular disease? The common soil hypothesis revisited. *Arteriosclerosis, thrombosis, and vascular biology*, *24*(5), 816-823.

Ceylan-Isik, A. F., Sreejayan, N., & Ren, J. (2011). Endoplasmic reticulum chaperon tauroursodeoxycholic acid alleviates obesity-induced myocardial contractile dysfunction. *Journal of molecular and cellular cardiology*, *50*(1), 107-116.

Chahal, H., McClelland, R. L., Tandri, H., Jain, A., Turkbey, E. B., Hundley, W. G., Barr, R. G., Kizer, J., Lima, J. A., & Bluemke, D. A. (2012). Obesity and right ventricular structure and function: the MESA-Right Ventricle Study. *Chest*, *141*(2), 388-395.

Chalupsky, K., Kračun, D., Kanchev, I., Bertram, K., & Görlach, A. (2015). Folic acid promotes recycling of tetrahydrobiopterin and protects against hypoxia-induced pulmonary hypertension by recoupling endothelial nitric oxide synthase. *Antioxidants & redox signaling*, *23*(14), 1076-1091.

Che, Y., Wang, Z. P., Yuan, Y., Zhang, N., Jin, Y. G., Wan, C. X., & Tang, Q. Z. (2018). Role of autophagy in a model of obesity: A long-term high fat diet induces cardiac dysfunction. *Molecular medicine reports*, *18*(3), 3251-3261.

Chen, J., Bardes, E. E., Aronow, B. J., & Jegga, A. G. (2009). ToppGene Suite for gene list enrichment analysis and candidate gene prioritization. *Nucleic acids research*, *37*(suppl_2), W305-W311.

Chen, K., Kirber, M. T., Xiao, H., Yang, Y., & Keaney Jr, J. F. (2008). Regulation of ROS signal transduction by NADPH oxidase 4 localization. *The Journal of cell biology*, *181*(7), 1129-1139.

Chen, Y., & Brandizzi, F. (2013). IRE1: ER stress sensor and cell fate executor. *Trends in cell biology*, *23*(11), 547-555.

Chen, Z., Smith, M., Du, H., Guo, Y., Clarke, R., Bian, Z., Collins, R., Chen, J., Qian, Y., & Wang, X. (2015). Blood pressure in relation to general and central adiposity among 500 000 adult Chinese men and women. *International journal of epidemiology*, *44*(4), 1305-1319.

Cheng, G., Cao, Z., Xu, X., Van Meir, E. G., & Lambeth, J. D. (2001). Homologs of gp91phox: cloning and tissue expression of Nox3, Nox4, and Nox5. *Gene*, *269*(1-2), 131-140.

Chin, K. M., & Rubin, L. J. (2008). Pulmonary arterial hypertension. *Journal of the American College of Cardiology*, *51*(16), 1527-1538.

Chinetti-Gbaguidi, G., & Staels, B. (2011). Macrophage polarization in metabolic disorders: functions and regulation. *Current opinion in lipidology*, *22*(5), 365.

Chipuk, J. E., Moldoveanu, T., Llambi, F., Parsons, M. J., & Green, D. R. (2010). The BCL-2 family reunion. *Molecular cell*, *37*(3), 299-310.

Christoffersen, C., Bollano, E., Lindegaard, M. L., Bartels, E. D., Goetze, J. P., Andersen, C. B., & Nielsen, L. B. (2003). Cardiac lipid accumulation associated with diastolic dysfunction in obese mice. *Endocrinology*, *144*(8), 3483-3490.

Cinti, S., Mitchell, G., Barbatelli, G., Murano, I., Ceresi, E., Faloia, E., Wang, S., Fortier, M., Greenberg, A. S., & Obin, M. S. (2005). Adipocyte death defines macrophage localization and function in adipose tissue of obese mice and humans. *Journal of lipid research*, *46*(11), 2347-2355.

Clark, R., Leidal, K., Pearson, D., & Nauseef, W. (1987). NADPH oxidase of human neutrophils. Subcellular localization and characterization of an arachidonate-activatable superoxide-generating system. *Journal of Biological Chemistry*, *262*(9), 4065-4074.

Colston, J. T., Sam, D., Strader, J. R., Anderson, M. A., & Freeman, G. L. (2005). H2O2 activates Nox4 through PLA2-dependent arachidonic acid production in adult cardiac fibroblasts. *FEBS letters*, *579*(11), 2533-2540.

Cominacini, L., Pasini, A. F., Garbin, U., Davoli, A., Tosetti, M. L., Campagnola, M., Rigoni, A., Pastorino, A. M., Cascio, V. L., & Sawamura, T. (2000). Oxidized low density lipoprotein (ox-LDL) binding to ox-LDL receptor-1 in endothelial cells induces the activation of NF-κB through an increased production of intracellular reactive oxygen species. *Journal of Biological Chemistry*, *275*(17), 12633-12638.

Corry, D. B., & Tuck, M. L. (1999). Obesity, hypertension, and sympathetic nervous system activity. *Current hypertension reports*, *1*(2), 119-126.

Cory, S., & Adams, J. M. (2002). The Bcl2 family: regulators of the cellular life-or-death switch. *Nature Reviews Cancer*, *2*(9), 647-656.

Cross, A. R., & Segal, A. W. (2004). The NADPH oxidase of professional phagocytes—prototype of the NOX electron transport chain systems. *Biochimica et Biophysica Acta (BBA)-Bioenergetics*, *1657*(1), 1-22.

Cuspidi, C., Rescaldani, M., Sala, C., & Grassi, G. (2014). Left-ventricular hypertrophy and obesity: a systematic review and meta-analysis of echocardiographic studies. *Journal of hypertension*, *32*(1), 16-25.

Cuspidi, C., Tadic, M., Grassi, G., & Mancia, G. (2018). Treatment of hypertension: The ESH/ESC guidelines recommendations. *Pharmacological research*, *128*, 315-321.

Das, S. R., Alexander, K. P., Chen, A. Y., Powell-Wiley, T. M., Diercks, D. B., Peterson, E. D., Roe, M. T., & De Lemos, J. A. (2011). Impact of body weight and extreme obesity on the presentation, treatment, and in-hospital outcomes of 50,149 patients with ST-segment elevation myocardial infarction: results from the NCDR (National Cardiovascular Data Registry). *Journal of the American College of Cardiology*, *58*(25), 2642-2650.

de Divitiis, O., Fazio, S., Petitto, M., Maddalena, G., Contaldo, F., & Mancini, M. (1981). Obesity and cardiac function. *Circulation*, *64*(3), 477-482.

De Figueiredo, A. S. P., Salmon, A. B., Bruno, F., Jimenez, F., Martinez, H. G., Halade, G. V., Ahuja, S. S., Clark, R. A., DeFronzo, R. A., & Abboud, H. E. (2015). Nox2 mediates skeletal muscle insulin resistance induced by a high fat diet. *Journal of Biological Chemistry*, *290*(21), 13427-13439.

De Jong, K. A., & Lopaschuk, G. D. (2017). Complex energy metabolic changes in heart failure with preserved ejection fraction and heart failure with reduced ejection fraction. *Canadian Journal of Cardiology*, *33*(7), 860-871.

De Oliveira, J., Hort, M., Moreira, E., Glaser, V., Ribeiro-do-Valle, R., Prediger, R., Farina, M., Latini, A., & De Bem, A. (2011). Positive correlation between elevated plasma cholesterol levels and cognitive impairments in LDL receptor knockout mice: relevance of cortico-cerebral mitochondrial dysfunction and oxidative stress. *Neuroscience*, *197*, 99-106.

De Pergola, G., & Pannacciulli, N. (2002). Coagulation and fibrinolysis abnormalities in obesity. *Journal of endocrinological investigation*, *25*(10), 899-904.

Den Hartigh, L. J., Omer, M., Goodspeed, L., Wang, S., Wietecha, T., O'Brien, K. D., & Han, C. Y. (2017). Adipocyte-specific deficiency of NADPH oxidase 4 delays the onset of insulin resistance and attenuates adipose tissue inflammation in obesity. *Arteriosclerosis, thrombosis, and vascular biology*, *37*(3), 466-475.

Dhalla, N. S., Temsah, R. M., & Netticadan, T. (2000). Role of oxidative stress in cardiovascular diseases. *Journal of hypertension*, *18*(6), 655-673.

Dirkx, E., Schwenk, R. W., Glatz, J. F., Luiken, J. J., & van Eys, G. J. (2011). High fat diet induced diabetic cardiomyopathy. *Prostaglandins, Leukotrienes and Essential Fatty Acids (PLEFA)*, *85*(5), 219-225.

Donovan, M., & Cotter, T. G. (2004). Control of mitochondrial integrity by Bcl-2 family members and caspase-independent cell death. *Biochimica et Biophysica Acta (BBA)-Molecular Cell Research*, *1644*(2-3), 133-147.

Doussière, J., Gaillard, J., & Vignais, P. V. (1996). Electron transfer across the O2-generating flavocytochrome b of neutrophils. Evidence for a transition from a low-spin state to a high-spin state of the heme iron component. *Biochemistry*, *35*(41), 13400-13410.

Drolet, R., Richard, C., Sniderman, A., Mailloux, J., Fortier, M., Huot, C., Rhéaume, C., & Tchernof, A. (2008). Hypertrophy and hyperplasia of abdominal adipose tissues in women. *International journal of obesity*, *32*(2), 283-291.

Du, C., Fang, M., Li, Y., Li, L., & Wang, X. (2000). Smac, a mitochondrial protein that promotes cytochrome c–dependent caspase activation by eliminating IAP inhibition. *Cell*, *102*(1), 33-42.

Dworakowski, R., Anilkumar, N., Zhang, M., & Shah, A. (2006). Redox signalling involving NADPH oxidase-derived reactive oxygen species. In: Portland Press Ltd.

Eaton, C. B., Pettinger, M., Rossouw, J., Martin, L. W., Foraker, R., Quddus, A., Liu, S., Wampler, N. S., Hank Wu, W.-C., & Manson, J. E. (2016). Risk factors for incident hospitalized heart failure with preserved versus reduced ejection fraction in a multiracial cohort of postmenopausal women. *Circulation: Heart Failure*, *9*(10), e002883.

Eletto, D., Chevet, E., Argon, Y., & Appenzeller-Herzog, C. (2014). Redox controls UPR to control redox. *Journal of cell science*, *127*(17), 3649-3658.

Ellgaard, L., & Helenius, A. (2003). Quality control in the endoplasmic reticulum. *Nature reviews Molecular cell biology*, *4*(3), 181-191.

Esser, N., Legrand-Poels, S., Piette, J., Scheen, A. J., & Paquot, N. (2014). Inflammation as a link between obesity, metabolic syndrome and type 2 diabetes. *Diabetes research and clinical practice*, *105*(2), 141-150.

Faxén, U. L., Hage, C., Benson, L., Zabarovskaja, S., Andreasson, A., Donal, E., Daubert, J.-C., Linde, C., Brismar, K., & Lund, L. H. (2017). HFpEF and HFrEF display different phenotypes as assessed by IGF-1 and IGFBP-1. *Journal of cardiac failure*, *23*(4), 293-303.

Fernández-Sánchez, A., Madrigal-Santillán, E., Bautista, M., Esquivel-Soto, J., Morales-González, Á., Esquivel-Chirino, C., Durante-Montiel, I., Sánchez-Rivera, G., Valadez-Vega, C., & Morales-González, J. A. (2011). Inflammation, oxidative stress, and obesity. *International journal of molecular sciences*, *12*(5), 3117-3132.

Fita, I., & Rossmann, M. G. (1985). The active center of catalase. *Journal of molecular biology*, *185*(1), 21-37.

Folli, F., Corradi, D., Fanti, P., Davalli, A., Paez, A., Giaccari, A., Perego, C., & Muscogiuri, G. (2011). The role of oxidative stress in the pathogenesis of type 2 diabetes mellitus micro-and macrovascular complications: avenues for a mechanistic-based therapeutic approach. *Current diabetes reviews*, *7*(5), 313-324.

Forrester, S. J., Kikuchi, D. S., Hernandes, M. S., Xu, Q., & Griendling, K. K. (2018). Reactive oxygen species in metabolic and inflammatory signaling. *Circulation research*, *122*(6), 877-902.

Fridlyand, L. E., & Philipson, L. H. (2004). Does the glucose-dependent insulin secretion mechanism itself cause oxidative stress in pancreatic β-cells? *Diabetes*, *53*(8), 1942-1948.

Friedman, S. E., & Andrus, B. W. (2012). Obesity and pulmonary hypertension: a review of pathophysiologic mechanisms. *Journal of obesity*, *2012*.

Fujita, K., Nishizawa, H., Funahashi, T., Shimomura, I., & Shimabukuro, M. (2006). Systemic oxidative stress is associated with visceral fat accumulation and the metabolic syndrome. *Circulation Journal*, *70*(11), 1437-1442.

Furukawa, S., Fujita, T., Shimabukuro, M., Iwaki, M., Yamada, Y., Nakajima, Y., Nakayama, O., Makishima, M., Matsuda, M., & Shimomura, I. (2017). Increased oxidative stress in obesity and its impact on metabolic syndrome. *The Journal of clinical investigation*, *114*(12), 1752-1761.

Gadde, K. M., Martin, C. K., Berthoud, H.-R., & Heymsfield, S. B. (2018). Obesity: pathophysiology and management. *Journal of the American College of Cardiology*, *71*(1), 69-84.

Gao, X., Wen, X., Esser, L., Quinn, B., Yu, L., Yu, C.-A., & Xia, D. (2003). Structural basis for the quinone reduction in the bc 1 complex: a comparative analysis of crystal structures of mitochondrial cytochrome bc 1 with bound substrate and inhibitors at the Qi site. *Biochemistry*, *42*(30), 9067-9080.

Garg, N., Senthilkumar, A., Nusair, M. B., Goyal, N., Garg, R. K., & Alpert, M. A. (2013). Heart Failure With a Normal Left Ventricular Ejection Fraction: Epidemiology Pathophysiology, Diagnosis and Management. *The American journal of the medical sciences*, *346*(2), 129-136.

Ge, C.-X., Xu, M.-X., Qin, Y.-T., Gu, T.-T., Lou, D.-S., Li, Q., Hu, L.-F., Wang, B.-C., & Tan, J. (2019). Endoplasmic reticulum stress-induced iRhom2 up-regulation promotes macrophage-regulated cardiac inflammation and lipid deposition in high fat diet (HFD)-challenged mice: Intervention of fisetin and metformin. *Free Radical Biology and Medicine*, *141*, 67-83.

Ge, S. X., Son, E. W., & Yao, R. (2018). iDEP: an integrated web application for differential expression and pathway analysis of RNA-Seq data. *BMC bioinformatics*, *19*(1), 534.

Geetha, R., Radika, M. K., Priyadarshini, E., Bhavani, K., & Anuradha, C. V. (2015). Troxerutin reverses fibrotic changes in the myocardium of high-fat high-fructose diet-fed mice. *Molecular and cellular biochemistry*, *407*(1), 263-279.

Geiszt, M., Kopp, J. B., Várnai, P., & Leto, T. L. (2000). Identification of renox, an NAD (P) H oxidase in kidney. *Proceedings of the National Academy of Sciences*, *97*(14), 8010-8014.

Geng, Z., Fan, W.-Y., Zhou, B., Ye, C., Tong, Y., Zhou, Y.-B., & Xiong, X.-Q. (2019). FNDC5 attenuates obesity-induced cardiac hypertrophy by inactivating JAK2/STAT3-associated inflammation and oxidative stress. *Journal of translational medicine*, *17*(1), 1-13.

Gonçalves, A. E. d. S. S., Rocha, G. Z., Marin, R., Camargo, R. L., Santos, A. d., Carmo, H. d., Guadagnini, D., Petrucci, O., Moysés, Z. P., & Salemi, V. M. C. (2021). Pulmonary Hypertension in Obese Mice Is Accompanied by a Reduction in PPAR-γ Expression in Pulmonary Artery. *Frontiers in Endocrinology*, *12*, 701994.

Goncalves, R. L., Rothschild, D. E., Quinlan, C. L., Scott, G. K., Benz, C. C., & Brand, M. D. (2014). Sources of superoxide/H2O2 during mitochondrial proline oxidation. *Redox biology*, *2*, 901-909.

Gorlach, A., Brandes, R., Nguyen, K., Amidi, M., Dehghani, F., & Busse, R. (2000). A gp91phox containing NADPH oxidase selectively expressed in endothelial cells is a major source of oxygen radical generation in the arterial wall. *Circulation research*, *87*(1), 26-32.

Grundy, S. M. (2002). Obesity, metabolic syndrome, and coronary atherosclerosis. In: Am Heart Assoc.

Gülçin, İ., Huyut, Z., Elmastaş, M., & Aboul-Enein, H. Y. (2010). Radical scavenging and antioxidant activity of tannic acid. *Arabian Journal of Chemistry*, *3*(1), 43-53.

Gürtl, B., Kratky, D., Guelly, C., Zhang, L., Gorkiewicz, G., Das, S. K., Tamilarasan, K. P., & Hoefler, G. (2009). Apoptosis and fibrosis are early features of heart failure in an animal model of metabolic cardiomyopathy. *International journal of experimental pathology*, *90*(3), 338-346.

Gurusamy, N., & Das, D. K. (2009). Autophagy, redox signaling, and ventricular remodeling. *Antioxidants & redox signaling*, *11*(8), 1975-1988.

Haber, C. A., Lam, T. K., Yu, Z., Gupta, N., Goh, T., Bogdanovic, E., Giacca, A., & Fantus, I. G. (2003). N-acetylcysteine and taurine prevent hyperglycemia-induced insulin resistance in vivo: possible role of oxidative stress. *American Journal of Physiology-Endocrinology and Metabolism*, *285*(4), E744-E753.

Hafstad, A. D., Hansen, S. S., Lund, J., Santos, C. X., Boardman, N. T., Shah, A. M., & Aasum, E. (2020). NADPH oxidase 2 mediates myocardial oxygen wasting in obesity. *Antioxidants*, *9*(2), 171.

Hansen, S. S., Aasum, E., & Hafstad, A. D. (2018). The role of NADPH oxidases in diabetic cardiomyopathy. *Biochimica et Biophysica Acta (BBA)-Molecular Basis of Disease*, *1864*(5), 1908-1913.

Harding, H. P., Novoa, I., Zhang, Y., Zeng, H., Wek, R., Schapira, M., & Ron, D. (2000). Regulated translation initiation controls stress-induced gene expression in mammalian cells. *Molecular cell*, *6*(5), 1099-1108.

Harding, H. P., Zhang, Y., & Ron, D. (1999). Protein translation and folding are coupled by an endoplasmic-reticulum-resident kinase. *Nature*, *397*(6716), 271-274.

Hasan-Ali, H., Abd El-Mottaleb, N. A., Hamed, H. B., & Abd-Elsayed, A. (2011). Serum adiponectin and leptin as predictors of the presence and degree of coronary atherosclerosis. *Coronary artery disease*, *22*(4), 264-269.

Herrington, W., Lacey, B., Sherliker, P., Armitage, J., & Lewington, S. (2016). Epidemiology of atherosclerosis and the potential to reduce the global burden of atherothrombotic disease. *Circulation research*, *118*(4), 535-546.

Hetz, C., Zhang, K., & Kaufman, R. J. (2020). Mechanisms, regulation and functions of the unfolded protein response. *Nature reviews Molecular cell biology*, *21*(8), 421-438.

Higaki, Y., Mikami, T., Fujii, N., Hirshman, M. F., Koyama, K., Seino, T., Tanaka, K., & Goodyear, L. J. (2008). Oxidative stress stimulates skeletal muscle glucose uptake through a phosphatidylinositol 3-kinase-dependent pathway. *American Journal of Physiology-Endocrinology and Metabolism*, *294*(5), E889-E897.

Hildebrandt, W., Hamann, A., Krakowski-Roosen, H., Kinscherf, R., Dugi, K., Sauer, R., Lacher, S., Nöbel, N., Bodens, A., & Bellou, V. (2004). Effect of thiol antioxidant on body fat and insulin reactivity. *Journal of molecular medicine*, *82*(5), 336-344.

Hill, M. M., Adrain, C., Duriez, P. J., Creagh, E. M., & Martin, S. J. (2004). Analysis of the composition, assembly kinetics and activity of native Apaf-1 apoptosomes. *The EMBO journal*, *23*(10), 2134-2145.

Hille, R., & Nishino, T. (1995). Xanthine oxidase and xanthine dehydrogenase. *The FASEB Journal*, *9*(11), 995-1003.

Hindricks, G., Potpara, T., Dagres, N., Arbelo, E., Bax, J. J., Blomström-Lundqvist, C., Boriani, G., Castella, M., Dan, G.-A., Dilaveris, P. E., Fauchier, L., Filippatos, G., Kalman, J. M., La Meir, M., Lane, D. A., Lebeau, J.-P., Lettino, M., Lip, G. Y. H., Pinto, F. J., . . . Group, E. S. D. (2020). 2020 ESC Guidelines for the diagnosis and management of atrial fibrillation developed in collaboration with the European Association for Cardio-Thoracic Surgery (EACTS): The Task Force for the diagnosis and management of atrial fibrillation of the European Society of Cardiology (ESC) Developed with the special contribution of the European Heart Rhythm Association (EHRA) of the ESC. *European Heart Journal*, *42*(5), 373-498. https://doi.org/10.1093/eurheartj/ehaa612

Hordijk, P. L. (2006). Regulation of NADPH oxidases: the role of Rac proteins. *Circulation research*, *98*(4), 453-462.

Horwich, T. B., Broderick, S., Chen, L., McCullough, P. A., Strzelczyk, T., Kitzman, D. W., Fletcher, G., Safford, R. E., Ewald, G., & Fine, L. J. (2011). Relation among body mass index, exercise training, and outcomes in chronic systolic heart failure. *The American journal of cardiology*, *108*(12), 1754-1759.

Hotamisligil, G. S. (2017). Inflammation, metaflammation and immunometabolic disorders. *Nature*, *542*(7640), 177-185.

Houstis, N., Rosen, E. D., & Lander, E. S. (2006). Reactive oxygen species have a causal role in multiple forms of insulin resistance. *Nature*, *440*(7086), 944-948.

Huang, B., Eberstadt, M., Olejniczak, E. T., Meadows, R. P., & Fesik, S. W. (1996). NMR structure and mutagenesis of the Fas (APO-1/CD95) death domain. *Nature*, *384*(6610), 638-641.

Hutcheson, R., & Rocic, P. (2012). The metabolic syndrome, oxidative stress, environment, and cardiovascular disease: the great exploration. *Experimental diabetes research*, *2012*.

Jaishy, B., Zhang, Q., Chung, H. S., Riehle, C., Soto, J., Jenkins, S., Abel, P., Cowart, L. A., Van Eyk, J. E., & Abel, E. D. (2015). Lipid-induced NOX2 activation inhibits autophagic flux by impairing lysosomal enzyme activity [S]. *Journal of lipid research*, *56*(3), 546-561.

Jalili, V., Afgan, E., Gu, Q., Clements, D., Blankenberg, D., Goecks, J., Taylor, J., & Nekrutenko, A. (2020). The Galaxy platform for accessible, reproducible and collaborative biomedical analyses: 2020 update. *Nucleic Acids Research*.

Jang, J.-H., & Surh, Y.-J. (2003). Potentiation of cellular antioxidant capacity by Bcl-2: implications for its antiapoptotic function. *Biochemical pharmacology*, *66*(8), 1371-1379.

Jay, D. B., Papaharalambus, C. A., Seidel-Rogol, B., Dikalova, A. E., Lassègue, B., & Griendling, K. K. (2008). Nox5 mediates PDGF-induced proliferation in human aortic smooth muscle cells. *Free Radical Biology and Medicine*, *45*(3), 329-335.

Jiang, S. Z., Lu, W., Zong, X. F., Ruan, H. Y., & Liu, Y. (2016). Obesity and hypertension. *Experimental and therapeutic medicine*, *12*(4), 2395-2399.

Joseph, L. C., Avula, U. M. R., Wan, E. Y., Reyes, M. V., Lakkadi, K. R., Subramanyam, P., Nakanishi, K., Homma, S., Muchir, A., & Pajvani, U. B. (2019). Dietary saturated fat promotes arrhythmia by activating NOX2 (nadph oxidase 2). *Circulation: Arrhythmia and Electrophysiology*, *12*(11), e007573.

Joza, N., Susin, S. A., Daugas, E., Stanford, W. L., Cho, S. K., Li, C. Y., Sasaki, T., Elia, A. J., Cheng, H.-Y. M., & Ravagnan, L. (2001). Essential role of the mitochondrial apoptosis-inducing factor in programmed cell death. *Nature*, *410*(6828), 549-554.

Judkins, C. P., Diep, H., Broughton, B. R., Mast, A. E., Hooker, E. U., Miller, A. A., Selemidis, S., Dusting, G. J., Sobey, C. G., & Drummond, G. R. (2010). Direct evidence of a role for Nox2 in superoxide production, reduced nitric oxide bioavailability, and early atherosclerotic plaque formation in ApoE−/− mice. *American Journal of Physiology-Heart and Circulatory Physiology*, *298*(1), H24-H32.

Juhan-Vague, I., Thompson, S., & Jespersen, J. (1993). Involvement of the hemostatic system in the insulin resistance syndrome. A study of 1500 patients with angina pectoris. The ECAT Angina Pectoris Study Group. *Arteriosclerosis and thrombosis: a journal of vascular biology*, *13*(12), 1865-1873.

Juhan-Vague, I., Alessi, M. C., Mavri, A., & Morange, P. (2003). Plasminogen activator inhibitor-1, inflammation, obesity, insulin resistance and vascular risk. *Journal of Thrombosis and Haemostasis*, *1*(7), 1575-1579.

Junge, W., & Nelson, N. (2015). ATP synthase. *Annu Rev Biochem*, *84*(1), 631-657.

Kanda, H., Tateya, S., Tamori, Y., Kotani, K., Hiasa, K.-i., Kitazawa, R., Kitazawa, S., Miyachi, H., Maeda, S., & Egashira, K. (2006). MCP-1 contributes to macrophage infiltration into adipose tissue, insulin resistance, and hepatic steatosis in obesity. *The Journal of clinical investigation*, *116*(6), 1494-1505.

Kang, P. M., & Izumo, S. (2000). Apoptosis and heart failure: a critical review of the literature. *Circulation research*, *86*(11), 1107-1113.

Karakikes, I., Chaanine, A. H., Kang, S., Mukete, B. N., Jeong, D., Zhang, S., Hajjar, R. J., & Lebeche, D. (2013). Therapeutic cardiac-targeted delivery of miR-1 reverses pressure overload-induced cardiac hypertrophy and attenuates pathological remodeling. *J Am Heart Assoc*, *2*(2), e000078. https://doi.org/10.1161/JAHA.113.000078

Karasoy, D., Bo Jensen, T., Hansen, M. L., Schmiegelow, M., Lamberts, M., Gislason, G. H., Hansen, J., Torp-Pedersen, C., & Olesen, J. B. (2013). Obesity is a risk factor for atrial fibrillation among fertile young women: a nationwide cohort study. *Europace*, *15*(6), 781-786.

Kaufman, L. N., Peterson, M. M., & Smith, S. M. (1991). Hypertension and sympathetic hyperactivity induced in rats by high-fat or glucose diets. *American Journal of Physiology-Endocrinology and Metabolism*, *260*(1), E95-E100.

Kelley, E. E., Baust, J., Bonacci, G., Golin-Bisello, F., Devlin, J. E., St. Croix, C. M., Watkins, S. C., Gor, S., Cantu-Medellin, N., Weidert, E. R., Frisbee, J. C., Gladwin, M. T., Champion, H. C., Freeman, B. A., & Khoo, N. K. H. (2014). Fatty acid nitroalkenes ameliorate glucose intolerance and pulmonary hypertension in high-fat diet-induced obesity. *Cardiovascular Research*, *101*(3), 352-363. https://doi.org/10.1093/cvr/cvt341

Kenchaiah, S., Evans, J. C., Levy, D., Wilson, P. W., Benjamin, E. J., Larson, M. G., Kannel, W. B., & Vasan, R. S. (2002). Obesity and the risk of heart failure. *New England Journal of Medicine*, *347*(5), 305-313.

Kikuchi, H., Hikage, M., Miyashita, H., & Fukumoto, M. (2000). NADPH oxidase subunit, gp91phox homologue, preferentially expressed in human colon epithelial cells. *Gene*, *254*(1-2), 237-243.

Kimes, B., & Brandt, B. (1976). Properties of a clonal muscle cell line from rat heart. *Experimental cell research*, *98*(2), 367-381.

Kischkel, F., Hellbardt, S., Behrmann, I., Germer, M., Pawlita, M., Krammer, P. H., & Peter, M. (1995). Cytotoxicity-dependent APO-1 (Fas/CD95)-associated proteins form a death-inducing signaling complex (DISC) with the receptor. *The EMBO journal*, *14*(22), 5579-5588.

Klapholz, M., Maurer, M., Lowe, A. M., Messineo, F., Meisner, J. S., Mitchell, J., Kalman, J., Phillips, R. A., Steingart, R., & Brown, E. J. (2004). Hospitalization for heart failure in the presence of a normal left ventricular ejection fraction: results of the New York Heart Failure Registry. *Journal of the American College of Cardiology*, *43*(8), 1432-1438.

Klinman, J. P. (2007). How do enzymes activate oxygen without inactivating themselves? *Accounts of Chemical Research*, *40*(5), 325-333.

Kotsis, V., Stabouli, S., Papakatsika, S., Rizos, Z., & Parati, G. (2010). Mechanisms of obesity-induced hypertension. *Hypertension research*, *33*(5), 386-393.

Kračun, D., Klop, M., Knirsch, A., Petry, A., Kanchev, I., Chalupsky, K., Wolf, C., & Görlach, A. (2020). NADPH oxidases and HIF1 promote cardiac dysfunction and pulmonary hypertension in response to glucocorticoid excess. *Redox Biology*, 101536.

Kračun, D., Rieß, F., Kanchev, I., Gawaz, M., & Görlach, A. (2014). The β3-integrin binding protein β3-endonexin is a novel negative regulator of hypoxia-inducible factor-1. *Antioxidants & redox signaling*, *20*(13), 1964-1976.

Krijnen, P., Meischl, C., Hack, C., Meijer, C., Visser, C., Roos, D., & Niessen, H. (2003). Increased Nox2 expression in human cardiomyocytes after acute myocardial infarction. *Journal of clinical pathology*, *56*(3), 194-199.

Kumar, D., Lou, H., & Singal, P. K. (2002). Oxidative stress and apoptosis in heart dysfunction. *Herz*, *27*(7), 662-668.

Kuroda, J., Ago, T., Matsushima, S., Zhai, P., Schneider, M. D., & Sadoshima, J. (2010). NADPH oxidase 4 (Nox4) is a major source of oxidative stress in the failing heart. *Proceedings of the National Academy of Sciences*, *107*(35), 15565-15570.

Lai, Y.-C., Potoka, K. C., Champion, H. C., Mora, A. L., & Gladwin, M. T. (2014). Pulmonary arterial hypertension: the clinical syndrome. *Circulation research*, *115*(1), 115-130.

Lakshmanan, A. P., Harima, M., Suzuki, K., Soetikno, V., Nagata, M., Nakamura, T., Takahashi, T., Sone, H., Kawachi, H., & Watanabe, K. (2013). The hyperglycemia stimulated myocardial endoplasmic reticulum (ER) stress contributes to diabetic cardiomyopathy in the transgenic non-obese type 2 diabetic rats: a differential role of unfolded protein response (UPR) signaling proteins. *The international journal of biochemistry & cell biology*, *45*(2), 438-447.

Lambeth, J. D. (2004). NOX enzymes and the biology of reactive oxygen. *Nature Reviews Immunology*, *4*(3), 181-189.

Landin, K., Stigendal, L., Eriksson, E., Krotkiewski, M., Risberg, B., Tengborn, L., & Smith, U. (1990). Abdominal obesity is associated with an impaired fibrinolytic activity and elevated plasminogen activator inhibitor-1. *Metabolism*, *39*(10), 1044-1048.

Landsberg, L., Aronne, L. J., Beilin, L. J., Burke, V., Igel, L. I., Lloyd-Jones, D., & Sowers, J. (2013). Obesity-related hypertension: Pathogenesis, cardiovascular risk, and treatment—A position paper of the The Obesity Society and the American Society of Hypertension. *Obesity*, *21*(1), 8-24.

Langbein, H., Brunssen, C., Hofmann, A., Cimalla, P., Brux, M., Bornstein, S. R., Deussen, A., Koch, E., & Morawietz, H. (2016). NADPH oxidase 4 protects against development of endothelial dysfunction and atherosclerosis in LDL receptor deficient mice. *European heart journal*, *37*(22), 1753-1761.

Lassègue, B., & Griendling, K. K. (2010). NADPH oxidases: functions and pathologies in the vasculature. *Arteriosclerosis, thrombosis, and vascular biology*, *30*(4), 653-661.

Lassègue, B., Sorescu, D., Szöcs, K., Yin, Q., Akers, M., Zhang, Y., Grant, S. L., Lambeth, J. D., & Griendling, K. K. (2001). Novel gp91 phox homologues in vascular smooth muscle cells: nox1 mediates angiotensin II–induced superoxide formation and redox-sensitive signaling pathways. *Circulation research*, *88*(9), 888-894.

Latif, N., Khan, M. A., Birks, E., O'Farrell, A., Westbrook, J., Dunn, M. J., & Yacoub, M. H. (2000). Upregulation of the Bcl-2 family of proteins in end stage heart failure. *Journal of the American College of Cardiology*, *35*(7), 1769-1777.

Lau, W. B., Ohashi, K., Wang, Y., Ogawa, H., Murohara, T., Ma, X.-L., & Ouchi, N. (2017). Role of adipokines in cardiovascular disease. *Circulation Journal*, *81*(7), 920-928.

Lauer, M. S., Anderson, K. M., Kannel, W. B., & Levy, D. (1991). The impact of obesity on left ventricular mass and geometry: the Framingham Heart Study. *Jama*, *266*(2), 231-236.

Lauer, M. S., Anderson, K. M., & Levy, D. (1992). Separate and joint influences of obesity and mild hypertension on left ventricular mass and geometry: the Framingham Heart Study. *Journal of the American College of Cardiology*, *19*(1), 130-134.

Lee, A.-H., Iwakoshi, N. N., & Glimcher, L. H. (2003). XBP-1 regulates a subset of endoplasmic reticulum resident chaperone genes in the unfolded protein response. *Molecular and cellular biology*, *23*(21), 7448-7459.

Lee, J. (2013). Adipose tissue macrophages in the development of obesity-induced inflammation, insulin resistance and type 2 diabetes. *Archives of pharmacal research*, *36*(2), 208-222.

Leloup, C., Tourrel-Cuzin, C., Magnan, C., Karaca, M., Castel, J., Carneiro, L., Colombani, A.-L., Ktorza, A., Casteilla, L., & Pénicaud, L. (2009). Mitochondrial reactive oxygen species are obligatory signals for glucose-induced insulin secretion. *Diabetes*, *58*(3), 673-681.

Li, G., Scull, C., Ozcan, L., & Tabas, I. (2010). NADPH oxidase links endoplasmic reticulum stress, oxidative stress, and PKR activation to induce apoptosis. *Journal of Cell Biology*, *191*(6), 1113-1125.

Li, Q., Song, X.-W., Zou, J., Wang, G.-K., Kremneva, E., Li, X.-Q., Zhu, N., Sun, T., Lappalainen, P., & Yuan, W.-J. (2010). Attenuation of microRNA-1 derepresses the cytoskeleton regulatory protein twinfilin-1 to provoke cardiac hypertrophy. *J Cell Sci*, *123*(14), 2444-2452.

Litwin, S. E. (2010). Cardiac remodeling in obesity: time for a new paradigm. In: American College of Cardiology Foundation Washington, DC.

Liu, R., Holik, A. Z., Su, S., Jansz, N., Chen, K., Leong, H. S., Blewitt, M. E., Asselin-Labat, M.-L., Smyth, G. K., & Ritchie, M. E. (2015). Why weight? Modelling sample and observational level variability improves power in RNA-seq analyses. *Nucleic acids research*, *43*(15), e97-e97.

Lob, H. E., Song, J., Hurr, C., Chung, A., Young, C. N., Mark, A. L., & Davisson, R. L. (2017). Deletion of p22phox-dependent oxidative stress in the hypothalamus protects against obesity by modulating β3-adrenergic mechanisms. *JCI insight*, *2*(2).

Locksley, R. M., Killeen, N., & Lenardo, M. J. (2001). The TNF and TNF receptor superfamilies: integrating mammalian biology. *Cell*, *104*(4), 487-501.

Loffreda, S., Yang, S., Lin, H., Karp, C., Brengman, M. L., Wang, D., Klein, A., Bulkley, G. B., Bao, C., & Noble, P. (1998). Leptin regulates proinflammatory immune responses. *The FASEB journal*, *12*(1), 57-65.

Loh, K., Deng, H., Fukushima, A., Cai, X., Boivin, B., Galic, S., Bruce, C., Shields, B. J., Skiba, B., & Ooms, L. M. (2009). Reactive oxygen species enhance insulin sensitivity. *Cell metabolism*, *10*(4), 260-272.

Loskutoff, D. J., & Samad, F. (1998). The adipocyte and hemostatic balance in obesity: studies of PAI-1. *Arteriosclerosis, thrombosis, and vascular biology*, *18*(1), 1-6.

Lu, J.-W., Liao, C.-Y., Yang, W.-Y., Lin, Y.-M., Jin, S.-L. C., Wang, H.-D., & Yuh, C.-H. (2014). Overexpression of endothelin 1 triggers hepatocarcinogenesis in zebrafish and promotes cell proliferation and migration through the AKT pathway. *PloS one*, *9*(1), e85318.

Madala, M. C., Franklin, B. A., Chen, A. Y., Berman, A. D., Roe, M. T., Peterson, E. D., Ohman, E. M., Smith, S. C., Gibler, W. B., & McCullough, P. A. (2008). Obesity and age of first non–ST-segment elevation myocardial infarction. *Journal of the American College of Cardiology*, *52*(12), 979-985.

Magnani, F., Nenci, S., Fananas, E. M., Ceccon, M., Romero, E., Fraaije, M. W., & Mattevi, A. (2017). Crystal structures and atomic model of NADPH oxidase. *Proceedings of the National Academy of Sciences*, *114*(26), 6764-6769.

Mailloux, R. J. (2015). Teaching the fundamentals of electron transfer reactions in mitochondria and the production and detection of reactive oxygen species. *Redox biology*, *4*, 381-398.

Mair, K. M., Harvey, K. Y., Henry, A. D., Hillyard, D. Z., Nilsen, M., & MacLean, M. R. (2019). Obesity alters oestrogen metabolism and contributes to pulmonary arterial hypertension. *European Respiratory Journal*, *53*(6).

Manson, J. E., Colditz, G. A., Stampfer, M. J., Willett, W. C., Rosner, B., Monson, R. R., Speizer, F. E., & Hennekens, C. H. (1990). A prospective study of obesity and risk of coronary heart disease in women. *New England journal of medicine*, *322*(13), 882-889.

Marques de Mattos, A., Marino, L. V., Ovidio, P. P., Jordão, A. A., Almeida, C. C., & Chiarello, P. G. (2012). Protein oxidative stress and dyslipidemia in dialysis patients. *Therapeutic Apheresis and Dialysis*, *16*(1), 68-74.

Martyn, K. D., Frederick, L. M., Von Loehneysen, K., Dinauer, M. C., & Knaus, U. G. (2006). Functional analysis of Nox4 reveals unique characteristics compared to other NADPH oxidases. *Cellular signalling*, *18*(1), 69-82.

Matsuda, M., & Shimomura, I. (2014). Roles of adiponectin and oxidative stress in obesity-associated metabolic and cardiovascular diseases. *Reviews in endocrine and metabolic disorders*, *15*(1), 1-10.

Matsuno, K., Iwata, K., Matsumoto, M., Katsuyama, M., Cui, W., Murata, A., Nakamura, H., Ibi, M., Ikami, K., & Zhang, J. (2012). NOX1/NADPH oxidase is involved in endotoxin-induced cardiomyocyte apoptosis. *Free Radical Biology and Medicine*, *53*(9), 1718-1728.

Matsushima, S., Kuroda, J., Ago, T., Zhai, P., Ikeda, Y., Oka, S., Fong, G.-H., Tian, R., & Sadoshima, J. (2013). Broad suppression of NADPH oxidase activity exacerbates ischemia/reperfusion injury through inadvertent downregulation of hypoxia-inducible factor-1α and upregulation of peroxisome proliferator–activated receptor-α. *Circulation research*, *112*(8), 1135-1149.

May, J. M., & de Haen, C. (1979). The insulin-like effect of hydrogen peroxide on pathways of lipid synthesis in rat adipocytes. *Journal of Biological Chemistry*, *254*(18), 9017-9021.

McCracken, E., Monaghan, M., & Sreenivasan, S. (2018). Pathophysiology of the metabolic syndrome. *Clinics in dermatology*, *36*(1), 14-20.

McGill Jr, H. C., McMahan, C. A., Herderick, E. E., Zieske, A. W., Malcom, G. T., Tracy, R. E., & Strong, J. P. (2002). Obesity accelerates the progression of coronary atherosclerosis in young men. *Circulation*, *105*(23), 2712-2718.

McGoon, M. D., Benza, R. L., Escribano-Subias, P., Jiang, X., Miller, D. P., Peacock, A. J., Pepke-Zaba, J., Pulido, T., Rich, S., & Rosenkranz, S. (2013). Pulmonary arterial hypertension: epidemiology and registries. *Journal of the American College of Cardiology*, *62*(25S), D51-D59.

McMurray, F., Patten, D. A., & Harper, M. E. (2016). Reactive oxygen species and oxidative stress in obesity—recent findings and empirical approaches. *Obesity*, *24*(11), 2301-2310.

Meng, Q., Lai, Y.-C., Kelly, N. J., Bueno, M., Baust, J. J., Bachman, T. N., Goncharov, D., Vanderpool, R. R., Radder, J. E., & Hu, J. (2017). Development of a mouse model of metabolic syndrome, pulmonary hypertension, and heart failure with preserved ejection fraction. *American journal of respiratory cell and molecular biology*, *56*(4), 497-505.

Miller, W. L., Grill, D. E., & Borlaug, B. A. (2013). Clinical features, hemodynamics, and outcomes of pulmonary hypertension due to chronic heart failure with reduced ejection fraction: pulmonary hypertension and heart failure. *JACC: Heart Failure*, *1*(4), 290-299.

Minamino, T., Komuro, I., & Kitakaze, M. (2010). Endoplasmic reticulum stress as a therapeutic target in cardiovascular disease. *Circulation research*, *107*(9), 1071-1082.

Mishima, Y., Stahlhut, C., & Giraldez, A. J. (2007). miR-1-2 gets to the heart of the matter. *Cell*, *129*(2), 247-249.

Mitchell, P. (1976). Possible molecular mechanisms of the protonmotive function of cytochrome systems. *Journal of theoretical biology*, *62*(2), 327-367.

Miyano, K., & Sumimoto, H. (2007). Role of the small GTPase Rac in p22phox-dependent NADPH oxidases. *Biochimie*, *89*(9), 1133-1144.

Mohan, S., Brown, L., & Ayyappan, P. (2019). Endoplasmic reticulum stress: a master regulator of metabolic syndrome. *European Journal of Pharmacology*, *860*, 172553.

Molarius, A., Seidell, J. C., Sans, S., Tuomilehto, J., & Kuulasmaa, K. (2000). Educational level, relative body weight, and changes in their association over 10 years: an international perspective from the WHO MONICA Project. *American journal of public health*, *90*(8), 1260.

Monteiro, C. A., Moura, E. C., Conde, W. L., & Popkin, B. M. (2004). Socioeconomic status and obesity in adult populations of developing countries: a review. *Bulletin of the world health organization*, *82*(12), 940-946.

Montero, D., Walther, G., Perez-Martin, A., Roche, E., & Vinet, A. (2012). Endothelial dysfunction, inflammation, and oxidative stress in obese children and adolescents: markers and effect of lifestyle intervention. *Obesity reviews*, *13*(5), 441-455.

Morawietz, H. (2011). Endothelial NADPH oxidases: friends or foes? *Basic research in cardiology*, *106*(4), 521-525.

Morawietz, H. (2018). Cardiovascular protection by Nox4. In: Oxford University Press.

Mozaffarian, D., Benjamin, E. J., Go, A. S., Arnett, D. K., Blaha, M. J., Cushman, M., De Ferranti, S., Després, J.-P., Fullerton, H. J., & Howard, V. J. (2015). Heart disease and stroke statistics—2015 update: a report from the American Heart Association. *circulation*, *131*(4), e29-e322.

Mruk, D. D., Silvestrini, B., Mo, M.-y., & Cheng, C. Y. (2002). Antioxidant superoxide dismutase-a review: its function, regulation in the testis, and role in male fertility. *Contraception*, *65*(4), 305-311.

Nakamura, K., Fuster, J. J., & Walsh, K. (2014). Adipokines: a link between obesity and cardiovascular disease. *Journal of cardiology*, *63*(4), 250-259.

Nakano, Y., Longo-Guess, C. M., Bergstrom, D. E., Nauseef, W. M., Jones, S. M., & Bánfi, B. (2008). Mutation of the Cyba gene encoding p22 phox causes vestibular and immune defects in mice. *The Journal of clinical investigation*, *118*(3), 1176-1185.

Naqui, A., Chance, B., & Cadenas, E. (1986). Reactive oxygen intermediates in biochemistry. *Annual review of biochemistry*, *55*(1), 137-166.

Nauseef, W. M. (2004). Assembly of the phagocyte NADPH oxidase. *Histochemistry and cell biology*, *122*(4), 277-291.

Nauseef, W. M. (2008). Biological roles for the NOX family NADPH oxidases. *Journal of Biological Chemistry*, *283*(25), 16961-16965.

Nazzareno, G., Marc, H., Jean, L., Simon, G., Irene, L., & Adam, T. (2016). ESC/ERS Guidelines for the diagnosis and treatment of pulmonary hypertension. The Joint Task Force for the

Diagnosis and Treatment of Pulmonary Hypertension of the European Society of Cardiology (ESC) and the European Respiratory Society (ERS). *Eur Heart J*, *37*(1), 67-119.

NEVIÈRE, R. M., FAUVEL, H., CHOPIN, C., FORMSTECHER, P., & MARCHETTI, P. (2001). Caspase inhibition prevents cardiac dysfunction and heart apoptosis in a rat model of sepsis. *American journal of respiratory and critical care medicine*, *163*(1), 218-225.

Nicholls, D. G., & Ferguson, S. J. (2002). *Bioenergetics*. Elsevier.

Nisimoto, Y., Motalebi, S., Han, C.-H., & Lambeth, J. D. (1999). The p67 phox Activation Domain Regulates Electron Flow from NADPH to Flavin in Flavocytochromeb 558. *Journal of Biological Chemistry*, *274*(33), 22999-23005.

Noll, N. A., Lal, H., & Merryman, W. D. (2020). Mouse models of heart failure with preserved or reduced ejection fraction. *The American journal of pathology*.

Nordberg, J., & Arnér, E. S. (2001). Reactive oxygen species, antioxidants, and the mammalian thioredoxin system. *Free Radical Biology and Medicine*, *31*(11), 1287-1312.

Obokata, M., Reddy, Y. N., Pislaru, S. V., Melenovsky, V., & Borlaug, B. A. (2017). Evidence supporting the existence of a distinct obese phenotype of heart failure with preserved ejection fraction. *Circulation*, *136*(1), 6-19.

Ochoa, C. D., Wu, R. F., & Terada, L. S. (2018). ROS signaling and ER stress in cardiovascular disease. *Molecular aspects of medicine*, *63*, 18-29.

Owan, T. E., Hodge, D. O., Herges, R. M., Jacobsen, S. J., Roger, V. L., & Redfield, M. M. (2006). Trends in prevalence and outcome of heart failure with preserved ejection fraction. *New England Journal of Medicine*, *355*(3), 251-259.

Ozgur, R., Uzilday, B., Iwata, Y., Koizumi, N., & Turkan, I. (2018). Interplay between the unfolded protein response and reactive oxygen species: a dynamic duo. *Journal of experimental botany*, *69*(14), 3333-3345.

Paffenholz, R., Bergstrom, R. A., Pasutto, F., Wabnitz, P., Munroe, R. J., Jagla, W., Heinzmann, U., Marquardt, A., Bareiss, A., & Laufs, J. (2004). Vestibular defects in head-tilt mice result from mutations in Nox3, encoding an NADPH oxidase. *Genes & development*, *18*(5), 486-491.

Palade, G. E. (1956). The endoplasmic reticulum. *The Journal of biophysical and biochemical cytology*, *2*(4), 85.

Panchal, S. K., Poudyal, H., Iyer, A., Nazer, R., Alam, A., Diwan, V., Kauter, K., Sernia, C., Campbell, F., & Ward, L. (2011). High-carbohydrate high-fat diet–induced metabolic syndrome and cardiovascular remodeling in rats. *Journal of cardiovascular pharmacology*, *57*(1), 51-64.

Papa, F. R. (2012). Endoplasmic reticulum stress, pancreatic β-cell degeneration, and diabetes. *Cold Spring Harbor perspectives in medicine*, *2*(9), a007666.

Pasarica, M., Sereda, O. R., Redman, L. M., Albarado, D. C., Hymel, D. T., Roan, L. E., Rood, J. C., Burk, D. H., & Smith, S. R. (2009). Reduced adipose tissue oxygenation in human obesity: evidence for rarefaction, macrophage chemotaxis, and inflammation without an angiogenic response. *Diabetes*, *58*(3), 718-725.

Pausova, Z., Jomphe, M., Houde, L., Vezina, H., Orlov, S. N., Gossard, F., Gaudet, D., Tremblay, J., Kotchen, T. A., & Cowley, A. W. (2002). A genealogical study of essential hypertension with and without obesity in French Canadians. *Obesity research*, *10*(6), 463-470.

Pedruzzi, E., Guichard, C., Ollivier, V., Driss, F., Fay, M., Prunet, C., Marie, J.-C., Pouzet, C., Samadi, M., & Elbim, C. (2004). NAD (P) H oxidase Nox-4 mediates 7-ketocholesterol-induced endoplasmic reticulum stress and apoptosis in human aortic smooth muscle cells. *Molecular and cellular biology*, *24*(24), 10703-10717.

Pendyala, S., & Natarajan, V. (2010). Redox regulation of Nox proteins. *Respiratory physiology & neurobiology*, *174*(3), 265-271.

Perrotta, F., Nigro, E., Mollica, M., Costigliola, A., D'Agnano, V., Daniele, A., Bianco, A., & Guerra, G. (2019). Pulmonary hypertension and obesity: Focus on adiponectin. *International journal of molecular sciences*, *20*(4), 912.

Petry, A., Djordjevic, T., Weitnauer, M., Kietzmann, T., Hess, J., & Görlach, A. (2006). NOX2 and NOX4 mediate proliferative response in endothelial cells. *Antioxidants & redox signaling*, *8*(9-10), 1473-1484.

Petry, A., Weitnauer, M., & Goerlach, A. (2010). Receptor activation of NADPH oxidases. *Antioxidants & redox signaling*, *13*(4), 467-487.

Petry, A., Zhang, Z., Trautz, B., Riess, F., & Görlach, A. (2018). Cross talk between p22phox and ATF4 in the endothelial unfolded protein response. *Antioxidants & redox signaling*, *30*(1), 40-55.

Pfaffl, M. W., Horgan, G. W., & Dempfle, L. (2002). Relative expression software tool (REST©) for group-wise comparison and statistical analysis of relative expression results in real-time PCR. *Nucleic acids research*, *30*(9), e36-e36.

Piccoli, C., Ria, R., Scrima, R., Cela, O., D'Aprile, A., Boffoli, D., Falzetti, F., Tabilio, A., & Capitanio, N. (2005). Characterization of mitochondrial and extra-mitochondrial oxygen consuming reactions in human hematopoietic stem cells Novel evidence of the occurrence of NAD (P) H oxidase activity. *Journal of Biological Chemistry*, *280*(28), 26467-26476.

Poirier, P., Giles, T. D., Bray, G. A., Hong, Y., Stern, J. S., Pi-Sunyer, F. X., & Eckel, R. H. (2006). Obesity and cardiovascular disease: pathophysiology, evaluation, and effect of weight loss: an update of the 1997 American Heart Association Scientific Statement on Obesity and Heart Disease from the Obesity Committee of the Council on Nutrition, Physical Activity, and Metabolism. *Circulation*, *113*(6), 898-918.

Ponikowski, P., Voors, A. A., Anker, S. D., Bueno, H., Cleland, J. G. F., Coats, A. J. S., Falk, V., González-Juanatey, J. R., Harjola, V.-P., Jankowska, E. A., Jessup, M., Linde, C., Nihoyannopoulos, P., Parissis, J. T., Pieske, B., Riley, J. P., Rosano, G. M. C., Ruilope, L. M., Ruschitzka, F., . . . Group, E. S. D. (2016). 2016 ESC Guidelines for the diagnosis and treatment of acute and chronic heart failure: The Task Force for the diagnosis and treatment of acute and chronic heart failure of the European Society of Cardiology (ESC)Developed with the special contribution of the Heart Failure Association (HFA) of the ESC. *European Heart Journal*, *37*(27), 2129-2200. https://doi.org/10.1093/eurheartj/ehw128

Porter, A. G., & Jänicke, R. U. (1999). Emerging roles of caspase-3 in apoptosis. *Cell death & differentiation*, *6*(2), 99-104.

Rebelato, E., Mares-Guia, T. R., Graciano, M. F. R., Labriola, L., Britto, L. R., Garay-Malpartida, H. M., Curi, R., Sogayar, M. C., & Carpinelli, A. R. (2012). Expression of NADPH oxidase in human pancreatic islets. *Life sciences*, *91*(7-8), 244-249.

Rector, R. S., Warner, S. O., Liu, Y., Hinton, P. S., Sun, G. Y., Cox, R. H., Stump, C. S., Laughlin, M. H., Dellsperger, K. C., & Thomas, T. R. (2007). Exercise and diet induced weight loss improves measures of oxidative stress and insulin sensitivity in adults with characteristics of the metabolic syndrome. *American Journal of Physiology-Endocrinology and Metabolism*, *293*(2), E500-E506.

Reed, J. C. (1998). Bcl-2 family proteins. *Oncogene*, *17*(25), 3225-3236.

Ren, J., Bi, Y., Sowers, J. R., Hetz, C., & Zhang, Y. (2021). Endoplasmic reticulum stress and unfolded protein response in cardiovascular diseases. *Nature Reviews Cardiology*, *18*(7), 499-521.

Ridker, P. M., Vaughan, D. E., Manson, J., Hennekens, C., & Stampfer, M. (1993). Endogenous tissue-type plasminogen activator and risk of myocardial infarction. *The Lancet*, *341*(8854), 1165-1168.

Roberts, C. K., & Sindhu, K. K. (2009). Oxidative stress and metabolic syndrome. *Life sciences*, *84*(21-22), 705-712.

Robinson, M. D., McCarthy, D. J., & Smyth, G. K. (2010). edgeR: a Bioconductor package for differential expression analysis of digital gene expression data. *Bioinformatics*, *26*(1), 139-140.

Rodrigues, A. C., Spagnol, A. R., Frias, F. D. T., De Mendonça, M., Araújo, H., Guimarães, D., Silva, W. J., & Silveira, L. R. (2021). Intramuscular injection of miR-1 reduces insulin resistance in obese mice. *Frontiers in physiology*, *12*, 1027.

Ronti, T., Lupattelli, G., & Mannarino, E. (2006). The endocrine function of adipose tissue: an update. *Clinical endocrinology*, *64*(4), 355-365.

Rosito, G. A., D Agostino, R. B., Massaro, J., Lipinska, I., Mittleman, M. A., Sutherland, P., Wilson, P. W., Levy, D., Muller, J. E., & Tofler, G. H. (2004). Association between obesity and a prothrombotic state: the Framingham Offspring Study. *THROMBOSIS AND HAEMOSTASIS-STUTTGART-*, *91*(4), 683-689.

Ross, R. (1999). Atherosclerosis—an inflammatory disease. *New England journal of medicine*, *340*(2), 115-126.

Ruiz-Núñez, B., Dijck-Brouwer, D. J., & Muskiet, F. A. (2016). The relation of saturated fatty acids with low-grade inflammation and cardiovascular disease. *The Journal of Nutritional Biochemistry*, *36*, 1-20.

Russo, C., Olivieri, O., Girelli, D., Faccini, G., Zenari, M. L., Lombardi, S., & Corrocher, R. (1998). Anti-oxidant status and lipid peroxidation in patients with essential hypertension. *Journal of hypertension*, *16*(9), 1267-1271.

Saelens, X., Festjens, N., Walle, L. V., Van Gurp, M., Van Loo, G., & Vandenabeele, P. (2004). Toxic proteins released from mitochondria in cell death. *Oncogene*, *23*(16), 2861-2874.

Salles, N., Szanto, I., Herrmann, F., Armenian, B., Stumm, M., Stauffer, E., Michel, J.-P., & Krause, K.-H. (2005). Expression of mRNA for ROS-generating NADPH oxidases in the aging stomach. *Experimental gerontology*, *40*(4), 353-357.

Samuel, V. T., & Shulman, G. I. (2012). Mechanisms for insulin resistance: common threads and missing links. *Cell*, *148*(5), 852-871.

Sancho, P., Mainez, J., Crosas-Molist, E., Roncero, C., Fernández-Rodriguez, C. M., Pinedo, F., Huber, H., Eferl, R., Mikulits, W., & Fabregat, I. (2012). NADPH oxidase NOX4 mediates stellate cell activation and hepatocyte cell death during liver fibrosis development. *PloS one*, *7*(9), e45285.

Sano, M., Abdellatif, M., Oh, H., Xie, M., Bagella, L., Giordano, A., Michael, L. H., DeMayo, F. J., & Schneider, M. D. (2002). Activation and function of cyclin T–CDK9 (positive transcription elongation factor-b) in cardiac muscle-cell hypertrophy. *Nature medicine*, *8*(11), 1310-1317.

Sano, M., Wang, S. C., Shirai, M., Scaglia, F., Xie, M., Sakai, S., Tanaka, T., Kulkarni, P. A., Barger, P. M., & Youker, K. A. (2004). Activation of cardiac Cdk9 represses PGC-1 and confers a predisposition to heart failure. *The EMBO journal*, *23*(17), 3559-3569.

Santos, C. X., Hafstad, A. D., Beretta, M., Zhang, M., Molenaar, C., Kopec, J., Fotinou, D., Murray, T. V., Cobb, A. M., & Martin, D. (2016). Targeted redox inhibition of protein phosphatase 1 by Nox4 regulates eIF 2α-mediated stress signaling. *The EMBO journal*, *35*(3), 319-334.

Santos, C. X., Tanaka, L. Y., Wosniak Jr, J., & Laurindo, F. R. (2009). Mechanisms and implications of reactive oxygen species generation during the unfolded protein response: roles of endoplasmic reticulum oxidoreductases, mitochondrial electron transport, and NADPH oxidase. *Antioxidants & redox signaling*, *11*(10), 2409-2427.

Savarese, G., Vedin, O., D'Amario, D., Uijl, A., Dahlström, U., Rosano, G., Lam, C. S., & Lund, L. H. (2019). Prevalence and prognostic implications of longitudinal ejection fraction change in heart failure. *JACC: Heart Failure*, *7*(4), 306-317.

Savji, N., Meijers, W. C., Bartz, T. M., Bhambhani, V., Cushman, M., Nayor, M., Kizer, J. R., Sarma, A., Blaha, M. J., & Gansevoort, R. T. (2018). The association of obesity and cardiometabolic traits with incident HFpEF and HFrEF. *JACC: Heart Failure*, *6*(8), 701-709.

Sayed, D., Hong, C., Chen, I.-Y., Lypowy, J., & Abdellatif, M. (2007). MicroRNAs play an essential role in the development of cardiac hypertrophy. *Circulation research*, *100*(3), 416-424.

Schenk, S., Saberi, M., & Olefsky, J. M. (2008). Insulin sensitivity: modulation by nutrients and inflammation. *The Journal of clinical investigation*, *118*(9), 2992-3002.

Scheper, W., & Hoozemans, J. J. (2015). The unfolded protein response in neurodegenerative diseases: a neuropathological perspective. *Acta neuropathologica*, *130*(3), 315-331.

Schinzari, F., Tesauro, M., & Cardillo, C. (2017). Endothelial and perivascular adipose tissue abnormalities in obesity-related vascular dysfunction: novel targets for treatment. *Journal of cardiovascular pharmacology*, *69*(6), 360-368.

Schröder, K., Zhang, M., Benkhoff, S., Mieth, A., Pliquett, R., Kosowski, J., Kruse, C., Luedike, P., Michaelis, U. R., & Weissmann, N. (2012). Nox4 is a protective reactive oxygen species generating vascular NADPH oxidase. *Circulation research*, *110*(9), 1217-1225.

Schunkert, H. (2002). Obesity and target organ damage: the heart. *International Journal of Obesity*, *26*(4), S15-S20.

Schürmann, C., Rezende, F., Kruse, C., Yasar, Y., Löwe, O., Fork, C., van de Sluis, B., Bremer, R., Weissmann, N., & Shah, A. M. (2015). The NADPH oxidase Nox4 has anti-atherosclerotic functions. *European heart journal*, *36*(48), 3447-3456.

Segal, A. W., & JONES, O. T. (1978). Novel cytochrome b system in phagocytic vacuoles of human granulocytes. *Nature*, *276*(5687), 515-517.

Seidell, J. C., & Halberstadt, J. (2015). The global burden of obesity and the challenges of prevention. *Annals of Nutrition and Metabolism*, *66*(Suppl. 2), 7-12.

Seok, H., Lee, H., Lee, S., Ahn, S. H., Lee, H.-S., Kim, G.-W. D., Peak, J., Park, J., Cho, Y. K., & Jeong, Y. (2020). Position-specific oxidation of miR-1 encodes cardiac hypertrophy. *Nature*, *584*(7820), 279-285.

Seravalle, G., & Grassi, G. (2017). Obesity and hypertension. *Pharmacological research*, *122*, 1-7.

Shah, D., Romero, F., Guo, Z., Sun, J., Li, J., Kallen, C. B., Naik, U. P., & Summer, R. (2017). Obesity-induced endoplasmic reticulum stress causes lung endothelial dysfunction and promotes acute lung injury. *American journal of respiratory cell and molecular biology*, *57*(2), 204-215.

Shiose, A., Kuroda, J., Tsuruya, K., Hirai, M., Hirakata, H., Naito, S., Hattori, M., Sakaki, Y., & Sumimoto, H. (2001). A novel superoxide-producing NAD (P) H oxidase in kidney. *Journal of Biological Chemistry*, *276*(2), 1417-1423.

Silvestri, P., Di Russo, C., Rigattieri, S., Fedele, S., Todaro, D., Ferraiuolo, G., Altamura, G., & Loschiavo, P. (2009). MicroRNAs and ischemic heart disease: towards a better comprehension of pathogenesis, new diagnostic tools and new therapeutic targets. *Recent patents on cardiovascular drug discovery*, *4*(2), 109-118.

Simmonds, S. J., Cuijpers, I., Heymans, S., & Jones, E. A. (2020). Cellular and molecular differences between HFpEF and HFrEF: a step ahead in an improved pathological understanding. *Cells*, *9*(1), 242.

Simonneau, G., Robbins, I. M., Beghetti, M., Channick, R. N., Delcroix, M., Denton, C. P., Elliott, C. G., Gaine, S. P., Gladwin, M. T., & Jing, Z.-C. (2009). Updated clinical classification of pulmonary hypertension. *Journal of the American college of cardiology*, *54*(1S), S43-S54.

Smedley, D., Haider, S., Durinck, S., Pandini, L., Provero, P., Allen, J., Arnaiz, O., Awedh, M. H., Baldock, R., & Barbiera, G. (2015). The BioMart community portal: an innovative alternative to large, centralized data repositories. *Nucleic acids research*, *43*(W1), W589-W598.

Sobey, C. G., Judkins, C. P., Rivera, J., Lewis, C., Diep, H., Lee, H. W., Kemp-Harper, B. K., Broughton, B. R., Selemidis, S., & Gaspari, T. A. (2015). NOX1 deficiency in apolipoprotein E-knockout mice is associated with elevated plasma lipids and enhanced atherosclerosis. *Free radical research*, *49*(2), 186-198.

Song, B., Scheuner, D., Ron, D., Pennathur, S., & Kaufman, R. J. (2008). Chop deletion reduces oxidative stress, improves β cell function, and promotes cell survival in multiple mouse models of diabetes. *The Journal of clinical investigation*, *118*(10), 3378-3389.

Spalding, K. L., Arner, E., Westermark, P. O., Bernard, S., Buchholz, B. A., Bergmann, O., Blomqvist, L., Hoffstedt, J., Näslund, E., & Britton, T. (2008). Dynamics of fat cell turnover in humans. *Nature*, *453*(7196), 783-787.

Srivastava, D., Thomas, T., Lin, Q., Kirby, M. L., Brown, D., & Olson, E. N. (1997). Regulation of cardiac mesodermal and neural crest development by the bHLH transcription factor, dHAND. *Nature genetics*, *16*(2), 154-160.

Starkov, A. A., Fiskum, G., Chinopoulos, C., Lorenzo, B. J., Browne, S. E., Patel, M. S., & Beal, M. F. (2004). Mitochondrial α-ketoglutarate dehydrogenase complex generates reactive oxygen species. *Journal of Neuroscience*, *24*(36), 7779-7788.

Steinhorn, B., Sartoretto, J. L., Sorrentino, A., Romero, N., Kalwa, H., Abel, E. D., & Michel, T. (2017). Insulin-dependent metabolic and inotropic responses in the heart are modulated by hydrogen peroxide from NADPH-oxidase isoforms NOX2 and NOX4. *Free Radical Biology and Medicine*, *113*, 16-25.

Stritzke, J., Markus, M. R. P., Duderstadt, S., Lieb, W., Luchner, A., Döring, A., Keil, U., Hense, H.-W., Schunkert, H., & Investigators, M. K. (2009). The aging process of the heart: obesity is the main risk factor for left atrial enlargement during aging: the MONICA/KORA (Monitoring of Trends and Determinations in Cardiovascular Disease/Cooperative Research in the Region of Augsburg) study. *Journal of the American College of Cardiology*, *54*(21), 1982-1989.

Suh, Y.-A., Arnold, R. S., Lassegue, B., Shi, J., Xu, X., Sorescu, D., Chung, A. B., Griendling, K. K., & Lambeth, J. D. (1999). Cell transformation by the superoxide-generating oxidase Mox1. *Nature*, *401*(6748), 79-82.

Sukumar, P., Viswambharan, H., Imrie, H., Cubbon, R. M., Yuldasheva, N., Gage, M., Galloway, S., Skromna, A., Kandavelu, P., & Santos, C. X. (2013). Nox2 NADPH oxidase has a critical role in insulin resistance–related endothelial cell dysfunction. *Diabetes*, *62*(6), 2130-2134.

Sumimoto, H., Hata, K., Mizuki, K., Ito, T., Kage, Y., Sakaki, Y., Fukumaki, Y., Nakamura, M., & Takeshige, K. (1996). Assembly and activation of the phagocyte NADPH oxidase specific interaction of the N-terminal Src homology 3 domain of p47phox with p22phox is required for activation of the NADPH oxidase. *Journal of Biological Chemistry*, *271*(36), 22152-22158.

Sun, F., Huo, X., Zhai, Y., Wang, A., Xu, J., Su, D., Bartlam, M., & Rao, Z. (2005). Crystal structure of mitochondrial respiratory membrane protein complex II. *Cell*, *121*(7), 1043-1057.

Szanto, I., Rubbia-Brandt, L., Kiss, P., Steger, K., Banfi, B., Kovari, E., Herrmann, F., Hadengue, A., & Krause, K. H. (2005). Expression of NOX1, a superoxide-generating NADPH oxidase, in colon cancer and inflammatory bowel disease. *The Journal of Pathology: A Journal of the Pathological Society of Great Britain and Ireland*, *207*(2), 164-176.

Szegezdi, E., Fitzgerald, U., & Samali, A. (2003). Caspase-12 and ER-stress-mediated apoptosis: the story so far. *Annals of the new York Academy of Sciences*, *1010*(1), 186-194.

Szegezdi, E., Logue, S. E., Gorman, A. M., & Samali, A. (2006). Mediators of endoplasmic reticulum stress-induced apoptosis. *EMBO reports*, *7*(9), 880-885.

Takaya, T., Ono, K., Kawamura, T., Takanabe, R., Kaichi, S., Morimoto, T., Wada, H., Kita, T., Shimatsu, A., & Hasegawa, K. (2009). MicroRNA-1 and MicroRNA-133 in spontaneous myocardial differentiation of mouse embryonic stem cells. *Circulation Journal*, *73*(8), 1492-1497.

Taraseviciute, A., & Voelkel, N. F. (2006). Severe pulmonary hypertension in postmenopausal obese women. *European journal of medical research*, *11*(5), 198.

Tarhriz, V., Wagner, K. D., Masoumi, Z., Molavi, O., Hejazi, M. S., & Ghanbarian, H. (2018). CDK9 regulates apoptosis of myoblast cells by modulation of microRNA-1 expression. *Journal of cellular biochemistry*, *119*(1), 547-554.

Thattaliyath, B. D., Livi, C. B., Steinhelper, M. E., Toney, G. M., & Firulli, A. B. (2002). HAND1 and HAND2 are expressed in the adult-rodent heart and are modulated during cardiac hypertrophy. *Biochemical and biophysical research communications*, *297*(4), 870-875.

Thompson, J. A., Larion, S., Mintz, J. D., Belin de Chantemèle, E. J., Fulton, D. J., & Stepp, D. W. (2017). Genetic deletion of NADPH oxidase 1 rescues microvascular function in mice with metabolic disease. *Circulation research*, *121*(5), 502-511.

Toth, A., Nickson, P., Mandl, A., Bannister, M. L., Toth, K., & Erhardt, P. (2007). Endoplasmic reticulum stress as a novel therapeutic target in heart diseases. *Cardiovascular & Haematological Disorders-Drug Targets (Formerly Current Drug Targets-Cardiovascular & Hematological Disorders)*, *7*(3), 205-218.

Touyz, R. M., Anagnostopoulou, A., Rios, F., Montezano, A. C., & Camargo, L. L. (2019). NOX5: Molecular biology and pathophysiology. *Experimental Physiology*, *104*(5), 605-616.

Trayhurn, P., de Heredia, F. P., Wang, B., Oliveira, C., González-Muniesa, P., & Wood, I. S. (2009). Cellular hypoxia: a key modulator of adipocyte function in obesity? *Adipobiology*, *1*, 19-26.

Tse, W., Maxwell, S., Thomason, H., Blann, A., Thorpe, G., Waite, M., & Holder, R. (1994). Antioxidant status in controlled and uncontrolled hypertension and its relationship to endothelial damage. *Journal of human hypertension*, *8*(11), 843-849.

Tsutsui, H., Kinugawa, S., & Matsushima, S. (2011). Oxidative stress and heart failure. *American Journal of Physiology-Heart and Circulatory Physiology*, *301*(6), H2181-H2190.

Turrens, J. F. (2003). Mitochondrial formation of reactive oxygen species. *The Journal of physiology*, *552*(2), 335-344.

Ueno, N., Takeya, R., Miyano, K., Kikuchi, H., & Sumimoto, H. (2005). The NADPH oxidase Nox3 constitutively produces superoxide in a p22phox-dependent manner: its regulation by oxidase organizers and activators. *Journal of Biological Chemistry*, *280*(24), 23328-23339.

Ueyama, T., Geiszt, M., & Leto, T. L. (2006). Involvement of Rac1 in activation of multicomponent Nox1-and Nox3-based NADPH oxidases. *Molecular and cellular biology*, *26*(6), 2160-2174.

Vallet, P., Charnay, Y., Steger, K., Ogier-Denis, E., Kovari, E., Herrmann, F., Michel, J.-P., & Szanto, I. (2005). Neuronal expression of the NADPH oxidase NOX4, and its regulation in mouse experimental brain ischemia. *Neuroscience*, *132*(2), 233-238.

Van Gaal, L. F., Mertens, I. L., & Christophe, E. (2006). Mechanisms linking obesity with cardiovascular disease. *Nature*, *444*(7121), 875-880.

van Heerebeek, L., Borbély, A., Niessen, H. W., Bronzwaer, J. G., van der Velden, J., Stienen, G. J., Linke, W. A., Laarman, G. J., & Paulus, W. J. (2006). Myocardial structure and function differ in systolic and diastolic heart failure. *Circulation*, *113*(16), 1966-1973.

Vignais, P. (2002). The superoxide-generating NADPH oxidase: structural aspects and activation mechanism. *Cellular and Molecular Life Sciences CMLS*, *59*(9), 1428-1459.

Vinciguerra, M., Santini, M. P., Claycomb, W. C., Ladurner, A. G., & Rosenthal, N. (2010). Local IGF-1 isoform protects cardiomyocytes from hypertrophic and oxidative stresses via SirT1 activity. *Aging (Albany NY)*, *2*(1), 43.

Vitsios, D. M., & Enright, A. J. (2015). Chimira: analysis of small RNA sequencing data and microRNA modifications. *Bioinformatics*, *31*(20), 3365-3367.

von Löhneysen, K., Noack, D., Jesaitis, A. J., Dinauer, M. C., & Knaus, U. G. (2008). Mutational analysis reveals distinct features of the Nox4-p22phox complex. *Journal of Biological Chemistry*, *283*(50), 35273-35282.

Wang, T. J., Parise, H., Levy, D., D'Agostino, R. B., Wolf, P. A., Vasan, R. S., & Benjamin, E. J. (2004). Obesity and the risk of new-onset atrial fibrillation. *Jama*, *292*(20), 2471-2477.

Weatherald, J., Huertas, A., Boucly, A., Guignabert, C., Taniguchi, Y., Adir, Y., Jevnikar, M., Savale, L., Jaïs, X., & Peng, M. (2018). Association between BMI and obesity with survival in pulmonary arterial hypertension. *Chest*, *154*(4), 872-881.

Wellen, K. E., & Hotamisligil, G. S. (2005). Inflammation, stress, and diabetes. *The Journal of clinical investigation*, *115*(5), 1111-1119.

Wendel, A. (1981). [44] Glutathione peroxidase. In *Methods in enzymology* (Vol. 77, pp. 325-333). Elsevier.

Weyemi, U., Caillou, B., Talbot, M., Ameziane-El-Hassani, R., Lacroix, L., Lagent-Chevallier, O., Al Ghuzlan, A., Roos, D., Bidart, J.-M., & Virion, A. (2010). Intracellular expression of reactive oxygen species-generating NADPH oxidase NOX4 in normal and cancer thyroid tissues. *Endocrine-related cancer*, *17*(1), 27.

Whitlock, G., Lewington, S., Sherliker, P., Clarke, R., Emberson, J., Halsey, J., Qizilbash, N., Collins, R., & Peto, R. (2009). Prospective Studies Collaboration Body-mass index and cause-specific mortality in 900 000 adults: collaborative analyses of 57 prospective studies. *Lancet*, *373*(9669), 1083-1096.

Wing, R. R., Bolin, P., Brancati, F. L., Bray, G. A., Clark, J. M., Coday, M., Crow, R. S., Curtis, J. M., Egan, C. M., & Espeland, M. A. (2013). Cardiovascular effects of intensive lifestyle intervention in type 2 diabetes. *The New England journal of medicine*, *369*(2), 145-154.

Wong, C. Y., O'Moore-Sullivan, T., Leano, R., Hukins, C., Jenkins, C., & Marwick, T. H. (2006). Association of subclinical right ventricular dysfunction with obesity. *Journal of the American College of Cardiology*, *47*(3), 611-616.

World Health Organization. (2021). *Obesity and overweight: fact sheet*. World Health Organization. Retrieved 06.12.2021 from https://www.who.int/news-room/fact-sheets/detail/obesity-and-overweight

Xu, J., Wang, G., Wang, Y., Liu, Q., Xu, W., Tan, Y., & Cai, L. (2009). Diabetes-and angiotensin II-induced cardiac endoplasmic reticulum stress and cell death: metallothionein protection. *Journal of Cellular and Molecular Medicine*, *13*(8a), 1499-1512.

Xu, J., Zhou, Q., Xu, W., & Cai, L. (2012). Endoplasmic reticulum stress and diabetic cardiomyopathy. *Experimental diabetes research*, *2012*.

Xu, L., Balzarolo, M., Robinson, E. L., Lorenz, V., Verde, G. D., Joray, L., Mochizuki, M., Kaufmann, B. A., Valstar, G., & de Jager, S. C. (2021). NOX1 mediates metabolic heart disease in mice and is upregulated in monocytes of humans with diastolic dysfunction. *Cardiovascular Research*.

Xue, R.-Q., Zhao, M., Wu, Q., Yang, S., Cui, Y.-L., Yu, X.-J., Liu, J., & Zang, W.-J. (2019). Regulation of mitochondrial cristae remodelling by acetylcholine alleviates palmitate-induced cardiomyocyte hypertrophy. *Free Radical Biology and Medicine*, *145*, 103-117.

Yamaguchi, N., Argueta, J. G. M., Masuhiro, Y., Kagishita, M., Nonaka, K., Saito, T., Hanazawa, S., & Yamashita, Y. (2005). Adiponectin inhibits Toll-like receptor family-induced signaling. *FEBS letters*, *579*(30), 6821-6826.

Yancy, C. W., Jessup, M., Bozkurt, B., Butler, J., Casey, D. E., Drazner, M. H., Fonarow, G. C., Geraci, S. A., Horwich, T., & Januzzi, J. L. (2013). 2013 ACCF/AHA guideline for the management of heart failure: a report of the American College of Cardiology Foundation/American Heart Association Task Force on Practice Guidelines. *Journal of the American College of Cardiology*, *62*(16), e147-e239.

Yang, L., Guan, G., Lei, L., Liu, J., Cao, L., & Wang, X. (2019). Oxidative and endoplasmic reticulum stresses are involved in palmitic acid-induced H9c2 cell apoptosis. *Bioscience reports*, *39*(5), BSR20190225.

Yang, X., & Trumpower, B. (1986). Purification of a three-subunit ubiquinol-cytochrome c oxidoreductase complex from Paracoccus denitrificans. *Journal of Biological Chemistry*, *261*(26), 12282-12289.

Yates, A. D., Achuthan, P., Akanni, W., Allen, J., Allen, J., Alvarez-Jarreta, J., Amode, M. R., Armean, I. M., Azov, A. G., & Bennett, R. (2020). Ensembl 2020. *Nucleic acids research*, *48*(D1), D682-D688.

Ye, J., Rawson, R. B., Komuro, R., Chen, X., Davé, U. P., Prywes, R., Brown, M. S., & Goldstein, J. L. (2000). ER stress induces cleavage of membrane-bound ATF6 by the same proteases that process SREBPs. *Molecular cell*, *6*(6), 1355-1364.

Yokota, T., Oritani, K., Takahashi, I., Ishikawa, J., Matsuyama, A., Ouchi, N., Kihara, S., Funahashi, T., Tenner, A. J., & Tomiyama, Y. (2000). Adiponectin, a new member of the family of soluble defense collagens, negatively regulates the growth of myelomonocytic progenitors and the functions of macrophages. *Blood, The Journal of the American Society of Hematology*, *96*(5), 1723-1732.

Yoshida, H., Haze, K., Yanagi, H., Yura, T., & Mori, K. (1998). Identification of the cis-acting endoplasmic reticulum stress response element responsible for transcriptional induction of mammalian glucose-regulated proteins Involvement of basic leucine zipper transcription factors. *Journal of Biological Chemistry*, *273*(50), 33741-33749.

Youn, J.-Y., Siu, K. L., Lob, H. E., Itani, H., Harrison, D. G., & Cai, H. (2014). Role of vascular oxidative stress in obesity and metabolic syndrome. *Diabetes*, *63*(7), 2344-2355.

Yu, L., Quinn, M. T., Cross, A. R., & Dinauer, M. C. (1998). Gp91phox is the heme binding subunit of the superoxide-generating NADPH oxidase. *Proceedings of the National Academy of Sciences*, *95*(14), 7993-7998.

Yu, S., Kim, S. R., Jiang, K., Ogrodnik, M., Zhu, X. Y., Ferguson, C. M., Tchkonia, T., Lerman, A., Kirkland, J. L., & Lerman, L. O. (2021). Quercetin reverses cardiac systolic dysfunction in mice fed with a high-fat diet: role of angiogenesis. *Oxidative medicine and cellular longevity*, *2021*.

Yu, X.-J., Huang, Y.-Q., Shan, Z.-X., Zhu, J.-N., Hu, Z.-Q., Huang, L., Feng, Y.-Q., & Geng, Q.-S. (2019). MicroRNA-92b-3p suppresses angiotensin II-induced cardiomyocyte hypertrophy via targeting HAND2. *Life sciences*, *232*, 116635.

Yusefzadeh, H., Rashidi, A., & Rahimi, B. (2019). Economic burden of obesity: A systematic review. *Social Health and Behavior*, *2*(1), 7.

Zelzer, S., Fuchs, N., Almer, G., Raggam, R. B., Prüller, F., Truschnig-Wilders, M., Schnedl, W., Horejsi, R., Möller, R., & Weghuber, D. (2011). High density lipoprotein cholesterol level is a robust predictor of lipid peroxidation irrespective of gender, age, obesity, and inflammatory or metabolic biomarkers. *Clinica chimica acta*, *412*(15-16), 1345-1349.

Zeyda, M., & Stulnig, T. M. (2009). Obesity, inflammation, and insulin resistance–a mini-review. *Gerontology*, *55*(4), 379-386.

Zha, B. S., & Zhou, H. (2012). ER stress and lipid metabolism in adipocytes. *Biochemistry research international*, *2012*.

Zhai, C., Tang, G., Peng, L., Hu, H., Qian, G., Wang, S., Yao, J., Zhang, X., Fang, Y., & Yang, S. (2015). Inhibition of microRNA-1 attenuates hypoxia/re-oxygenation-induced apoptosis of cardiomyocytes by directly targeting Bcl-2 but not GADD45Beta. *American journal of translational research*, *7*(10), 1952.

Zhang, D., Li, Y., Wang, W., Lang, X., Zhang, Y., Zhao, Q., & Yan, J. (2022). NOX1 promotes myocardial fibrosis and cardiac dysfunction via activating the TLR2/NF-κB pathway in diabetic cardiomyopathy. *Frontiers in pharmacology*, *13*.

Zhang, M., Brewer, A. C., Schröder, K., Santos, C. X., Grieve, D. J., Wang, M., Anilkumar, N., Yu, B., Dong, X., & Walker, S. J. (2010). NADPH oxidase-4 mediates protection against chronic load-induced stress in mouse hearts by enhancing angiogenesis. *Proceedings of the National Academy of Sciences*, *107*(42), 18121-18126.

Zhang, M., Mongue-Din, H., Martin, D., Catibog, N., Smyrnias, I., Zhang, X., Yu, B., Wang, M., Brandes, R. P., & Schröder, K. (2018). Both cardiomyocyte and endothelial cell Nox4 mediate protection against hemodynamic overload-induced remodelling. *Cardiovascular Research*, *114*(3), 401-408.

Zhang, Q., Liu, J., Chen, S., Liu, J., Liu, L., Liu, G., Wang, F., Jiang, W., Zhang, C., & Wang, S. (2016). Caspase-12 is involved in stretch-induced apoptosis mediated endoplasmic reticulum stress. *Apoptosis*, *21*(4), 432-442.

Zhang, Y., Yang, S., Fu, J., Liu, A., Liu, D., & Cao, S. (2020). Inhibition of endoplasmic reticulum stress prevents high-fat diet mediated atrial fibrosis and fibrillation. *Journal of Cellular and Molecular Medicine*, *24*(23), 13660-13668.

Zhang, Z., Trautz, B., Kračun, D., Vogel, F., Weitnauer, M., Hochkogler, K., Petry, A., & Görlach, A. (2019). Stabilization of p22phox by hypoxia promotes pulmonary hypertension. *Antioxidants & redox signaling*, *30*(1), 56-73.

Zhao, Y., Samal, E., & Srivastava, D. (2005). Serum response factor regulates a muscle-specific microRNA that targets Hand2 during cardiogenesis. *Nature*, *436*(7048), 214.

Zhu, G., & Lee, A. S. (2015). Role of the unfolded protein response, GRP78 and GRP94 in organ homeostasis. *Journal of cellular physiology*, *230*(7), 1413-1420.

Zile, M. R., Gottdiener, J. S., Hetzel, S. J., McMurray, J. J., Komajda, M., McKelvie, R., Baicu, C. F., Massie, B. M., & Carson, P. E. (2011). Prevalence and significance of alterations in cardiac structure and function in patients with heart failure and a preserved ejection fraction. *Circulation*, *124*(23), 2491-2501.

Zorio, E., Medina, P., Rueda, J., Millán, J., Arnau, M., Beneyto, M., Marín, F., Gimeno, J., Osca, J., & Salvador, A. (2009). Insights into the role of microRNAs in cardiac diseases: from biological signalling to therapeutic targets. *Cardiovascular & Hematological Agents in Medicinal Chemistry (Formerly Current Medicinal Chemistry-Cardiovascular & Hematological Agents)*, *7*(1), 82-90.